universität wien

MASTERARBEIT

Titel der Masterarbeit

A screen for cold-induced plant metabolites that promote RNA folding

Verfasser

Thomas Gstrein, Bakk.Biol.

angestrebter akademischer Grad

Master of Science (MSc)

Wien, 2011

Studienkennzahl lt. Studienblatt:	A 066 877
Studienrichtung lt. Studienblatt:	Masterstudium Genetik und Entwicklungsbiologie
Betreuerin:	Univ.-Prof. Dr. Renée Schröder

This work was conducted in collaboration with the laboratory of Univ.-Prof. Dr. Wolfram Weckwerth.

TABLE OF CONTENTS

ABBREVIATIONS

ApR	Ampicillin resistance gene
amp	Ampicillin
BSA	Bovine serum albumin
CBD	Chitin binding domain
CSD	Cold-shock domain
CSDP	Cold-shock domain protein
CSE6	Cold-shock extract 6 hours after cold-induction
CSE48	Cold-shock extract 48 hours after cold-induction
CTAB	Cetyltrimethylammonium bromide
FRET	Fluorescence resonance energy transfer
GC-MC	Gas chromatography–mass spectrometry
GRP	Glycine-rich RNA binding protein
IPTG	Isopropyl β-D-1-thiogalactopyranoside
K_a	Equilibrium-affinity constant
ori	Origin of replication
PAA	Polyacrylamide gel
PCR	Polymerase chain reaction
PMSF	Phenylmethylsulfonyl fluoride
PNK	Polynucleotide kinase
rRNA	ribosomal ribonucleic acid
rpm	Revolutions per minute
RRM	RNA recognition motif
TIC	Total ion chromatogram
tRNA	Transfer ribonucleic acid
T_m	Melting temperature

1. INTRODUCTION

1. 1. RNA STRUCTURE

For decades, RNA was seen as a transport molecule, delivering information from DNA to protein. The discovery of transfer RNAs (tRNAs) and ribosomal RNA (rRNA) in the nineteen fifties didn't change much about the notion that RNA only plays a minor role in cellular processes. tRNA nucleotide sequences and evolutionary comparisons revealed important folding patterns. The first three-dimensional structure of a tRNA was determined by X-ray crystallography in the nineteen eighties. From this structure it became apparent that RNAs need to fold into distinct three-dimensional structures in order to execute their cellular function. The final breakthrough in RNA biology was the discovery of the group I intron, which is able to catalyze its own removal from the precursor RNA molecule. The finding that such RNA enzymes (ribozymes) have both functions, the transport of genetic information as well as a catalytic activity, made RNA a possible candidate for a important role in a pre-biotic or rather a pre-protein world. This hypothesis is nowadays commonly known as the "RNA world hypothesis". In the past years until now, RNA has been found to play key roles in nearly all cellular processes, ranging from catalytic functions in the ribosome and splicosome to the regulation of gene expression on the post-transcriptional level (mRNA autoregulation, small RNAs) and the transcriptional level (X-chromosome inactivation). In any case, the correct three-dimensional structure is the key to RNA function.

1. 1. 1. RNA Secondary Structure

Under physiological conditions, RNA exists in a structured, well ordered arrangement of secondary and tertiary elements. RNA secondary structure consists of mostly short helical regions with single-stranded interceptions (figure 1A). Such helices are stabilized by hydrogen bonding of complementary bases and stacking interactions of the coplanar aromatic rings of bases. The most common base-pairs in RNA secondary structure are the canonical Watson-Crick base-pairs between guanine (G) and cytosine (C) as well as adenine (A) and uracil (U). G and C are able to form three hydrogen bonds as compared to only two hydrogen bonds between A and U. This explains the higher

thermodynamic stability of G:C rich sequences. The presence of the 2'-hydroxyl group causes RNA helices to predominantly adopt the A-form geometry. A-form RNA has a deep and narrow major groove (deep groove) and a broad and shallow minor groove (shallow groove). This burial of discriminating base characteristics in the major groove leaves less possibility for proteins to interact specifically with a regular A-form RNA (reviewed in Weeks and Crothers 1993). Regions for specific ligand and protein binding and catalytic sites are mostly found in single-stranded regions and in regions where the helix geometry is perturbed by non Watson-Crick base-pairs, loops or bulges (reviewed in Lescoute and Westhof 2006). Among the various non canonical base-pairs found in RNA structures, the “wobble” base-pair G:U is the most common. In helices, G:U base-pairs introduce regions of higher structural flexibility and distinct structural, chemical and thermodynamic properties. The pairing results in an additional, non-paired amino group in the minor groove and a deeply negative electrostatic potential in the major groove and makes such regions important recognition sites for proteins and ligands (reviewed in Varani and McClain 2000).

Hairpins consist of a helical region that is closed by a single-stranded loop. The most frequently found hairpin loops in RNA structures are tetraloops (figure 1A), most likely due to their high thermodynamic stability (Woese et al. 1990). Small hairpins are generally more stable, since the entropic penalty to form a hairpin increases with the loop size (reviewed in Tinoco and Bustamante 1999). Hairpin loops are key functional elements, with many of them being involved in tertiary structure formation, as discussed in the next section. In addition, hairpins can be sites of specific recognition.

Internal loops are single-stranded regions linking two helical segments. In comparison, regions linking three or more helical segments are called *junctions*. Internal loops can be as small as one or two base-pairs like pyrimidine-pyrimidine or purine-purine mismatches. Larger internal loops are suggested to be frequently highly structured and important protein binding sites. A prominent example for an internal loop is the 11nt GAAA tetraloop receptor (figure 1A).

Bulges form when there is an excess of bases on one side of a helix (figure 1A). Single base bulges are either looped out of the helix or stack between the bases of the helix. In the latter case they reduce the overall stability of the helix. Bulges can introduce a

backbone bend and thereby increase the major groove accessibility at base-pairs flanking the bulge.

1. 1. 2. Tertiary Structure

An RNA tertiary structure is a three-dimensional arrangement of secondary elements, which is stabilized by the interaction of mainly non-Watson-Crick base-pairs of different secondary structure elements and base-backbone or backbone-backbone interactions (reviewed in Brion and Westhof 1997, Lescoute and Westhof 2006 and Woodson 2010). As mentioned in the previous section, regular A-helical segments have less potential to form specific interactions, because discriminatory base-pair edges are buried in the deep and narrow major groove (reviewed in Weeks and Crothers 1993). Therefore, tertiary interactions occur mainly in stretches of single-stranded RNA or at helical regions that are perturbed by mismatched bases, loops or bulges. This explains the generally lower thermodynamic stability of tertiary interactions compared to secondary interactions. Another factor contributing to the low stability of the overall tertiary fold of an RNA molecule is that in many cases backbone-phosphate burial goes along with these folding events, resulting in electrostatic repulsion and the loss of chain entropy (Moghaddam et al. 2009).
The classification of tertiary interactions and motifs is inconsistent in the literature. In this section, a distinction is made between tertiary structure motifs and tertiary architecture. A motif is defined as an elementary tertiary interaction, with one or more motifs being necessary to stabilize an overall tertiary architecture.

1. 1. 2. 1. Motifs

Tertiary motifs involve hydrogen bonds between bases, backbone-phosphates and backbone-riboses. Some of the best-studied motifs, such as base triplets and base- and ribose-zippers, give a good representation of possible interactions contributing to the stabilization of RNA architectures.

Base triplets and quadruplets. Mismatched bases are a common source of tertiary contacts, with G:U and A:G being among the most frequently observed (Gautheret et al. 1994; reviewed in Hermann and Patel 1999 and Varani and McClain 2000). By changing the helix geometry, such mismatched bases allow for the formation of triple

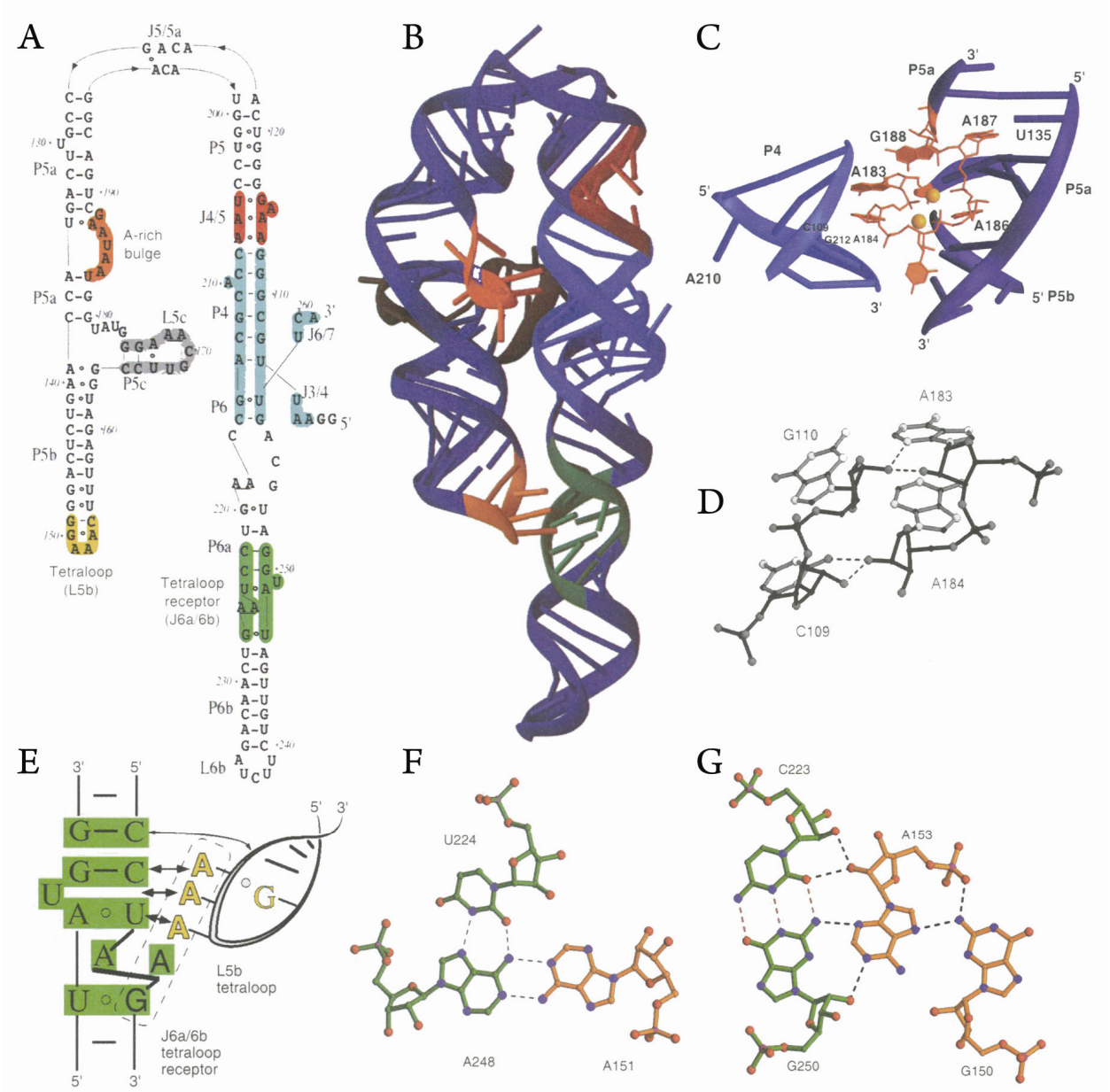

Figure 1. The P4-P6 domain of the *Tetrahymena thermophila* group I self-splicing intron as an example for RNA secondary and tertiary structure. Figures A – G were adapted from Cate et al. (1996) **(A)** The secondary structure of the ribozyme consists of paired regions (P) that are linked by junctions (J). **(B)** The colours correspond to figure A. The helices P4 and P6 as well as P5a and P5b are coaxially stacked. A sharp kink in J5/5a allows the side-by-side docking of the two quasi-continuous helices. Two major sets of tertiary interactions contribute significantly to the overall stability of the ribozyme. The first are interactions of residues of the A-rich bulge (coloured in orange) with the minor groove of helix P4. The second is the docking of the GAAA tetraloop (coloured in gold) into its receptor (coloured in green). **(C)** The backbone of the A-rich bulge makes a sharp turn which is stabilized by specific binding of two magnesium ions (yellow spheres). The residues of the bulge are flipped out and interact with the minor groove of helix P4 as well as with the three helix junction of P5a, P5b and P5c via a network of stacking and base-pairing interactions. The interaction between the A-rich bulge and helix P4 is further stabilized by a ribose zipper as shown in figure D. The hydrogen bonds are shown as dashed lines. **(E)** Schematic representation of the interaction of the GAAA tetraloop with the internal loop of helix J6a/6b (tetraloop receptor). Three adenosines of the tetraloop stack on an adenine and a guanine of the receptor, indicated by a dashed box. The first adenine (GAAA) is involved in a triple

base-pair as shown in figure F. The packing of an adenine into the minor groove of an acceptor base-pair is also called an “A-minor interaction”. The third adenine (GAAA) forms a quadruple base-pair with a guanine from the tetraloop and a G:C base-pair of the receptor as shown in figure G. The dashed lines in figures F and G represent hydrogen bonds.

and quadruple base-pairs (figure 1F and 1G). Triple base-pairs occur when a single-stranded region or a single, for example bulged out residue approaches the major or minor groove of a helical segment. A well-known example for a triple base-pair is the “A-minor” interaction, which was identified in high abundance in the 50S ribosomal subunit and in almost every other tertiary folded RNA. As the name suggests, the interaction comprises an adenine residue packed against the 2'-hydroxyls and the minor groove edge of an acceptor base-pair (figure 1E and 1F) (Strobel 2002). The energetic contribution of A-minor interactions is usually lower than 1 kcal mol^{-1} (reviewed in Woodson 2010). An example for a base quadruple is the GAAA tetraloop receptor motif of the P4-P6 domain of the group I ribozyme (figure 1A and 1G) (Cate et al. 1996).

Cross-strand stacking of bases. Single “free” bases and mismatched base-pairs can be involved in stacking interactions with other strands. Due to their sometimes periodic occurrence, such interactions are also referred to as “interdigitation” or “base zippers” (figure 2). Interdigitation contributes significantly to the stability and compactness of tertiary structures (reviewed in Hermann and Patel 1999).

Ribose zippers are hydrogen bonding interactions of the backbone-ribose 2'-hydroxyls of different strands. One 2'-hydroxyl group is able to form two hydrogen bonds to both the 2'-hydroxyl group of another ribose and either the O2 atom of a pyrimidine or the N3 atom of a purine nucleotide (reviewed in Hermann and Patel 1999). Although the minor groove edge of bases is also involved in these hydrogen bonds, the interaction is not sequence specific (reviewed in Strobel and Doudna 1997). The contribution of ribose zippers to the overall thermodynamic stability of the RNA fold is as small as 1 kcal mol^{-1} or even lower (reviewed in Woodson 2010).

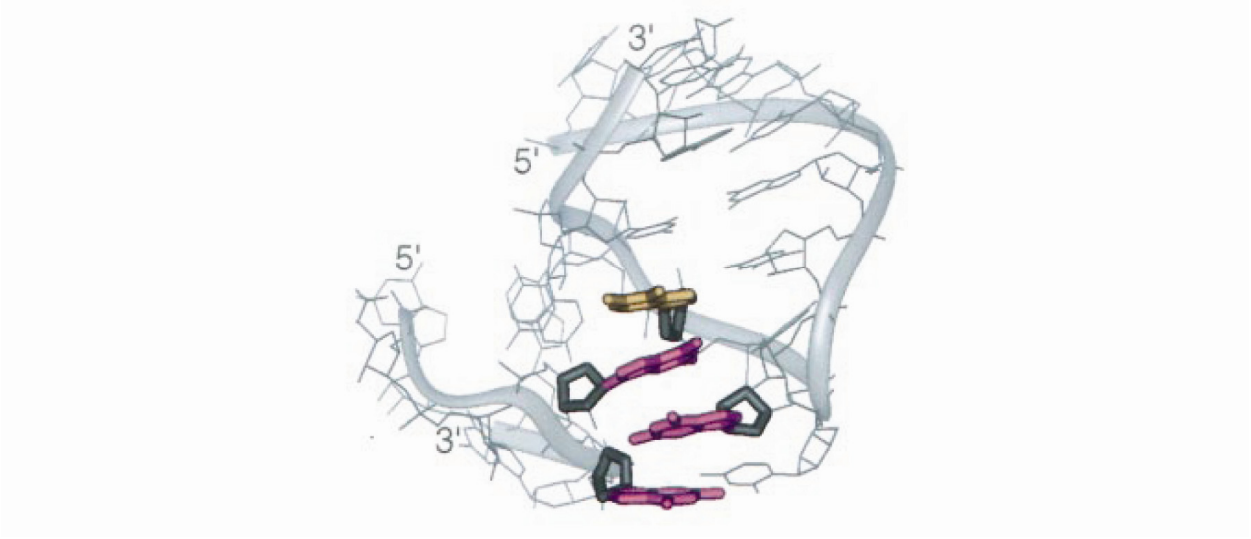

Figure 2. The T and D loop in tRNA interact via cross-strand stacking of bases. This arrangement is sometimes referred to as “interdigitation” or “base zipper”. The two loops are shown in grey. The stacked coplanar bases are highlighted in magenta (guanine) and yellow (adenine). The figure was obtained from Hermann and Patel (1999).

1. 1. 2. 2. Architectures

The overall spatial arrangement of RNA segments is called an architecture. Such an architecture can be mediated by above mentioned tertiary motifs as well as by standard Watson-Crick base-pairs. In most cases, tertiary architectures lead to strong twists and sharp turns of the backbone that have to be stabilized by specific ion binding and further tertiary motifs (figure 1C).

Stacking and docking. Coaxial stacking and side-by-side docking of helical segments are universal themes that change the overall architecture of RNA structures (figure 1B) (reviewed in Strobel and Doudna 1997). Coaxial stacking describes the arrangement of two or more helices to a quasi-continuous helix. Since such helices are linked by single-stranded regions, this interaction involves significant backbone aberrations, which are stabilized by further tertiary interaction motifs. The organization of helices via their sides is called helix docking. Docking is mainly mediated by the interaction of backbone-ribose 2'-hydroxyl groups, but can involve further tertiary contacts.

Pseudoknots are formed by base-pairing of a hairpin loop with a nearby complementary single-stranded region (figure 3) (Pleij et al. 1985; Puglisi et al. 1988). This architecture

has a thermodynamic stability that is comparable to secondary structures due to the involvement of standard Watson-Crick base-pairs (reviewed in Russell 2008). However, the backbone arrangement in pseudoknots leads to highly compact folds with coaxial and non-coaxial stacking of helices (reviewed in Hermann and Patel 1999). These arrangements are further stabilized by extensive tertiary interactions like base quadruples and ribose zippers (Ferré-D'Amaré et al. 1998; Su et al. 1999).

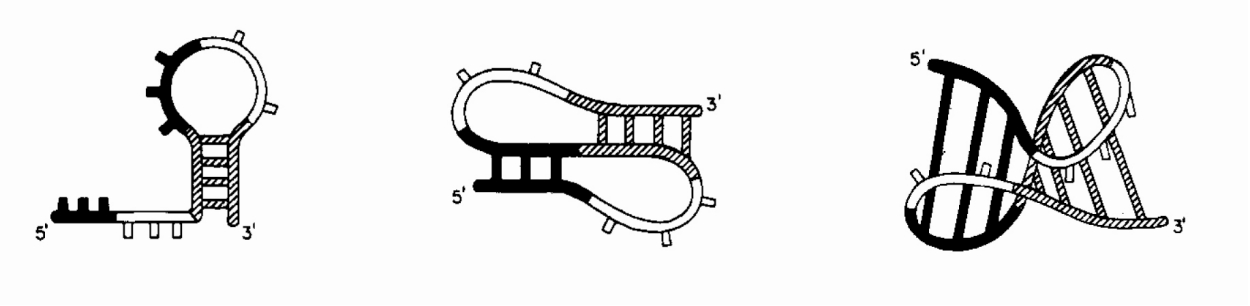

Figure 3. Schematic representation of the folding of an RNA pseudoknot. The complementary regions between the hairpin loop and the 5' end of the RNA molecule form an additional hairpin. The two helices stack coaxially to form a quasi-continuous helix. The figure was adapted from Puglisi et al. (1988).

Kissing complex. The base-pairing of complementary regions of two loops is called a kissing complex (Rist and Marino 2001). Like pseudoknots, kissing complexes have a high thermodynamic stability of -6 to -13 kcal mol^{-1} because they mainly consist of standard Watson-Crick base-pairs (reviewed in Woodson 2010). In many cases, the overall structure of a kissing loop resembles a quasi-continuous helix due to coaxial stacking of the flanking stems (reviewed in Hermann and Patel 1999). A prominent example comes from tRNA, where the D and the T loop form a kissing complex, which is stabilized by additional tertiary contacts of the flanking regions (Quigley and Rich 1976).

Tetraloop-tetraloop receptor interactions play an important role for long-range interactions in the tertiary fold of many RNAs (Costa and Michel 1995). A common example is the GAAA tetraloop interaction with its 11-nucleotide tetraloop receptor duplex in the *Tetrahymena* group I ribozyme (figure 1A and 1E) (Strobel 2002). The three adenines of the tetraloop are stacked on the bases of the tetraloop-receptor helix. This conformation results in a kink in the receptor backbone opening up the minor

groove, which can be accessed by the first adenine (GAAA) of the tetraloop to form a base triple with an A:U base-pair of the receptor (A-minor interaction). The third adenine (GAAA) is involved in a base quadruple with a guanine of the tetraloop and a G:C base-pair of the receptor (figure 1G). The interaction is stabilized by further hydrogen bonds and a ribose zipper between the backbones of the tetraloop and the receptor (reviewed in Strobel and Doudna 1997). However, the overall stability of this interaction is small with only -2 to -4 kcal mol^{-1} (reviewed in Woodson 2010).

1. 2. RNA FOLDING

RNAs need to fold into distinct three-dimensional structures in order to execute their multiple cellular functions like the translational regulation of mRNAs, catalysis, ligand binding, protein binding and many more (reviewed in Brion and Westhof 1997). The notion that folding is not just a simple collapse into a native structure but rather a complex task arose with the finding of stable alternative conformers in isolated tRNAs (Hawkins et al. 1977). RNAs inability to easily fold into the functional structure *in vitro* as well is *in vivo* is commonly accepted (Waldsich et al. 2002; Jackson et al. 2006) and is the central issue of the "RNA folding problem". Herschlag (1995) proposed that the RNA folding problem consists of two distinct challenges for a newly synthesized RNA strand. First, the RNA has the tendency to get kinetically trapped into non-native conformations, and second, some RNA molecules can have different tertiary folds of similar thermodynamic stability. However, not all of them are native.

1. 2. 1. RNA Folding is a Hierarchical Process

The general framework for RNA folding is a hierarchical process (figure 4) (reviewed in Brion and Westhof 1997). The initial collapse of an RNA strand towards more compact structures is induced by the shielding of backbone-charges and leads to the formation of stable secondary structures. The largest fraction is formed by simple hairpins of < 10 bp (reviewed in Russell 2008). Subsequently, interactions of secondary elements lead to the formation of higher order tertiary architectures (reviewed in Brion and Westhof 1997). However, a factor that makes this process more complex is that in some cases, the formation of secondary and tertiary structures is coupled during folding. The propagation of secondary structures can be mediated by tertiary structure formation (reviewed in Woodson 2010) and sometimes the formation of tertiary structures changes the secondary structure (Hilbers et al. 1976; reviewed in Wu and Tinoco 1998).

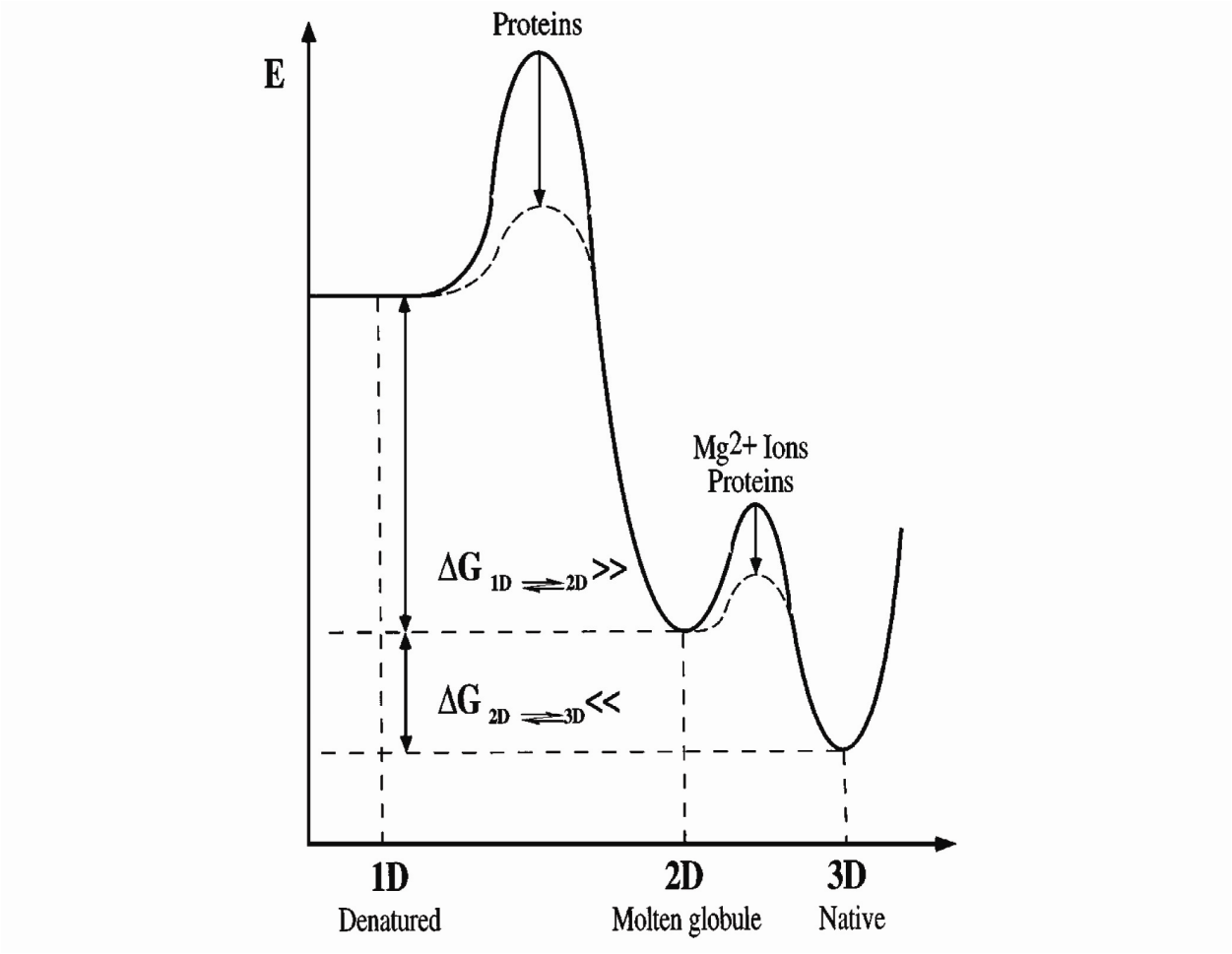

Figure 4. The free energy (E) of RNA secondary structure (1D > 2D) and tertiary structure (2D > 3D) formation. Tertiary folding is the spatial arrangement of stable secondary structures. Due to their high thermodynamic stability, secondary structures are usually not altered by the process of tertiary folding. Therefore, RNA folding is hierarchical. The figure was obtained from Brion and Westhof (1997)

1. 2. 2. Thermodynamics of Folding

The folding can be thought of as the sum of all favourable and unfavourable energies acting on the RNA primary sequence as well as the chronological order of their influence. Base-pairing and base-stacking drive secondary structure formation, but are opposed by unfavourable interactions such as the electrostatic repulsion of the backbone-phosphates and the loss of chain entropy (Heilman-Miller et al. 2001b). Electrostatic repulsion plays an important role in the burial of phosphate-backbones upon tertiary structure formation. In order to create active sites in an RNA structure, the backbone often adopts sharp turns and kinks. Such arrangements have a low thermodynamic stability and, in addition, often are created at the cost of canonical

Watson-Crick base-pairs (reviewed in Woodson 2010). Formation of secondary structures and formation of such architectures is only possible in the presence of cations that neutralize the backbone-charge and allow the strands to get in proximity to each other (Soto et al. 2007). Stretches of Watson-Crick base-paired structures have a high thermal stability. Once some stable base-pairs have formed, the zipping, i. e. the propagation of base-pairing interactions, is fast. Zipping is mainly driven by base-stacking with a nearest neighbour free energy contribution of -1 to -3.6 kcal mol^{-1} per base-pair (1 M NaCl, 37 °C) (Freier et al. 1986).

1. 2. 3. The Rough Folding Energy Landscape

Despite the fact that there is a thermodynamically most stable interaction for each stretch on an RNA molecule, chances are still high that there are alternative interactions with a similar thermal stability. Given the length of time needed to search all potentially accessible conformational states the question remains how RNA manages to fold on a biologically relevant time scale. One solution to this question, known as the Levinthal paradox, is the presence of intermediate organizational levels (reviewed in Brion and Westhof 1997). Such intermediates are generally described in the framework of folding from an unfolded state (U) to one or several intermediate states (I) consisting of native and non-native interactions. Such “metastable” intermediates have to be disrupted and refolded in order to find the functional, native state (N). Only a small fraction of U (Φ) is expected to collapse directly into a native-like conformation, thereby bypassing the slow refolding process. The underlying mechanism of two factions of intermediates is called the “kinetic partitioning mechanism” (Thirumalai and Woodson 1996) and can be explained by the framework of a rough energy landscape (figure 5) (Thirumalai et al. 2001; reviewed in Chen 2008). In such a landscape, mountains represent conformations of low stability such as unfolded structures and accordingly, valleys represent conformations of higher stability. The unfolded RNA sits on the highest mountain and has to find its way through the rough landscape of valleys and mountains to the deepest valley, which is usually the native state. The barrier between valleys represents the energy that has to be overcome in order to refold from one conformation to the other. Overcoming such barriers slows down the folding process. Accordingly, the

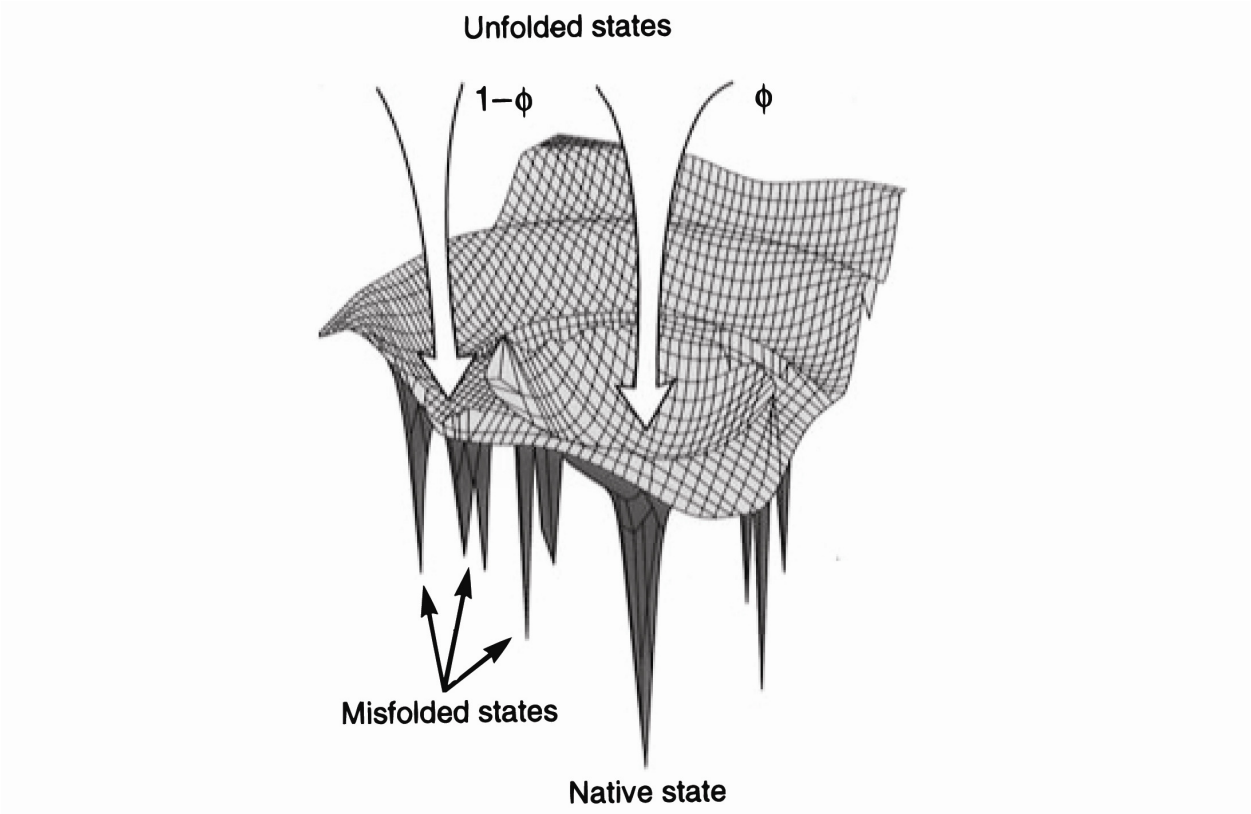

Figure 5. RNA folding can be explained by the framework of a rough energy landscape. The highest point corresponds to the highest free energy, which is the unfolded state of the molecule, and accordingly the deepest valley represents the lowest free energy which is usually the native state. A fraction (Φ) of the molecules directly collapses into the native state whereas the rest (1- Φ) adopts alternative conformations with similar thermodynamic stability as the native state. Such misfolded states have to be refolded in order to reach the native state. The figure was obtained from Thirumalai and Woodson (1996).

folding of complex RNAs can take from 1 – 1000 seconds (reviewed in Woodson 2010) compared to only about 10 ms in tRNA (Crothers et al. 1974). If the valley is too deep, i.e. the thermodynamic stability of the interaction is too high, the molecule may be trapped in this non-native intermediate conformation. Individual RNAs may take different routes through this landscape, because of slight variations in the environments of individual molecules. This explains why individual molecules with the same sequence may need different times to fold (reviewed in Woodson 2010).

1. 2. 4. Sequential Folding

A second solution to the Levinthal paradox is the fact that during transcription, sequences become available sequentially. The transcription rate of the RNA

polymerase II is about 100 nucleotides per second. In contrast, secondary structures are formed on a micro- to millisecond timescale (reviewed in Woodson 2010). One can assume that the timing, with which regions of the RNA become available during transcription, strongly influences the folding pathway. This idea of a sequential fold is supported by studies of transcriptional pausing, circular permutations and elongation kinetics (Mahen et al. 2010 and references therein). However, interactions that occur during transcription are not necessarily functional. Mahen et al. (2010) showed that non-native interactions can exchange rapidly *in vivo*, but not *in vitro.* Interestingly, this is true for interactions up to a certain threshold of thermal stability. Above this threshold, the interaction is trapped even if an alternative interaction with a higher thermal stability is available. These results are in line with a study of Giuliodori et al. (2010) on the cspA mRNA, in which the RNA was shown to adopt two different conformations at 37 °C and at cold-shock temperatures (< 20 °C). Since the 37 °C structure cannot switch to the cold-shock structure upon decreasing the temperature, the structures are expected to be determined by co-transcriptional folding at the respective temperatures. Likely, during transcription at low temperature, secondary structures are too stable to exchange and remain trapped in these interactions. In such a case, the functional RNA structure is not the most stable one.

1. 2. 5. Metal Ions and Folding

As mentioned earlier, RNA requires cations (counterions) in order to neutralize the negative backbone-charge of RNA (Heilman-Miller et al. 2001b and references therein). RNA-ion interactions are complex and it is not easy to break them down into distinct classes or simple rules. The effects of ions on RNA depend on the charge, size and topology of the ions. It is useful to distinct between ions that are bound to specific sites of the RNA molecule and ions that interact indirectly (territorially bound) as part of a delocalized ion atmosphere covering the negative surface of RNA (figure 6). Most ions remain hydrated when interacting with RNA (outer sphere coordination) (Granot and Kearns 1982). However, if the binding energy exceeds the energy of ion hydration, at least some or even all water molecules of the hydration layer are removed (inner sphere coordination).

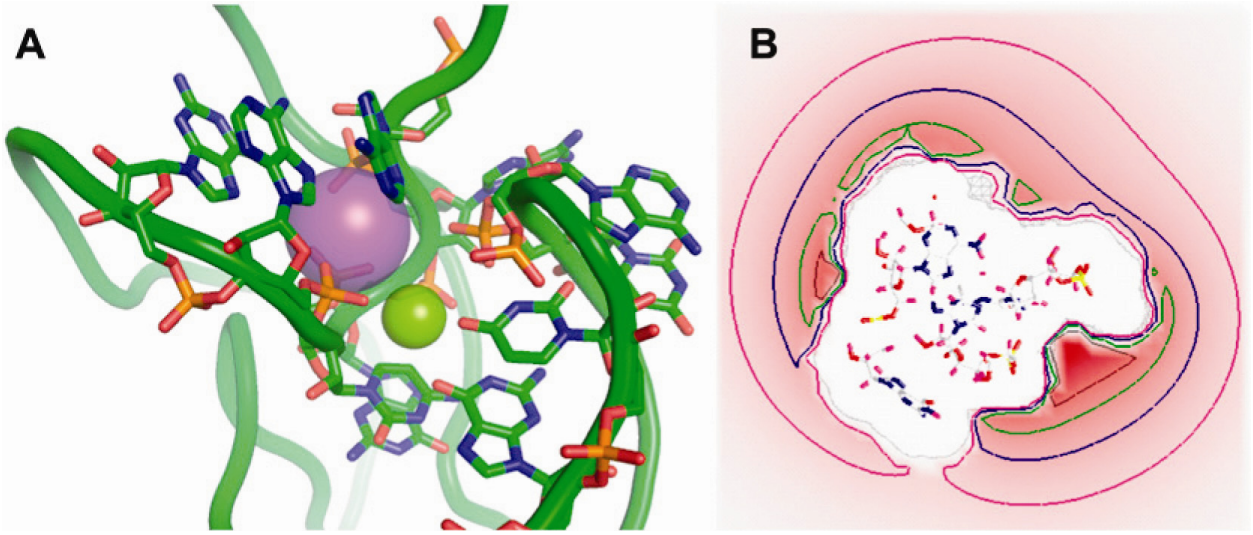

Figure 6. RNA-ion interactions. **(A)** A potassium ion (violet sphere) and a magnesium ion (green sphere) bound to specific sites of an rRNA fragment. Specific ion binding neutralizes sites of high negative charge density and can stabilize fragile backbone architectures. **(B)** An ion atmosphere around a cross section of an RNA hairpin. The red shading indicates the electrostatic potential and the contour lines show the concentrations of counterions of 1.6, 0.8, 0.4, 0.2 and 0.1 M (from the inside out). The figure was obtained from Draper (2008).

Specific ion binding. Backbone-phosphates that come into proximity upon tertiary structure formation form cavities of high negative charge density. This is especially true for backbone regions that are deformed in order to create active sites of ribozymes. Specifically bound magnesium or potassium ions are able to stabilize such fragile architectures (Soto et al. 2007 and references therein; reviewed in Draper 2008 and Woodson 2010). The strength of this interaction usually exceeds the hydration energy and at least some of the water molecules of the first hydration layer are removed. Another important contribution of specifically bound ions is their impact on the folding pathway. The stabilization of specific regions during the folding process adds a further strategy to the variety of folding pathways. Although these effects are essential for RNA folding, the energetic contribution of specifically bound ions is thought to be rather small, considering the actual number of such ions in all known tertiary structures. Most high-resolution crystal structures do not show bound Mg^{2+} ions at all (reviewed in Draper 2008) and only about 200 cations have been shown to be bound in the large subunit of the *Haloarcula marismortui* ribosome (Klein et al. 2004).

Delocalized ions represent the major contribution to the free energy of RNA folding (Soto et al. 2007) This is attributed to the long-range character of electrostatic interactions (Leipply et al. 2009). As a result, the RNA molecule is influenced by all ions surrounding it (Misra and Draper 2001). Delocalized ions are suggested to remain hydrated and mobile relative to the RNA surface (Granot and Kearns 1982). Therefore, instead of tight binding, this interaction resembles an atmosphere of fluctuating ions surrounding the negatively charged backbone. Anions are excluded from this atmosphere, adding a further contribution to the neutralization of backbone-charges (Leipply et al. 2009; reviewed in Draper 2008).

1. 2. 5. 1. Charge Density

In vitro, the most efficient folding and refolding of RNAs can be achieved in counterion mixtures of approximately physiological concentrations (Furtig et al. 2010). This can be explained by the diverse effects of different ions on RNA folding. Crucial for the effect of ions on RNA folding is the charge density, which can be simplified to the term $\zeta = Z / V$, where Z is the valence and V is the volume of the counterion (Koculi et al. 2004). Heilman-Miller et al. studied the influence of ions of different charge density on the folding as well as on the folding kinetics of the *Tetrahymena* group I ribozyme (Heilman-Miller et al. 2001a; Heilman-Miller et al. 2001b). An increasing charge density correlates with a more effective stabilization of RNA structures but with slower folding kinetics. This is not surprising, considering that folding of the group I ribozyme involves the refolding of misfolded intermediates. A stabilization of these intermediates is equivalent to an increase of the energetic barrier for refolding (see section 1. 2. 3.). In line with these findings is that subdenaturing concentrations of urea increase the rate of folding of RNAs in Mg^{2+} (Pörschke 1976; Pan et al. 1997; Rook et al. 1998; Heilman-Miller et al. 2001a).

The impact of size is explained by the excluded volume of the counterions, limiting the number of ions allowed in the atmosphere at the same time. Larger ions cannot approach the RNA surface as closely as small ions. This results in weaker electrostatic interactions with RNA and weaker competitive binding with monovalent salts (Koculi et al. 2004).

1. 2. 5. 2. Entropic Contributions

Entropy changes have considerable influence on the RNA folding energy. This is not only true for the loss of chain entropy during the compaction of RNA chains, but also for every molecule that interacts with RNA. Ions, proteins and other small molecules lose translational entropy upon binding. The fewer molecules that have to bind in order to execute the same function, e.g. the neutralization of backbone-charges, the smaller is this entropy penalty. Accordingly, there is a more favourable entropy term for Mg^{2+} binding than for Na^{+} binding (reviewed in Draper 2008). The same principle applies for ion release. The release of monovalent ions upon RNA folding and multivalent ion binding results in a favourable entropy (Misra and Draper 2000). This explains the lower activation energy of transition states in monovalent salts, since more monovalent than multivalent ions have to be released (Heilman-Miller et al. 2001b).

1. 3. FACTORS THAT INFLUENCE RNA FOLDING

The folding pathway is affected in multiple ways by the direct environment around the RNA molecule. The two probably strongest impacts are metal ions and temperature. A decrease in temperature strongly increases the thermodynamic stability of RNA-RNA interactions. *In vitro*, the stabilization of non-native intermediates in the RNA folding pathway results in slower folding kinetics or kinetically trapped RNAs. A cell usually compensates for this increase in stability by the production of balancing factors such as RNA chaperones.

The following chapter focuses on proteins and small metabolites that are upregulated during cold-shock and in addition influence RNA folding. For small metabolites, the influence on RNA stability was only shown *in vitro* so far. Whether it is of relevance under cold-shock conditions still has to be elucidated.

1. 3. 1. RNA Chaperones

Although the rules governing RNA folding seem to be the same *in vivo* and *in vitro*, RNA often misfolds *in vitro* (Zuker 1989; reviewed in Uhlenbeck 1995) but folds efficiently *in vivo*. The reason for this is that cells contain proteins with RNA chaperone activity, which guide the RNA folding process by resolving misfolded conformations (reviewed in Herschlag 1995 and Weeks 1997).

Rajkowitsch et al. (2007) defined RNA chaperones as proteins that are able to displace one strand on an RNA helix with an alternative one. Such proteins have to be discriminated from proteins that support RNA folding by only enhancing hybridization rates of complementary sequences or that stabilize tertiary structures by specific binding. *In vitro*, RNA chaperones are defined by following features:

(i) An RNA chaperone has non-specific and transient, mostly electrostatic interactions to the RNA substrate and does not require ATP to enhance RNA folding (Mayer et al. 2007). (ii) The RNA chaperone is only needed during the folding process, but can be removed afterwards, showing that the RNA chaperone acts by resolving non-native intermediates rather than stabilizing the native fold (Coetzee et al. 1994; Zhang et al. 1995). (iii) An excess of protein over RNA is needed (Mayer et al. 2007; reviewed in Cristofari and Darlix 2002). As testing RNA chaperone activity *in vivo* is technically not trivial, it remains to be elucidated whether these features also apply inside the cell. *In*

vivo, all RNA chaperones known so far have distinct cellular functions, such as hnRNPA1, a protein involved in the mRNA processing and export, the ribosomal proteins S1 and S12, bacterial proteins involved in the transcription regulation like histone-like protein StpA as well as the bacterial cold-shock protein cspA. Interestingly, all these proteins do not share any common sequence, structural motif or fold, indicating that there might be more than one mechanism behind RNA chaperone activity (reviewed in Rajkowitsch et al. 2007). Nevertheless, a common structural feature is that many RNA chaperones like NCp7, StpA and HNS, Hfq or CspE have an overall positive charge or interact with RNA via a positive surface. A positive charge allows for the interaction with the negative backbone-phosphates and seems to be of special importance in the annealing process (reviewed in Rajkowitsch et al. 2007). However, at least for CspE, the positively charged surface is not sufficient for its nucleic acid melting activity. Binding of CspE to the RNA is assumed to involve stacking of aromatic side chains with RNA bases. A mutant lacking the central aromatic residues of the RNA binding region loses its RNA nucleic acid melting activity but not its ability to bind to RNA (Phadtare et al. 2002). One interesting theory as to how proteins might be able to promote strand-exchange without consuming energy is the “entropy transfer theory”. Proteins with a high level of intrinsically disordered regions can undergo induced folding upon binding (Love et al. 2004; Dyson and Wright 2005). The folding might be accompanied by the unfolding of non-native interactions (Tompa and Csermely 2004).

1. 3. 2. Small Molecules and RNA Folding

Small organic compounds represent a main fraction of the cellular milieu. As discussed later, their composition changes dramatically upon biotic and abiotic stress. It is therefore important to understand their impact on macromolecules. Previous studies concentrated on polyhydric alcohols and sugars, amino acids, N-methylated glyines and urea and their influence on DNA and protein stability, but only little is known about their impact on RNA. The following section gives an overview of metabolites that are most prominent in literature and their impact on RNA folding (figure 7). There are no simple rules to explain the impact of small molecules on RNA folding because RNAs can react differently to their environment dependent on the abundance and type of their secondary and tertiary structures. That is why one metabolite can have opposing effects on RNA depending on the identity of the RNA substrate (Lambert and Draper 2007). In

general, small molecules have three distinct ways to influence RNA folding. First, ions interact mainly with backbone-phosphates via electrostatic attraction or repulsion (see section 1. 2. 5.). Second, small molecules compete with water for the solvation of RNA and are either accumulated at or excluded from phosphates, backbone-sugars or bases. Third, small molecules can interact with ions, thereby changing their activity, the strength of their electrostatic interactions with RNA or their solvation free energy (Lambert and Draper 2007).

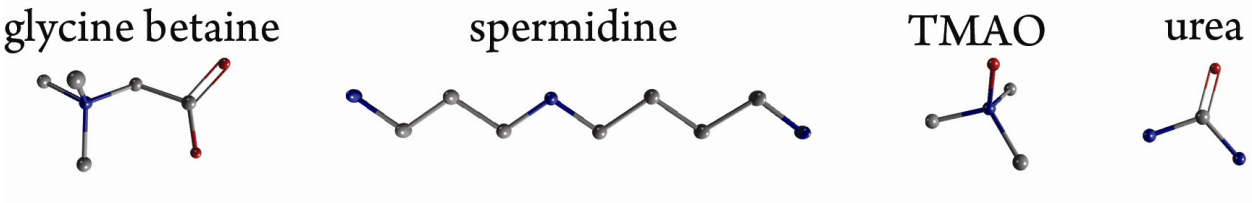

Figure 7. Small molecules that influence RNA folding. The figures were created with Pc3D viewer v2.0 from http://pubchem.ncbi.nlm.nih.gov/. Carbon atoms are shown in grey, nitrogen atoms in blue and oxygen atoms in red. **(Glycine betaine)** is an osmolyte commonly accumulated in plants in response to various stress conditions. It stabilizes proteins but destabilizes RNA secondary structures. Its effects on RNA tertiary structure vary between strongly stabilizing and strongly destabilizing, depending on the RNA substrate and the metal ion concentration. **(Spermidine)** belongs to the class of polyamines, a group of organic compounds comprising two or more amino groups. Many polyamines were shown to influence RNA folding by predominantly interacting with the negative backbone-phosphates. Most studies have been conducted on spermidine, which was shown to stabilize secondary structures and distinct folding-conformers as well as to increase base flexibility. **(TMAO)** is a ubiquitous osmolyte in sea organisms. It has a weak destabilizing effect on secondary structures and a stabilizing effect on most tertiary structures. **(Urea)** is a protein and nucleic-acid denaturant. As such it is able to increase the folding rate of certain RNA substrates by destabilizing non-native interactions.

Polyamines are organic compounds containing two ore more primary amino groups. The concentration of polyamines in cells is tightly regulated (Koculi et al. 2004), and, due to non-specific interactions with other cellular factors, held low (Rubin 1977; Kusama-Eguchi et al. 1991; Williams et al. 1992). Koculi et al. (2004) studied the folding of the *Tetrahymena* group I ribozyme in polyamines of different charge density and topology. The same rules governing metal ion induced folding were found to apply for polyamines, namely a higher charge density and a higher concentration go in line with a more effective stabilization of folding intermediates and a therefore decreased overall folding rate. However, there are some exceptions to this rule. (i) Polyamines with a spacing of amino-groups resembling one of the backbone-phosphates are more effective in compacting the ribozyme than would be expected of their size alone. The

interacting surface of such polyamines is similar to basic peptides that interact with RNA like RNA chaperones (Koculi et al. 2004). (ii) Spermidine increases the flexibility of RNA bases although increasing the overall stability of secondary structures as shown by CD spectroscopy (Furtig et al. 2010). (iii) Spermidine increases the folding rate of a bistable hairpin studied by (Furtig et al. 2010), but decreases the folding rate of the *Tetrahymena* group I ribozyme (Koculi et al. 2004). This is explained by the fact that spermidine can stabilize distinct conformers. These conformers may be native-like structures in the folding pathway of the bistable hairpin, or they may be non-native intermediates such as in the folding of the *Tetrahymena* group I ribozyme.

Urea is commonly known to act as a protein (Liu and Bolen 1995; Bolen and Baskakov 2001) and nucleic acid (Klump and Burkart 1977) denaturant at high concentrations. It lowers the melting temperature for secondary and tertiary unfolding transitions of RNA, with a stronger effect on AU-rich sequences (Schwinefus et al. 2007 and references therein). Interestingly, the addition of 4,5 M urea, although destabilizing, does not change the structure of RNA hairpins (Furtig et al. 2010). The destabilization goes hand in hand with a higher fraction of more open conformers in a Boltzmann distribution. In line with these findings is that moderate concentrations of urea can enhance overall RNA folding. This was shown for the folding of the *Tetrahymena* group I ribozyme and attributed to the ability of urea to resolve non-native intermediates (Heilman-Miller et al. 2001a and references therein) and for a 34mer bistable hairpin by Fürtig et al. (2010), which was explained by the destabilization of the ground states but not the transition state of the bistable hairpin. In addition, subdenaturing concentrations of urea oppose the effects of stabilizing metabolites like cobalt hexamine (Heilman-Miller et al. 2001a). This may explain why cells that accumulate urea often also accumulate stabilizing metabolites like glycine betaine or TMAO (Lin and Timasheff 1994; reviewed in Yancey et al. 1982). Surprisingly, urea is not able to stimulate the reconstitution of a folding-retarded 23S RNA, which was effectively stimulated by the RNA chaperone StpA and the osmolytes TMAO and glycine betaine (Semrad and Green 2002).
The destabilizing effect of urea is explained by its accumulation around amide functional groups that become exposed upon unfolding (Shelton et al. 1999; Hong et al. 2004; Schwinefus et al. 2007). This leads to an accumulation around single-stranded nucleic acids and an increased solubility of bases (Lambert and Draper 2007). Urea shows

neither accumulation at nor exclusion from backbone-oxygens of DNA (Hong et al. 2004).

Trimethylamine-N-oxide (TMAO) is an osmolyte that is commonly found in various sea organisms to compensate for high extracellular salt concentrations (reviewed in Yancey 2005). As such, its effects on protein and nucleic acid stability were examined in various studies. As mentioned above, TMAO is able to stimulate the reconstitution of a folding-retarded 23S RNA (Semrad and Green 2002). In addition, TMAO was shown to be able to induce the Mg^{2+} dependent native fold of a 58mer RNA even in the absence of Mg^{2+} (Lambert et al. 2010). This is especially surprising since the mechanisms of TMAO and Mg^{2+} induced folding have to be considerably different. Mg^{2+} has a strong attraction to negative backbone-phosphates from which TMAO is strongly excluded. This strong exclusion from the backbone is assumed to reduce the penalty for phosphate dehydration, which is accompanied by tertiary structure formation (Lambert et al. 2010) and therefore to effectively stabilize tertiary structures. This stabilization of tertiary structures was shown for different RNA substrates, even though the extent of the stabilization is considerably different depending on which RNA substrate is studied (Lambert and Draper 2007). However, TMAO shows a weak destabilizing effect on secondary structures. Lambert et al. (2010) explained this effect on secondary structures by a mutual elimination of favourable and unfavourable effects of TMAO with base surfaces. TMAO should serve as a good hydrogen bond acceptor but not as a hydrogen bond donor (Noto et al. 1995). The melting of a helix exposes an equal number of acceptors and donors on the base surface to the solvent. The favourable interactions with donors and the unfavourable ones with acceptors give rise to an equilibrium that is slightly destabilizing (Lambert et al. 2010).

Glycine betaine (GB) is an osmolyte that is accumulated upon various stress responses including cold acclimation in plants (reviewed in Janska et al. 2010). As for TMAO, GB was shown to stimulate the reconstitution of a folding-retarded 23 S RNA (Semrad and Green 2002) and was shown to stimulate translation *in vitro* (Brigotti et al. 2003). Another similarity to TMAO is that some cells tend to increase their GB concentration in response to an accumulation of urea (Lin and Timasheff 1994; reviewed in Yancey et al. 1982). GB probably compensates for the destabilizing effects of urea on proteins, since GB was shown to act as a protein stabilizer (Santoro et al. 1992). Interestingly, GB

either strongly stabilizes or strongly destabilizes RNA tertiary structure, depending on which RNA substrate is studied, whereas urea has a general destabilizing effect. Whether GB stabilizes or destabilizes tertiary structures seems to be at least partially dependent on the presence and concentration of salts. The human telomerase RNA (hTR) pseudoknot studied by (Schwinefus et al. 2007) is destabilized by increasing GB concentrations in 40 m*m* NaCl while it is stabilized in 135 m*m* NaCl. Another factor that might explain the behaviour of glycine betaine is its isostabilizing character (Rees et al. 1993; Barone et al. 1996). That is, the high preference of GB to destabilize G:C base-pairs over A:U base-pairs lowers the dependence of the melting temperature on G:C base-pairs. Therefore, the extent by which GB destabilizes secondary structures depends on their GC content (Lambert and Draper 2007). Similar to TMAO, the destabilization is explained by favourable interactions with hydrogen bond donors like amide nitrogens and unfavourable ones with hydrogen bond acceptors like amide oxygens (Capp et al. 2009), giving a destabilizing equilibrium by the accumulation of GB on base surfaces (Lambert and Draper 2007; Schwinefus et al. 2007). However, GB is strongly excluded from protein and dsDNA surfaces (Schwinefus et al. 2007 and references therein; Hong et al. 2004).

1. 4. COLD-SHOCK RESPONSE

Plants and microorganisms cannot escape from abiotic and biotic stresses like temperature changes, which is why they have developed strategies to tolerate them. A decrease in temperature leads to a number of physiological and biochemical changes in order to inhibit ice nucleation, to maintain the cells osmolarity, to maintain the stability of the cell membrane and macromolecules as well as to scavenge reactive oxygen species (ROS) (Kaplan et al. 2004; reviewed in Janska et al. 2010). Such adaption involves the change of the metabolite and protein profile as well as changes in the membrane structure and in the tissue water content.

In general, the metabolism is redirected towards synthesis of cryoprotectant molecules (reviewed in Janska et al. 2010). Although modern high throughput methods for metabolite and protein profiling allow for the detection of these changes and their correlations, little is known about their actual function. This is especially true for the role of metabolites in the cold-shock response.

1. 4. 1. Changes in the Protein Profile of Plants

A temperature decrease results in a global change of the protein profile in a plant cell. As would be expected, proteins linked to the common cell metabolism are generally down-regulated. This involves photosynthesis, cell wall, lipid and nucleotide metabolism (Atienza et al. 2004; Hannah et al. 2006). In addition, proteins known to be involved in the cold-tolerance are up-regulated. Their prevalent function is thought to be the maintenance of hydrophobic interactions and ion homeostasis as well as the scavenging of reactive oxygen species (ROS) (reviewed in Janska et al. 2010). Dehydrins and heat-shock proteins (HSPs) are thought to protect membranes and proteins by their protein chaperone activity (Renaut et al. 2006; Nakayama et al. 2008; Timperio et al. 2008). In addition, the level of cold-regulated (COR) proteins shows a strong correlation to the level of cold hardiness of plants (Pearce et al. 1996) as well as to levels of cold-induced metabolites (Cook et al. 2004).

Several proteins involved in metabolite synthesis and transport are also up-regulated. This includes the metabolism of amino acids, osmolytes, secondary metabolites and raffinose family oligosaccharides (Fowler and Thomashow 2002; Atienza et al. 2004; Hannah et al. 2006; Renaut et al. 2006) as well as transporters of the carbohydrate

metabolism (Kaplan et al. 2007; reviewed in Guy et al. 2008). Cold-induced changes in the metabolite profile are discussed in section 1. 4. 3.

1. 4. 2. Cold-Shock Proteins as RNA Chaperones

Low temperatures increase the thermodynamic stability of RNA-RNA interactions. This also involves a stabilization of non-native intermediates. As discussed in section 1. 2. 3., an increased stability of non-native interactions is equivalent to an increased energetic barrier for refolding. This slows down the folding rate of RNA molecules or even traps RNAs in non-native conformations. It is therefore not surprising that some cold-induced proteins have RNA chaperone activity. This is in line with the finding that malfunction of RNA chaperones *in vivo* often leads to a cold-sensitive phenotype.

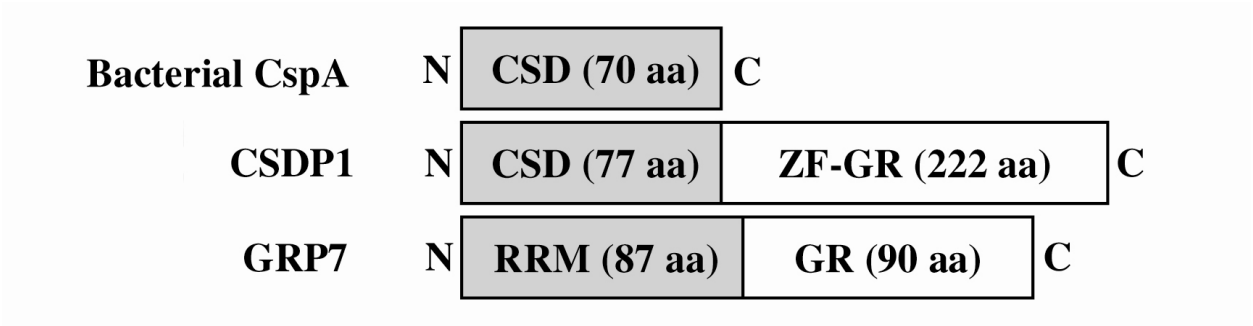

Figure 8. Schematic representation of different cold-induced proteins that act as RNA chaperones. Plant CSDPs such as CSDP1 are comprised of an N-terminal cold-shock domain (CSD) as well as a C-terminal glycine-rich region interspersed with zinc fingers. The CSD shows a high sequence similarity to the bacterial cold-shock protein A (CspA). Cyanobacteria lack cold-shock proteins but instead have cold-inducible glycine-rich RNA binding proteins (GRPs) containing an RNA recognition motif (RRM) as well as a C-terminal glycine-rich region. Many GRPs from *Arabidopsis thaliana*, such as GRP7, are as well cold-induced. The figure was adapted from Kim et al. (2007).

Cold-shock proteins (CSPs) are a well-studied group of small and mostly acid proteins (figure 8) including RNA chaperones like CspA (reviewed in Graumann and Marahiel 1998).

Cold-shock domain proteins (CSDP). The counterpart of bacterial CSPs in plants are cold-shock domain proteins (CSDPs) (figure 8). Their N-terminal cold-shock domain shows a high similarity to CSPs, but in addition CSDPs contain a glycine-rich region interspersed with CCHC-type zinc fingers at the C-terminus. Also CSDPs have been

shown to function as RNA chaperones (Nakaminami et al. 2006; Kim et al. 2007). In a study by Kim et al. (2007), CSDP1 was shown to have a DNA melting activity as well as the ability to complement the cold-sensitivity of the *E. coli* BX04 mutant (which lacks CspA, CspB, CspE and CspG). Surprisingly, these activities are attributed to the zinc fingers in the glycine-rich region rather than to the cold-shock domain (Kim et al. 2007).

Glycine-rich RNA binding proteins (GRPs). Cyanobacteria lack CSPs, but instead have cold-inducible proteins containing an RNA recognition motif (RRM) (figure 8). This led to the hypothesis that RRM proteins substitute the function of CSPs in cyanobacteria (Maruyama et al. 1999; reviewed in Graumann and Marahiel 1998). GRPs in plants contain one or more RRMs at the N-terminus and a glycine-rich region at the C-terminus and are highly induced by low temperature in a wide variety of plants (Kim et al. 2007 and references therein; Sachetto-Martins et al. 2000 and references therein). The *Arabidopsis thaliana* protein GRP7 was shown to have DNA melting activity, to complement the cold-sensitivity of the *E. coli* mutant BX04 and to increase the susceptibility of RNA to RNAse T_1 cleavage (Kim et al. 2007). RNAse T_1 is an endonuclease that specifically cleaves single-stranded RNA but nut double-stranded RNA indicating that GRP7 favours open RNA conformers. The N-terminal RRM is more effective than the C-terminal glycine-rich region. Another GRP assumed to have an RNA chaperone activity is the *Arabidopsis thaliana* protein atRZ-1a, also consisting of an N-terminal RRM and a C-terminal glycine rich region interspersed with zinc fingers (Kim et al. 2005).

1. 4. 3. Cold-Induced Metabolites in Plants

The concentrations of low molecular weight metabolites like carbohydrates, amines or other polar metabolites are significantly changed upon a plant cells response to biotic and abiotic stress (Cook et al. 2004; Kaplan et al. 2004; Wienkoop et al. 2008; reviewed in Yancey 2005 and Janska et al. 2010). They have been shown to act as signalling and regulatory agents, as antioxidants, as defense against pathogens and as compatible solutes (Kaplan et al. 2004). Interestingly, many metabolites cannot be assigned to a specific stress response but seem to play a more general role (Kaplan et al. 2004). This might be explained by the fact that the same cellular stress can be induced by different environmental stimuli. Biotic and abiotic impacts can result in the formation of free

radicals (reviewed in Mittler 2002) and osmotic stress can be a result of drought, salt, cold- and heat-shock as well as of radiation (Kaplan et al. 2004). As an example, an ensemble of osmolytes is up-regulated during cold-stress, acting supposably predominantly as compatible solutes (reviewed in Janska et al. 2010).
In this study, the focus is set on the change of the metabolite profile upon cold acclimation and cold-shock in plants. Cold acclimation describes the changes in cells upon preparation for overwintering and goes hand in hand with acquired freezing tolerance upon previous induction at low temperatures. In contrast, cold-shock describes the cells response to a sudden decrease in temperature. These two conditions are not well distinguished in the literature for studies with *Arabidopsis* species. However, most of the metabolites used in this work show the same change upon cold acclimation and cold-shock (table 5).

1. 4. 3. 1. Changes in the Metabolite Profile Upon Cold Acclimation

During the cold acclimation in plants, concentrations of metabolites with cryoprotective properties increase, while the major part of the metabolism is reduced to a minimum. The cell needs to stabilize membrane phospholipids, stabilize proteins and retain their hydrophobic interactions, maintain ion homeostasis and scavenge reactive oxygen species (reviewed in Janska et al. 2010). For this purpose, the metabolite profile changes dramatically. The function of different metabolites or metabolite groups, however, is poorly understood. Here, an overview of the most prominent changes is given.

Sugars and sugar alcohols. During cold acclimation, the raffinose oligosaccharide pathway is up-regulated, resulting in the accumulation of mono- and disaccharides like glucose, fructose, sucrose, galactinol, melbiose and raffinose (table 5) (Cook et al. 2004; Hannah et al. 2006; Usadel et al. 2008). Concentrations of other sugars like saccharose, stachyose and trehalose as well as sugar alcohols like sorbitol, ribitol and *myo*-inositol were also found to increase (reviewed in Janska et al. 2010). Many of these metabolites are up-regulated in multiple stress situations (Kaplan et al. 2004) indicating that they predominantly act as osmoprotectants and compatible solutes.
Considering that the raffinose pathway is significantly up-regulated under cold-stress, it is interesting that a raffinose accumulation on its own is neither sufficient nor necessary for the induction of freezing tolerance or cold acclimation in *A. thaliana* (Zuther et al.

2004). In contrast, overexpression of the *E. coli* trehalose biosynthetic gene in rice increased tolerance against drought, salinity and cold (Garg et al. 2002). Moreover, the *Arabidopsis* mutant *eskimo1* contains high levels of soluble sugars and proline and possesses an enhanced freezing tolerance (Xin and Browse 1998). In line, failure to accumulate sucrose and glucose results in reduced freezing tolerance in *Arabidopsis* (McKown et al. 1996).
Maltose and fructose have also been shown to increase during cold acclimation (table 5) (reviewed in Janska et al. 2010). Kaplan et al. (2006) hypothesized that the synthesis of maltose may provide some protection of the photosystem II photochemical efficiency. Fructose based polymers (fructans) stabilize membranes by binding to the phosphate and choline groups of membrane lipids, resulting in a reduced water loss upon dehydratization (reviewed in Valluru and Van den Ende 2008).

Amino acids and other nitrogenous compounds. Transcript levels of proteins involved in amino acid metabolism like proline, cysteine and polyamine synthesis as well as glutamate and ornithine pathways are up-regulated in *Arabidopsis thaliana* (reviewed in Janska et al. 2010). In line is the increase of nitrogenous compounds like proline and glycine betaine upon cold acclimation (table 5).

Lipids. Cold acclimation leads to a general suppression of the lipid metabolism (Hannah et al. 2006). Nevertheless, an increase of free fatty acids can be detected (reviewed in Janska et al. 2010).

Secondary metabolites. Freezing tolerance in *Arabidopsis* generally correlates well with the expression of secondary metabolism genes (Hannah et al. 2006; Usadel et al. 2008). Concentrations of flavonoids and anthocyanins along with glucosinolates, terpenoids and phenylpropanoids tend to be increased in *Arabidopsis thaliana*. Anthocyanin is known to help to protect chlorophyll against over-excitement at very low temperatures (Hannah et al. 2006; Korn et al. 2008). The role of other secondary metabolites in cold acclimation is yet largely unknown.

Antioxidants. Many environmental stress factors like drought, cold, heat or radiation can result in the formation of reactive oxidative species (ROS). Accordingly, antioxidants like

tripeptidthiol, glutathione, ascorbic acid and alpha-tocopherol are up-regulated under cold-stress (Chen and Li 2002).

1. 4. 3. 2. Changes in the Metabolite Profile Upon Cold-Shock

A series of metabolites is well-known to be up-regulated upon cold-shock in *Arabidopsis* species. GC-TOF studies reported hundreds of metabolites to be influenced by temperature. The most prominent are presented here.

In a study of Cook et al. (2004), 325 low molecular weight carbohydrates, amines, organic acids and other polar molecules were shown to be up-regulated. Along with proline, glucose, fructose, *myo*-inositol, galactinol, raffinose and sucrose, which are already known from previous studies, they further identified glutamine, asparagine, trehalose, putrescine, ascorbate and many others to be strongly induced by cold-shock (table 5). Interestingly, the majority of these metabolites are also induced by heat-shock. While the early responses to temperature were more diverse, the late responses were more collinear. One reason for this may be that many of these metabolites are well-known compatible solutes. Moreover, many of these metabolites are expected to be precursors for secondary metabolites. Nevertheless, the plant cells response is far more profound for cold-shock than for heat-shock (Kaplan et al. 2004). Some metabolites show no response or even decrease upon heat-shock in contrast to an increase upon cold-shock (table 5). Wienkoop et al. (2008) identified glutamine, raffinose, galactinol, sucrose and proline to be the most prominent metabolites to be increased upon cold-shock in *Arabidopsis* (table 5). Sucrose is known to act as an osmoprotectant as well as a signalling molecule (reviewed in Janska et al. 2010). More interestingly, concentrations of glutamine and proline show strong correlations with the protein level of GRP7 (see section 1. 4. 2.), a cold-induced protein that was previously proposed to act as an RNA chaperone (Kim et al. 2007), but not with raffinose or galactinol. Raffinose family oligosaccharides (RFOs) are general temperature stress markers, whereas proline and glutamine are cold-shock specific (Wienkoop et al. 2008).

Also for *Chlamydomonas reinhardtii*, a model organism used in this work, the Weckwerth laboratory showed a change in the metabolite profile for sugars, amino acids and other low molecular weight compounds upon cold-shock (unpublished data, Weckwerth laboratory, personal communication). The abundance of metabolites such as lactic acid, glycolic acid, alanine, serine, glutamic acid and *myo*-inositol increases

upon cold-shock whereas the abundance of metabolites such as urea, ethanolamine, sorbitol and sucrose decreases (figure 9).

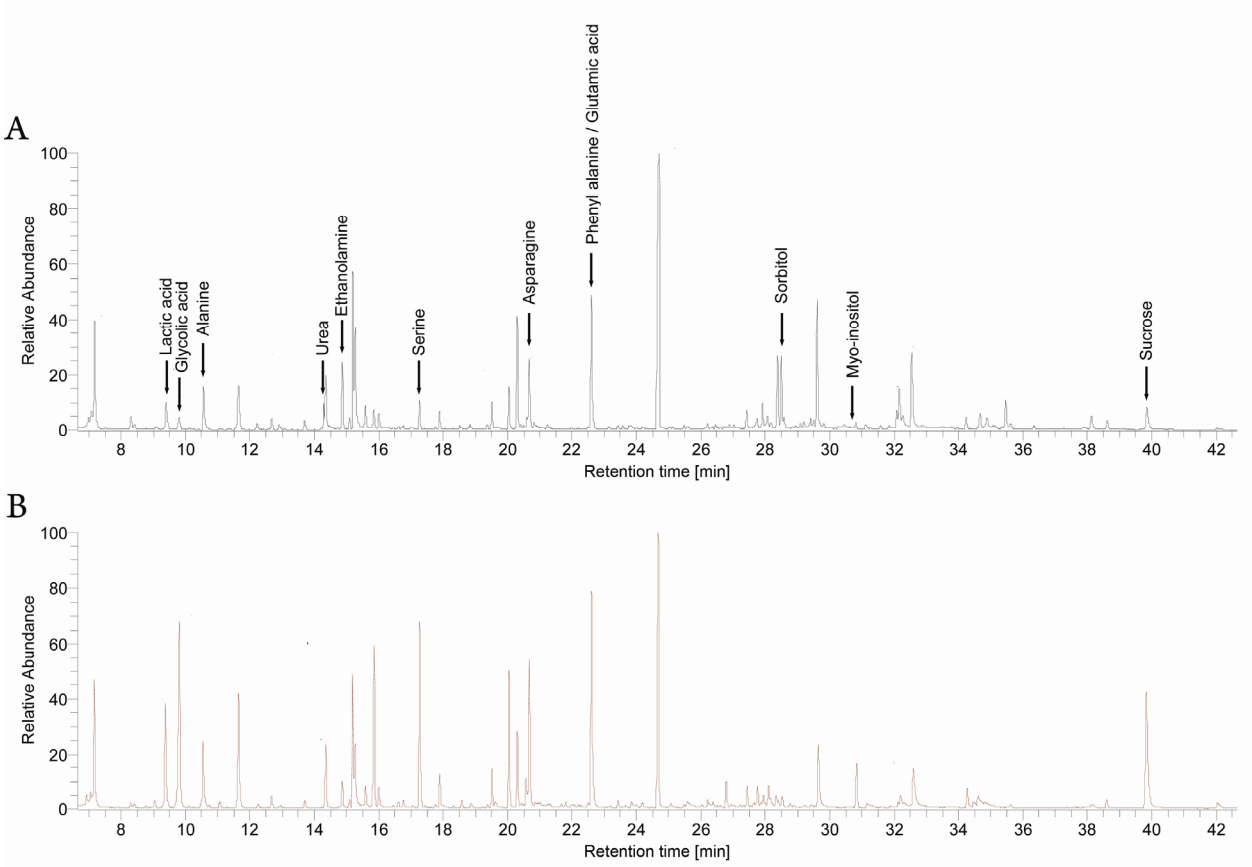

Figure 9. A metabolite profile from *Chlamydomonas reinhardtii* cells under standard growth conditions **(A)** and from cold-shock treated cells **(B)** analyzed with gas chromatography-mass spectrometry (GC-MS) visualized in a total ion chromatogram (TIC). The peaks represent a sum of ions with the same retention time. The abundance of metabolites such as lactic acid, glycolic acid, alanine, serine, glutamic acid and *myo*-inositol increases upon cold-shock whereas the abundance of metabolites such as urea, ethanolamine, sorbitol and sucrose decreases. GC-MS measurements and data analysis were carried out by the Weckwerth laboratory (unpublished data, personal communication), the figure was adapted from chromatograms provided by Dr. Takeshi Furuhashi and Dr. Luis Valledor (Weckwerth laboratory).

.

Weckwerth and Fiehn (2002) showed that the dynamic fluctuations of experimentally determined metabolite concentrations in a cell are connected with the elasticity of the underlying enzymatic pathways, and that such fluctuations propagate throughout the cells regulatory network. Although these results show that metabolite levels may change over time even under a constant environment, they also underline the tight regulation of metabolite levels in cells. Therefore, a dramatic change in the metabolite profile as seen upon cold-shock reflects the change in the protein pattern. But considering that a cell needs to keep its cell environment compatible with the stability and functionality of all

present macromolecules, the question remains whether a cell simply compensates for the presence of functional metabolites with other compounds, e.g. to create an equilibrium between stabilizing and destabilizing metabolites, or whether a previously unknown functionality exists behind these changes besides the few functions known so far.

1. 5. SCIENTIFIC AIM

Plant cells react to cold-shock by a dramatic change of the metabolite profile. Only little is known about the function of these metabolites. Previous studies predominantly concentrated on metabolites that help to sustain the cells osmolarity during stress but that do not interact with proteins or nucleic acids. However, many metabolites shown to increase during cold-stress were also shown to influence the structural stability of RNA. Interestingly, the extent to which these metabolites influence RNA stability differs considerably depending on which RNA is studied. Some metabolites even have opposing effects on secondary and tertiary structures. Such interactions may be of functional importance for a plant cell.

In this study, cold-shock metabolites were examined for their ability to help the cell to cope with the increased thermodynamic stability of RNA-RNA interactions at low temperatures by acting as RNA chaperones. A FRET-based annealing and strand-displacement assay was applied for individual metabolites as well as metabolite groups. Melting studies were carried out in order to link the RNA chaperone activity with RNA structural stability. Physiological metabolite combinations were approximated with polar metabolite-extracts from *Chlamydomonas reinhardtii* cells. The extracts were tested for their ability to enhance the *trans*-splicing activity of a splicing-retarded group I intron as well as to promote the strand-displacement of a double-stranded RNA oligonucleotide by a fully complementary competitor RNA.

In addition, a protein purification protocol for a tag-free protein GRP7 was developed. GRP7 is a proposed RNA-chaperone that is upregulated upon cold-stress in *Arabidopsis thaliana*. During the cold adaption process, the concentration of GRP7 correlates with the cold-shock metabolites proline and glutamine (Wienkoop et al. 2008).

2. MATERIAL AND METHODS

2. 1. MATERIALS, BUFFERS AND SOLUTIONS

2. 1. 1. Materials

RNA Oligonucleotides

Table 1. RNA oligonucleotides used for annealing and strand-displacement assays as well as thermal melting studies.

	Sequence (5' to 3')
$21R^+$	AUG UGG AAA AUC UCU AGC AGU
$21R^-$	ACU GCU AGA GAU UUU CCA CAU
$32R^-$	ACU GCU AGA GAU UUU CCA CAU AGU AUC GAA UU
J1	AAU UUA AUG UUU UAU UUA UUA
M1	UAA UAA AUA AAA CAU UAA AUU
SAM	GGA GUC UUU UCG AAA UGG GAA AGA UUC CC

DNA Oligonucleotides

Table 2. DNA oligonucleotides used for polymerase chain reaction (PCR). Bold letters mark the start- and stop-codons.

	Sequence (5' to 3')
21660 forward primer	AA ACC ATG GCA **ATG** GCG TCC GGT G
21660 reverse primer	AA GGA TCC **TTA** CCA TCC TCC ACC AC
37220 forward primer	TGC AAG ACC **ATG** GCT GCT TCA GC
37220 reverse primer	AAA GGA TCC **TCA** ATA TTG GCG CCT TG
53460 forward primer	AA ACC ATG GCC **ATG** TCT GCC TCT G
53460 reverse primer	GAA GGA TCC **TCA** AAA TTG GCC TCT TGG

Plasmids

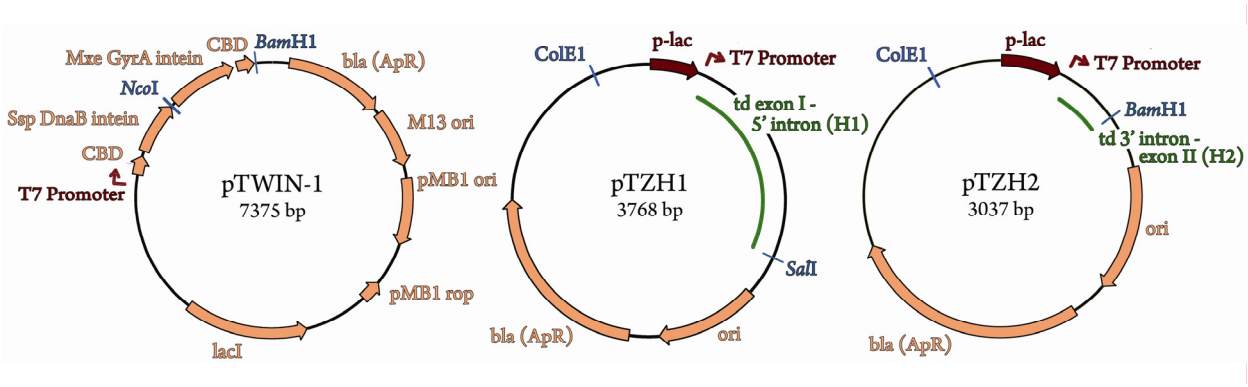

Figure 10. Plasmids used in this study. pTWIN-1 was used for protein purification. pTZH1 and pTZH2 carry the fragments H1 and H2 of the td group I self-splicing intron, respectively. bla (ApR), ampicillin resistance gene; ori, origin of replication; CBD, chitin binding domain.

2. 1. 2. Buffers and Solutions

Buffer B1

20 mM	TRIS-HCl pH 8.4
500 mM	NaCl
1 mM	EDTA pH 8.0
0.2 %	Tween-20
20 µM	PMSF

Buffer B2

40 mM	TRIS-HCl pH 7.0
1 M	NaCl
2 mM	EDTA pH 8.0
20 µM	PMSF

PAA gel elution buffer

10 mM	MOPS pH 6.0
1 mM	EDTA pH 8.0
250 mM	sodium acetate

LTE solution

10 mg	lysozyme diluted in
1 mL	TE-buffer

Sørensen phosphate buffer

330 mM	KH_2PO_4
670 mM	Na_2HPO_4

adjusted to pH 7.2 with additional KH_2PO_4 or Na_2HPO_4

Splicing buffer

4 mM	TRIS-HCl pH 7.0
3 mM	$MgCl_2$
400 µM	spermidine
4 mM	DTT

STET-buffer

8 %	sucrose
0.5 %	Triton X-100
10 mM	TRIS-HCl pH 8.0

STOP solution for strand-displacement gels

9 %	sucrose
0.2x	TBE
0.04 %	bromphenol blue
50 mM	EDTA pH 8.0

prepared in 100 % formamide

T7 RNA polymerase buffer

40 mM	TRIS-HCl pH 7.0
26 mM	$MgCl_2$
3 mM	spermidine
10 mM	DTT

TE-buffer

10 mM	TRIS-HCl pH 8.0
1 mM	EDTA pH 8.0

adjusted to pH 8.0

TER-solution

10 µg	RNAse A diluted in
1 mL	TE-buffer

P-solution (for Chlamydomonas reinhardtii culture medium)

1.65 M	K_2HPO_4
1.06 M	KH_2PO_4

HP salts (for Chlamydomonas reinhardtii culture medium)

280 mM	NH_4Cl
16 mM	$MgSO_4$
14 mM	$CaCl_2$

Hunters trace (for Chlamydomonas reinhardtii culture medium)

135 mM	EDTA pH 8.0
185 mM	H_3BO_3
77 mM	$ZnSO_4$
26 mM	$MnCl_2$
18 mM	$FeSo_4$
7 mM	$CoCl_2$
6 mM	$CuSO_4$
890 µM	$(NH_4)_6Mo_7O_{24}$

EDTA was added to the boiling solution. The pH was adjusted to pH 6.7 at 70 °C with KOH. The solution was sealed with a cotton plug and incubated for 1-2 weeks at room temperature and shaken once a day. The precipitate was removed by filtration.

Chlamydomonas reinhardtii culture medium

0.375 mL	P-solution
25 mL	HP salts
1 mL	Hunter's Trace

prepared in 20 mM HEPES buffer pH 7.0

adjusted to pH 7.0 with HCl and KOH

2. 2. EXPERIMENTAL STANDARD-PROCEDURES

2. 2. 1. Plasmid Minipreparation According to Holmes and Quigley (1981)

2 mL of an *E. coli* overnight culture were harvested at 6800 rpm for 3 minutes. All following centrifugal steps were carried out at maximum speed in a tabletop centrifuge for 5 minutes at room temperature. The pellet was resuspended in 500 µL STET-buffer. The enzymatic lysis was started by the addition of 50 µL LTE-solution. The reaction proceeded for 3 minutes at room temperature and was stopped by incubation at 95 °C for 90 seconds. The lysate was centrifuged and the pellet removed with an autoclaved toothpick. The nucleic acids in the supernatant were precipitated by centrifugation after addition of 50 µL 7.5 M ammonium acetate and 500 µL isopropyl alcohol. The pellet was resuspended in 500 µL cold (-20 °C) 70 % ethanol and the suspension again centrifuged. The pellet was dried and resuspended in 100 µL TER-solution for 30 minutes at 37 °C on a shaker. The solution was purified by PCI extraction when DNA was used for sequencing.

2. 2. 2. Bradford Assay According to Bradford (1976)

Standard curves were prepared with BSA dilutions in 0.15 M NaCl. 1 mL of Bradford dye (AppliChem) was added to 100 µL of protein sample. Protein concentrations were measured in an Eppendorf BioPhotometer® at 595 nm. The time between the addition of dye and the measurement were equal for every sample.

2. 2. 3. Colony PCR

Colonies were picked from culture plates and transferred to an empty PCR tube, the rest was used to inoculate 5 mL LB (amp) for future plasmid preparation. The cells break upon the first cycles of the PCR. A standard PCR protocol for Taq-polymerase (Promega GoTaq®) was carried out and the reactions were examined on a 1.5 % agarose gel.

2. 2. 4. Ethanol Precipitation (for DNA and RNA Samples)

Precipitation with ethanol was used for sample volumes between 10 µL and 500 µL. 0.1 volume of 3 M sodium acetate pH 7.5 and 2.5 volumes of cold (-20 °C) ethanol were added to the sample. The mixture was incubated at -20 °C for at least 20 minutes and in succession centrifuged at 16000 rmp at 4 °C for at least 20 minutes. The pellet was flushed with 1 mL of cold (-20 °C) 70 % ethanol, then dried and resuspended in desired buffer.

2. 2. 5. Elution of RNA from Polyacrylamide Gels

RNA bands were cut out from PAA gels using UV shadowing. Gel pieces were covered with elution buffer and incubated over night at 4 °C on a shaker (~ 1000 rpm). Eluted RNA was precipitated with ethanol.

2. 2. 6. In Vitro Transcription

Plasmids pTZH1 and pTZH2 were linearized with SalI and BamHI, respectively. The restriction was tested on a 1 % agarose gel and the plasmids purified by PCI extraction. In vitro transcription of H1 and H2 constructs was carried out as follows:
100 µL reaction

- 5 µg linearized plasmid
- 5 mM ATP
- 5 mM CTP
- 5 mM GTP
- 2.5 mM UTP
- 3 mM ^{35}S-α-UTP
- 100 U T7 RNA polymerase (New England Biolabs)
- 1x T7 RNA polymerase buffer
- 40 U ribonuclease inhibitor (Promega, RNasin®)

After incubation for 3 hour at 37 °C, 4 U of RNase free DNase (New England Biolabs) were added to the sample and the reaction proceeded for another 30 minutes at 37 °C. RNA was purified by separation over a 5 % denaturing PAA gel and subsequent gel

elution. The purified RNA was resuspended in 20 µL TE buffer. The RNA concentration was determined with the equation

$$C = DF * (\frac{A_{260}}{e_{ave} * P})$$

where DF is the dilution factor, A_{260} is the absorbance of the sample at 260 nm, e_{ave} is the approximate extinction coefficient of RNA (0,027 $(\mu g/mL)^{-1}cm^{-1}$) and P is the path length of the cuvette (1 cm).

2. 2. 7. Kits

Table 3. List of applications that were carried out with purchased systems according to the protocol provided by the manufacturer.

Application	Kit
Agarose-gel elution	Promega wizard® SV gel and PCR clean-up kit
Midiprep	Promega Pure Yield™ Plasmid Midiprep System
Miniprep	Promega Pure Yield™ Plasmid Purification System
PCR purification	Promega wizard® SV gel and PCR clean-up kit

2. 2. 8. PCI extraction of nucleic acids

The extraction with PCI was used for watery samples with a volume of at least 100 µL. One volume of phenol:chloroform:isoamyl alcohol (25:24:1) (AppliChem) was added and the sample mixed thoroughly. The phases were separated by centrifugation at maximum speed for 2 minutes at room temperature. The aqueous phase was collected and the phenol-phase mixed with an additional volume of RNAse-free water. The procedure was repeated and nucleic acids in collected aqueous phases were recovered by ethanol precipitation.

2. 2. 9. RNA hybridization (21R and JM1)

Equimolar concentrations of complementary RNA strands were heated to 95 °C for 2 minutes and subsequently slowly cooled to < 40 °C over a time span of 15 to 30 minutes. The samples were protected from light when RNA was fluorescently labeled.

2. 2. 10. T4 Polynucleotide Kinase (PNK) labelling

T4 PNK catalyzes the transfer of the γ-phosphate of ATP to a free 5' hydroxyl group of DNA or RNA. The reaction mix contained 12 pmoles of RNA, 10 pmol of ^{32}P-γ-ATP (6000 Ci / mmol, 25 µCi / µL), 30 U T4 PNK (New England Biolabs) and 40 U RNAse inhibitor (Promega, RNasin®). The reaction was carried out in T4 PNK buffer (New England Biolabs) and was allowed to proceed for 1 hour at 37 °C. The reaction was stopped by PCI extraction and succeeding ethanol precipitation.

2. 2. 11. Transformation of *E. coli* strains *DH5α* and *ER2566*

Chemically competent cells were kept on -80 °C until usage. 100 µL thawed competent cells were added directly to a ligation reaction (100 ng plasmid DNA) and incubated for 20 minutes on ice. The cells were heat-shocked at 42 °C for 45 seconds. 800 µL antibiotic-free LB medium was added and the sample was shaken at 400 rpm for 30 minutes at 37 °C. The cells were harvested at 6800 rpm for 3 minutes and the supernatant was poured off. The cells were resuspended in the remaining supernatant (~100 µL) and plated on LB (+100 µg/mL amp) plates. Plates were incubated at 37 °C over night.

2. 2. 12. UV melting analysis

UV melting studies were carried out in a Varian “Cary Bio100” UV/VIS spectrophotometer. The absorbance was measured at 260 nm in Quartz cuvettes with 1 cm path length (500 µL sample volume). The samples were heated and cooled at a rate of 0.2 °C per minute with two temperature ramps (10 °C to 80 °C, 80 °C to 10 °C for SAM RNA and 10 °C to 85 °C, 85 °C to 10 °C for 21R RNA.
Samples contained 500 nM RNA, 50 mM Sørensen phosphate buffer pH 7.2, 100 µM NaCl, 500 µM EDTA and respective metabolite at different concentrations. Temperature dependent absorbance was manually blanked. Blanks contained all components except for RNA. The melting temperature and thermodynamic parameters were evaluated by manual baseline setting. ΔH^0 and ΔS^0 were obtained from the slope ($-\Delta H^0/R$) and the Y-axis intercept ($\Delta S^0/R$) of a $\ln(K_a)$ vs. $1/T$ representation of the melting profile as described by Mergny and Lacroix (2003). K_a is the equilibrium-affinity constant and is

the ratio between the folded and the unfolded fraction of the RNA as extracted from the melting profile. The linear regression of values in the $\ln(K_a)$ vs. 1/T representation was restricted to a fraction of folded RNA between 0.15 and 0.85.

2. 3. METHODS

2. 3. 1. Protein Purification

The protein purification of *Arabidopsis thaliana* proteins At2g21660, At2g37220 and At3g53460 was carried out according to the protocol of vector pTWIN-1 accessible on http://www.neb.com/nebecomm/products/productE6950.asp. The protocol was adapted as presented here.

Cloning. Sequences were obtained by PCR with Pfu-polymerase (Promega) from *Arabidopsis thaliana* cDNA. At3g53460 was amplified with KOD polymerase (Novagen) according to protocol due to low yield with Pfu-polymerase. Primers introduced a NcoI restriction-site at the 5' end of the fragment and a BamHI restriction-site at the 3' end. Two to three nucleotides were added to the 5’ end of the primer to enhance the restriction efficiency and to match the melting temperatures. For At2g21660 and At3g53460, the primers extended the 5' protein coding sequence by an additional ATG start codon and one alanine residue. Vector pTWIN-1 was prepared by double restriction with NcoI and BamHI to remove the coding sequence for the Mxe intein and the C-terminal chitin binding domain (CBD). Ligation of the fragment into the prepared pTWIN-1 vector created a *CBD-Ssp intein-protein of interest* fusion protein.

Transformation and sequence verification. The ligation product was transformed into the chemically competent *E. coli* strain *DH5α* via heat shock and the presence of the fragment was confirmed by Colony PCR and restriction analysis. The sequence accuracy of the insert was confirmed by sequencing (AGOWA genomics, Germany). For protein purification, the vector was transformed into the chemically competent *E. coli* expression strain *ER2566* via heat shock.

Overexpression and lysate preparation. Cells were grown in 1 L LB medium (+100 µg/mL ampicillin) at 37 °C at 180 rpm to an OD_{600} between 0.5 and 0.7. Protein expression was induced by addition of isopropyl-β-D-thiogalactopyranoside (IPTG) to a final concentration of 0.3 mM and incubation at 18 °C over night. Cells were harvested at 5000 g for 15 minutes at 4 °C and put on -80 °C for at least 5 hours. Cells were resuspended in 50 mL of buffer B1 at 4 °C and lysed by 3 cycles of freezing in liquid

nitrogen and thawing in a water bath at 25 °C and subsequent sonification. The lysate was centrifuged at 15000 g for 30 minutes at 4 °C to remove the cell debris. The clarified cell extract was used for protein purification.

Protein purification. Proteins were purified via gravity flow through a column packed with 10 mL of chitin beads (New England Biolabs) per litre of culture medium. All steps were performed at 4 °C except for the on-column cleavage reaction. After equilibration of the column with ten bed volumes of buffer B1, the clarified cell extract was loaded with a flow rate of 0.5 mL – 1 mL per minute. The column was again washed with ten bed volumes of buffer B1, and then the on-column cleavage reaction was induced by flushing the column with ten bed volumes of buffer B2. The cleavage reaction was allowed to proceed in one bed volume of buffer B2 over night at room temperature on a slow shaker. The protein was eluted with additional buffer B2 at 4 °C. The fractions with the highest protein concentration were re-buffered in 50 mM TRIS-HCl pH 7.0 with a centrifugal concentration device and stored at 4 °C.

2. 3. 2. Polar Metabolite-Extracts from *Chlamydomonas reinhardtii* Cells

Chlamydomonas reinhadtii culture conditions. All experimental cultures were obtained from the same agar stock culture. Each culture was grown on a shaker at 110 rpm at constant light (100 µE m^{-2} s^{-1} in a 12 hours / 12 hours light-dark cycle) and constant temperature (20 °C) to an OD_{750} = 1. For cold-induction, the cultures at OD_{750} = 1 were grown for further 48 hours on 7 °C.

Extraction of polar metabolites. Polar metabolites were extracted from *Chlamydomonas reinhardtii* cultures as described by Weckwerth et al. (2004) with modifications (Lena Fragner and Anne-Mette Hanak, Weckwerth laboratory, personal communication). Samples were drawn 6 hours and 48 hours after cold-induction. 20 mL of culture were quenched with the same volume of methanol at -70 °C. The sample was lyophilized and the remaining cell debris resuspended in 10 mL of methanol:chloroform:water (2.5:1:0.5 v:v:v). The suspension was vortexed every 5 minutes while incubating on ice for a total of 45 minutes, then aliquoted in 2 mL Eppendorf tubes and centrifuged at 14000 g for 4 minutes at 4 °C. After addition of 500 µL sterile water and another centrifugation step at 14000 g for 4 minutes at 4 °C, the solution separated into two

clear phases. The aqueous phase was collected and dried in a centrifugal vacuum concentrator. The remaining pellet was stored at -80 °C until usage.

2. 3. 3. Trans-Splicing Assay

The self-splicing group I intron derived from the bacteriophage T4 thymidylate synthase (td) gene was *in vitro* transcribed as two separate parts (namely H1 and H2) to largely repress its catalytic activity due to misfolding at 37 °C. The fraction of RNA with the functional conformation can be increased *in vitro* by high temperatures (55 °C) and proteins with RNA chaperone activity (Coetzee et al. 1994). The system was used to test *Chlamydomonas reinhardtii* metabolite extracts for their ability to promote the splicing-competent conformation.

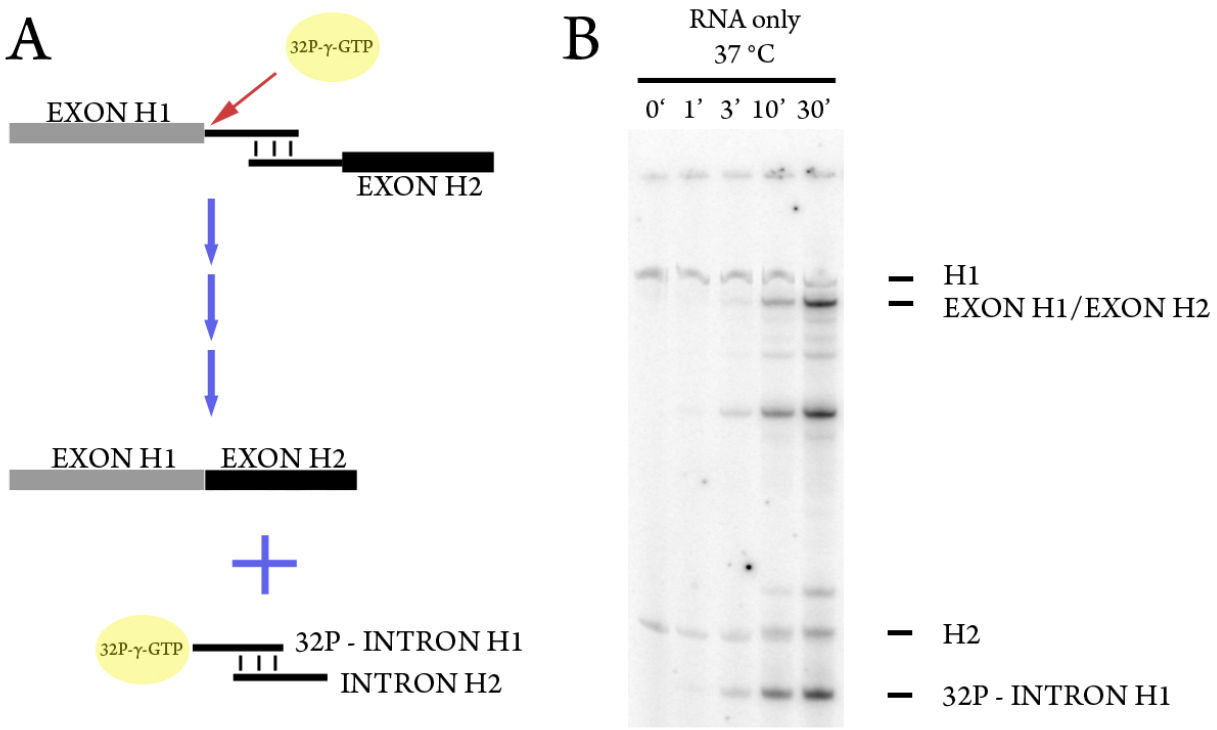

Figure 11. Self-splicing reaction of the *Tetrahymena* group I intron. **(A)** Schematic representation of the splicing reaction. The *in vitro* transcribed RNA fragments H1 and H2 associate *in trans*. The addition of radiolabeled GTP as a splicing cofactor starts the reaction that results in the exclusion of the intron sequence. The intron is released with GTP covalently joined to its 5’ end. **(B)** *In vitro* splicing is inefficient at 37 °C whereas the splicing competent conformation can be promoted by high temperatures (55 °C) and by the presence of RNA chaperones. Aliquots were drawn from the reaction at different time points (0, 1, 3, 10 and 30 minutes) and loaded onto a 12 % denaturing PAA gel. The efficiency of the reaction was monitored by the presence of the splicing product Intron H1 with ^{32}P covalently coined to its 5’ end.

The reaction mixture contained ^{35}S body-labeled H1 and H2 (200 nM each) in splicing buffer and different concentrations of metabolite extracts. The reaction was started with the addition of 0.8 pmol ^{32}P-γ-GTP (5000 Ci / mmol) and proceeded at 37 °C. The "RNA only" reaction mix containing no cold-shock metabolites served as the negative control at 37 °C, and as the positive control at 55 °C. 2.5 µL aliquots were drawn from the reaction mix at different time-points and stopped by the addition of 7.5 µL STOP solution. Bands were separated on a 12 % denaturing PAA gel (figure 11). The bands were quantified with ImageQuant®. The relative splicing efficiency was calculated with the equation RSE = Intron H1 / H1 + H2 + Intron H1

2. 3. 4. FRET-based Annealing and Strand-Displacement Assay

The annealing and strand-displacement reaction of fluorescently labeled (Cy3 and Cy5), complementary short RNA oligonucleotides was monitored with a FRET-based assay, previously described by Rajkowitsch and Schroeder (2007). Fluorescence resonance energy transfer (FRET) occurs when two fluorophores with overlapping excitation and emission spectra come into sufficient proximity. The excited state energy of the donor fluorophore is partially transferred to the acceptor fluorophore. This results in a time-dependent change in fluorescence which is equivalent to the change of the fraction-size of double-stranded RNA present in the sample (figure 12). These data can be fit to the following equations with GraphPadPrism® and can be used to derive the observed rate constants (k_{obs}) for both the annealing (1) and the strand displacement (2) reaction (with Y being the normalized FRET index (ratio of FCy5:FCy3) and t being time)

$$(1) \quad Y = amplitude * (1 - (\frac{1}{k_{obs} * t + 1}))$$

$$(2) \quad Y = Y_0 + amplitude * e^{-k_{obs} * t}$$

The change of fluorescence was monitored in a TECAN Infinite® F500 Microplate Reader with one data point per second. All measurements were carried out at 30 °C (± 0.5 °C). The reaction was carried out in a final concentration of 50 mM TRIS-HCl pH 7.0, 500 µM $MgCl_2$ as well as the tested metabolite in concentrations ranging between 400 nM and 100 mM in a total volume of 50 µL. Cy3-labeled RNA was pre-incubated in buffer. The annealing reaction was started by the injection of Cy5-labeled

RNA (phase I) (figure 12). Both RNAs were added to a final concentration of 10 nM. The reaction was allowed to proceed for 180 seconds, then 5 µL of an unlabeled fully complementary competitor RNA was added to a final concentration of 100 nM to start the strand-displacement reaction (phase II). The strand-displacement reaction was monitored for another 180 seconds.

As a control experiment, the strand-displacement reaction was also carried out without previous annealing-reaction with pre-annealed double-stranded RNA at a concentration of 10 nM over a time-period of 240 seconds.

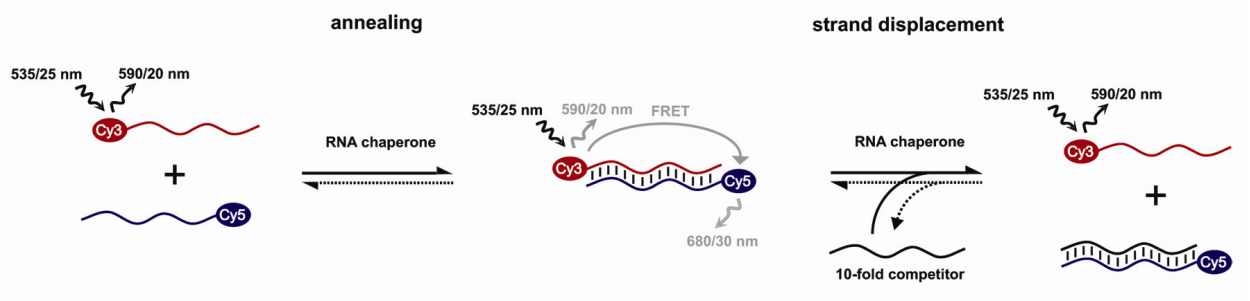

Figure 12. A FRET-based annealing and strand-displacement assay. Two fluorescently labeled short RNA oligonucleotides are allowed to anneal (phase I). Annealing places the two dyes in sufficient proximity to promote fluorescence resonance energy transfer (FRET) to occur when the donor dye (Cy3) is excited. The addition of a fully complementary, unlabeled competitor RNA starts the strand-displacement reaction (phase II). The displacement of a labeled strand leads to a decrease in FRET. The figure was obtained from Rajkowitsch & Schroeder (2007).

2. 3. 5. Strand-Displacement Gels

Polar metabolite extracts from *Chlamydomonas reinhardtii* were tested for their ability to enhance the strand-displacement reaction between a 21R double-strand and $32R^-$, a fully complementary 32mer competitor RNA. Similar assays were previously described by Tsuchihashi and Brown (1994) and Zhang et al. (1995). The $21R^+$ strand was 5' radiolabeled with a polynucleotide kinase to be able to monitor this reaction on a gel even at low RNA concentrations. $21R^+$ and $21R^-$ were pre-annealed in 50 mM TRIS-HCl pH 7.5, 1 mM EDTA pH 8.0 and 3 mM $MgCl_2$ by heating to 95 °C for 5 minutes and slow cooling to 37 °C over a time span of 30 minutes. A two-fold excess of $21R^-$ was used for pre-annealing to assure that no radiolabeled single-strand is present in solution. 500 nM $32R^-$ in 50 mM TRIS-HCl pH 7.5, 1 mM EDTA pH 8.0 and 3 mM $MgCl_2$ and varying concentrations of metabolite extract were pre-incubated at 37 °C. The reaction was

started by the addition of 21R double-strand to a final concentration of 10 nM. The reaction was allowed to proceed for 30 minutes at 37 °C. To stop the reaction and to remove metabolites that interfere with the RNA migration on native PAA gels, the RNA was ethanol precipitated. The RNA was separated on a 12 % native PAA gel. The bands were quantified with ImageQuant®.

3. RESULTS AND DISCUSSION

3. 1. COLD-INDUCED METABOLITES AND RNA FOLDING

RNA chaperones assist RNA folding by resolving non-native intermediates (reviewed in Herschlag 1995). Such non-native intermediates are believed to be resolved by a strand-exchange mechanism rather than simple helix dissociation with succeeding re-annealing. Mahen et al. (2010) showed that the rate of helix melting is the same *in vitro* and *in vivo* whereas the rate of strand-exchange is considerably enhanced in the cellular milieu. Moreover, urea has been shown to increase the folding rate of kinetically trapped RNA molecules but is not able to promote strand-displacement (Boris Fürtig, personal communication). However, it can be assumed that factors that destabilize helical segments also facilitate a strand-exchange mechanism, considering that the competitor-strand has a higher chance to catch a part of the partially opened helix.

RNA chaperones commonly have an overall positive charge or interact with RNA via a positively charged surface (reviewed in Rajkowitsch et al. 2007). A positive charge may lower the energetic cost for a competitor to approach a double-stranded segment and may further provide residual positive charges to attract other RNA strands. Centrimonium bromide (CTAB), a substance comprised of a positive trimethylamine group and a long hydrophobic tail, effectively enhances annealing and strand-exchange (Homann et al. 1996; Nedbal et al. 1997).

So far, no other small metabolite is known to enhance the strand-exchange between RNA molecules. However, it is reasonable to assume that other small molecules also fulfill the requirements. A FRET-based annealing and strand-displacement assay was carried out to screen for such metabolites. The assay was combined with UV-melting studies to further understand the relationship between an RNA chaperone activity and secondary structure stability.

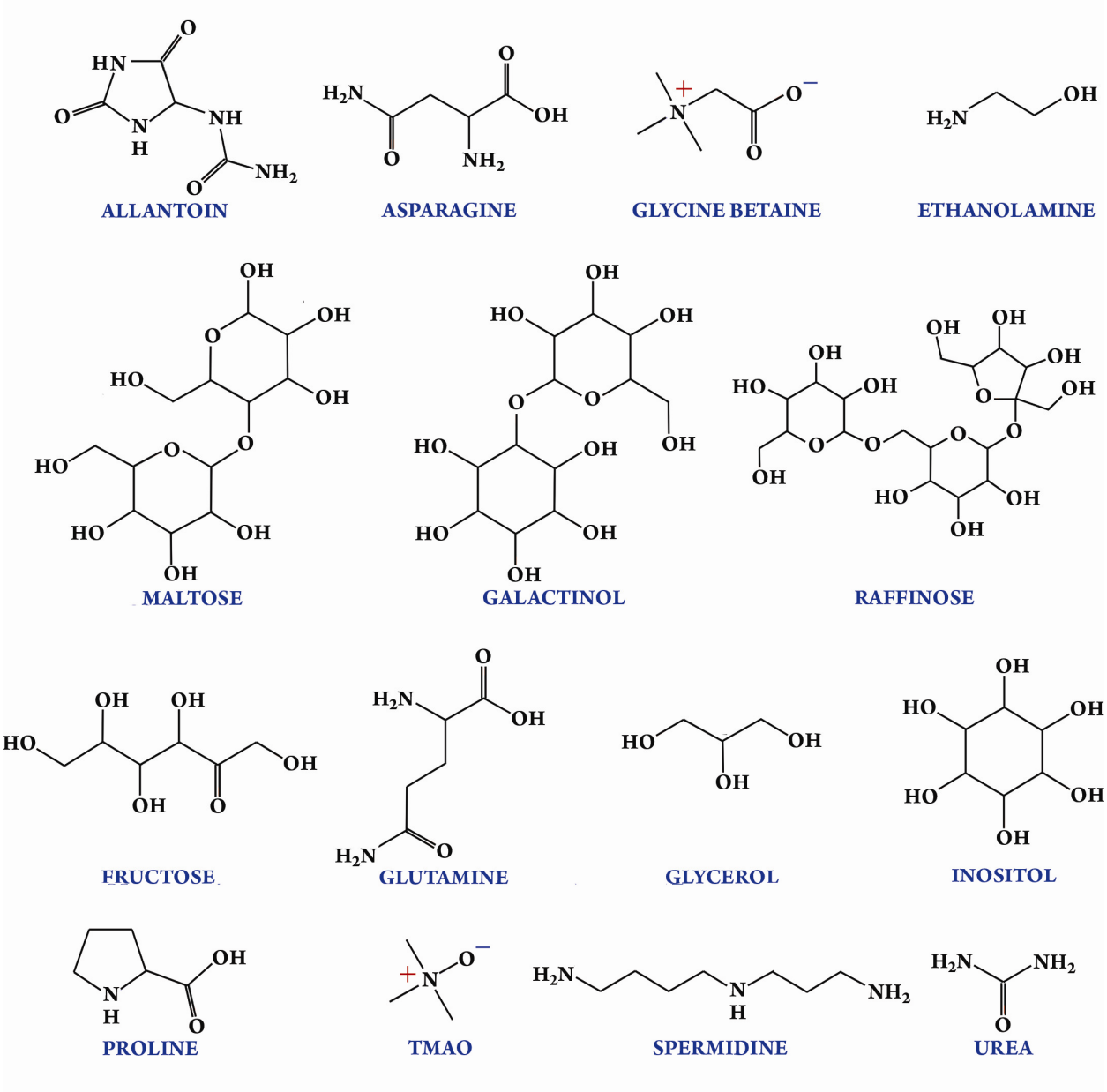

Figure 13. Secondary structure representation of cold-induced metabolites that were used in a FRET-based annealing and strand-displacement assay as well as in thermal melting studies.

3. 1. 1. Choice of Metabolites

The metabolites used in this study were selected based on following criteria. First, the intracellular concentration of the metabolites changes upon temperature stress in plants. In addition, the metabolites were shown to have effects on the secondary or tertiary structure stability of RNA and/or were shown to influence RNA folding. All metabolites used in this study, the dependence of their concentration on temperature

change in plants and their influence on secondary and tertiary structure stability are summarized in table 5. Their structure is shown in figure 13.

3. 1. 2. The Thermal Melting of a Hairpin RNA is Unaffected by the Presence of Cold-Shock Metabolites

The objective of UV melting studies was to gain a more comprehensive picture of the relationship between the influence of small metabolites on strand-displacement and on RNA structural stability. To monitor the effects of metabolites on secondary structure of RNA, the simple hairpin RNA "SAM" was chosen for this study. The hairpin loop is closed by an 11 bp helix with a predicted thermodynamic stability of -13.8 kcal mol^{-1} (1 M NaCl, 37 °C) (Zuker 2003) and an experimentally determined thermodynamic stability of -4.6 kcal mol^{-1} (100 µM NaCl, 37 °C) (figure 14). The large number of base-pairs and high stability make it a good model RNA to screen for metabolites that should act on RNAs with an increased thermodynamic stability due to low temperatures. Helices in natural occurring RNAs rarely succeed 10 bp (Fuertig et al. 2007). The thermodynamic stability of longer stretches is usually too high to be exchanged by a competing RNA strand *in vivo* (Mahen et al. 2010). Due to the high stability of the substrate, a low salt concentration of 100 µM NaCl had to be used in order to be able resolve the melting profile.

UV-melting studies were carried out at metabolite concentrations that were considered biologically relevant. However, the absolute quantities of all metabolites in plant cells are not known. A study of Lewis et al. (2007) showed that the concentrations of the most abundant metabolites in *Arabidopsis* are about 1 mM – 10 mM (table 5). This study was used as a guideline for concentrations used in UV melting studies.

In the absence of metabolites, the midpoint of the melting transition (T_m) of SAM is 59.3 °C ± 0.5 °C. The effects of spermidine and urea on RNA structural stability have been previously shown. As anticipated, 1 mM spermidine effectively stabilizes the hairpin by 6.2 °C and 1 M urea destabilizes the hairpin by -3.4 °C (figure 14 and 15, table 4). Other metabolites tested here are neither able to significantly change the melting temperature nor the shape of the melting transition (figure 15B). To understand whether the lack of effect of metabolites presented here is due to structural features or due to the base-pair composition of the RNA substrate, each metabolite was in addition tested at least once with 21R RNA (data not shown). For this substrate, the melting

temperature and the shape of the melting transition also remain unaltered by the presence of cold-shock metabolites.

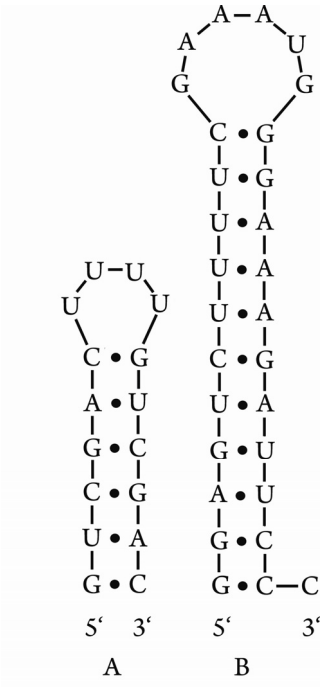

Figure 14. Hairpin RNAs. **(A)** A small hairpin designed by Lambert and Draper (2007). The melting temperature of the hairpin is slightly decreased in the presence of high concentrations of urea, proline, glycine betaine, glycerol and TMAO. **(B)** Hairpin RNA (SAM) used in this study. The melting temperature remains unaltered in the presence of cold-shock metabolites.

Table 4. Melting temperature (T_m) of a 29mer hairpin RNA (SAM) in the presence or absence of approximately physiological concentrations of metabolites. C, concentration. The deviation is presented as 2 x standard error of mean. Spermidine and urea were used as a positive control.

	C [mM]	T_m [°C]
SAM only	-	59.2 ± 0.3
allantoin	1	59.5 ± 0.3
allantoin	10	59.6 ± 1.0
asparagine	1	59.8 ± 0.8
betaine	10	59.7 ± 0.5
ethanolamine	10	59.9 ± 0.3
fructose	1	59.2 ± 0.8
galactinol	1	59.5 ± 0.6
glutamine	1	59.4 ± 0.1
glycerol	10	59.5 ± 0.5
myo-inositol	10	59.4 ± 0.5
maltose	10	59.4 ± 0.1
proline	10	59.5 ± 0.1
spermidine	1	65.4 ± 0.6
TMAO	1	59.4 ± 0.2
urea	1000	55.7 ± 0.2

Interestingly, CTAB is not able to change the melting temperature of the 21R duplex at a concentration of 100 µM. As will be discussed later (see section 3. 1. 3.), 100 µM CTAB is sufficient to effectively enhance annealing, but not to catalyze strand-displacement of the same RNA substrate. It was not possible to record melting curves at higher concentrations of CTAB. At 500 µM CTAB, the absorbance profile showed a slow but continuous decrease in absorbance with time that may result from precipitation.

	change in concentration upon cold acclimation	change in concentration upon cold-shock	change in concentration upon heat shock	effects on sec. structure stability	effects on tertiary structure stability	reconstitution of a folding retarded 23S rRNA	intracellular concentration
allantoin	-	I [3] / N [4]	I [4] / N [3]	-	-	-	-
asparagine	I [1]	I [3]	I [3] / N [4]	-	-	-	61.5 mM [9]
glycine betaine	I [2]	-	-	D [5][6]	D + I [5] [6]	I [8]	-
ethanolamine	-	D [4]	-	-	-	-	4.6 mM [9]
fructose	I [1] [2]	I [3] / N [4]	I [3] [4]	-	-	-	5.9 mM [9]
galactinol	I [1] [2]	I [3] [4]	I [3] [4]	-	I [5]	-	-
glutamine	I [1]	I [3] [4]	N [3] [4]	-	-	-	37.4 mM [9]
glycerol	I [1]	I [3] / N [4]	I [3] [4]	D + I [5]	-	N [8]	10.4 mM [9]
maltose	I [1]	I [3]	I [3]	-	-	-	0.1 mM [9]
***myo*-inositol**	I [1] [2]	I [4] / D [3]	I [3] [4]	-	-	-	-
proline	I [1] [2]	I [3] [4]	N [3] / D [4]	D [5]	D [5]	-	1.9 mM [9]
raffinose	I [1] [2]	I [3] [4]	I [3] [4]	-	-	-	-
spermidine	I [1]	N [4]	N [4]	I [7]	-	-	-
TMAO	-	-	-	D + I [5]	I [5]	I [8]	-
urea	I [1]	-	-	D [5]	D [5]	N [8]	-

Table 5. Metabolites used in UV-melting studies and in the FRET-based annealing and strand-displacement assay. Metabolites that change in concentration upon temperature stress and metabolites that influence the thermodynamic stability of RNA-RNA interactions are considered candidates as RNA chaperones. I, increase; D, decrease; N, no influence; -, not determined in given references. Glycine betaine, glycerol and TMAO were shown to increase and decrease RNA structural stability depending on which RNA substrate was studied. The numbers refer to the following references: [1] Cook et al. (2004); [2] Janska et al. (2010); [3] Kaplan et al. (2004); [4] Wienkoop et al. (2008); [5] Lambert and Draper (2007); [6] Schwinefus et al. (2007); [7] Furtig et al. (2010); [8] Semrad and Green (2002); [9] Lewis et al. (2007).

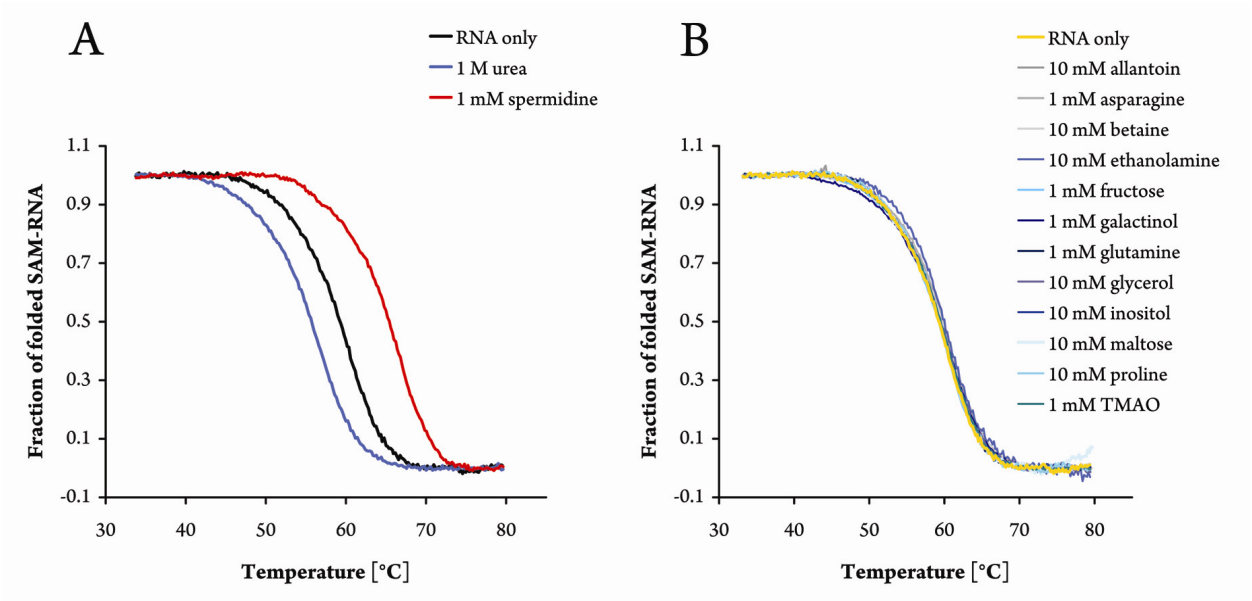

Figure 15. Thermal melting of a 29mer hairpin RNA (SAM) in the presence of different metabolites. At the melting temperature (T_m), the fraction of folded RNA is 0.5. **(A)** Spermidine and urea were used as positive controls: 1 mM spermidine increases the T_m by 6.2 °C and 1 M urea decreases the T_m by 3.4 °C. The shape of the melting transition remains unaltered. **(B)** At approximated physiological concentrations of metabolites, neither the T_m nor the shape of the melting transition of SAM is altered.

The lack of effect is also true for metabolites for which a stabilizing or destabilizing effect has previously been published. This may be explained by the fact that previous studies were carried out with very high metabolite concentrations. Lambert and Draper (2007) published a weak destabilizing effect of urea, proline, glycine betaine, glycerol and TMAO on a small hairpin shown in figure 14. However, the ΔG only changed by a factor of 0.08 kcal mol^{-1} to 0.57 kcal mol^{-1} per molal of metabolite. The experimental setup of melting studies presented here is not able to resolve effects that small.

The effects of different osmolytes such as glycine betaine and urea on the DNA stability can be influenced by the presence of monovalent salts in high concentrations. However, the salt dependence of osmolyte-DNA interactions is small (Lambert and Draper 2007). Therefore, a detrimental influence of the used sodium concentration can be excluded.

3. 1. 3. Testing Metabolites for their Ability to Enhance Annealing and Strand-Displacement.

A FRET-based assay developed by Rajkowitsch & Schroeder (2007) monitors the annealing and strand-displacement of short oligonucleotides in a fast and simple approach. Two fluorescently labeled short RNA oligonucleotides are annealed in the presence or absence of small metabolites (phase I). After 3 minutes, a competitor-strand is added which starts the strand-displacement reaction (phase II). Annealing increases the FRET index whereas strand-displacement decreases it. It has to be considered that the FRET signal from phase II also includes residual annealing from phase I. These measurements allowed the calculation of the observed rate-constant (k_{obs}) which is a measure of the velocity of the reaction.
All measurements were carried out at least twice in quadruplicates for four different metabolite concentrations ranging from 400 nM to higher than 5 mM. The concentration of 400 nM was chosen as the lower limit because at this concentration, the number of small metabolite molecules equals the number of backbone-phosphates for both RNA substrates studied. The upper limit varied depending on the solubility of the metabolite in water as specified by the manufacturer.

3. 1. 3. 1. Neither Destabilization nor a Positive Charge is Sufficient to Promote Strand-Displacement

Screen of individual metabolites
The screen was carried out with two RNA substrates, namely 21R and JM1. Both substrates are 5' fluorescently labeled (Cy5-21R$^+$ and Cy3-21R$^-$; Cy5-J1$^+$ and Cy3-M1$^-$) and are able to form a fully complementary 21mer duplex. 21R has a higher thermodynamic stability due to a higher G:C content of 38 % compared to only 5 % in JM1. All single-strands were specifically designed such that they do not form secondary structures at the reaction temperature of 30 °C. Therefore, phase I does not involve the unwinding of any secondary structures. In the absence of enhancers (RNA only), JM1 anneals slightly faster than 21R (table 6).

Table 6. Rate constants (k_{obs}) for the annealing and strand-displacement for two RNA substrates, JM1 and 21R, in the presence and absence of small metabolites as determined with a FRET-based assay. The deviation is presented as 2 x standard error of mean. nd, not determined. -, no activity.

	annealing (k_{obs} ($M^{-1}sec^{-1}$))		strand-displacement (k_{obs} ($M^{-1}sec^{-1}$))	
	JM1	21R	JM1	21R
RNA only	$2.3 \cdot 10^5 \pm 1.5 \cdot 10^4$	$1.9 \cdot 10^5 \pm 1.5 \cdot 10^4$	-	-
500 µM CTAB	$6.3 \cdot 10^6 \pm 1.4 \cdot 10^6$	$3.9 \cdot 10^6 \pm 8.0 \cdot 10^5$	$1.9 \cdot 10^6 \pm 1.2 \cdot 10^5$	$1.6 \cdot 10^6 \pm 1.0 \cdot 10^5$
100 µM spermidine	$1.3 \cdot 10^5 \pm 2.9 \cdot 10^4$	nd	-	-
1 mM spermidine	$2.8 \cdot 10^5 \pm 3.6 \cdot 10^4$	nd	-	-
10 mM spermidine	$7.0 \cdot 10^5 \pm 3.9 \cdot 10^4$	nd	-	-

Cetyltrimethylammonium bromide (CTAB) was used as a positive control for the strand-displacement reaction. In the combined assay, CTAB mediated rate constants vary considerably in phase I (annealing), whereas they are comparable to each other in phase II (strand-displacement). Annealing rate constants are in good agreement with previously published results (table 6). The slightly higher CTAB-mediated annealing rate presented by Nedbal et al. (1997) may be a result from the higher reaction temperature (37 °C). CTAB mediated strand-displacement of JM1 and 21R is more than 2000-fold more efficient than the strand-displacement between a 56 bp duplex and 645 nt competing RNA studied by Homann et al. (1996). The RNA substrate and factors such as the concentration of competitor RNA and the experimental set-up may strongly influence the velocity of the strand-displacement reaction. However, the exact reason for this discrepancy remains a matter of speculation.

CTAB shows slightly slower kinetics in a FRET-based strand-displacement assay with pre-annealed duplexes (data not shown) compared to the combined assay. This may be due to a higher concentration of competitor molecules in the combined assay because annealing is not completed at the end of phase I.

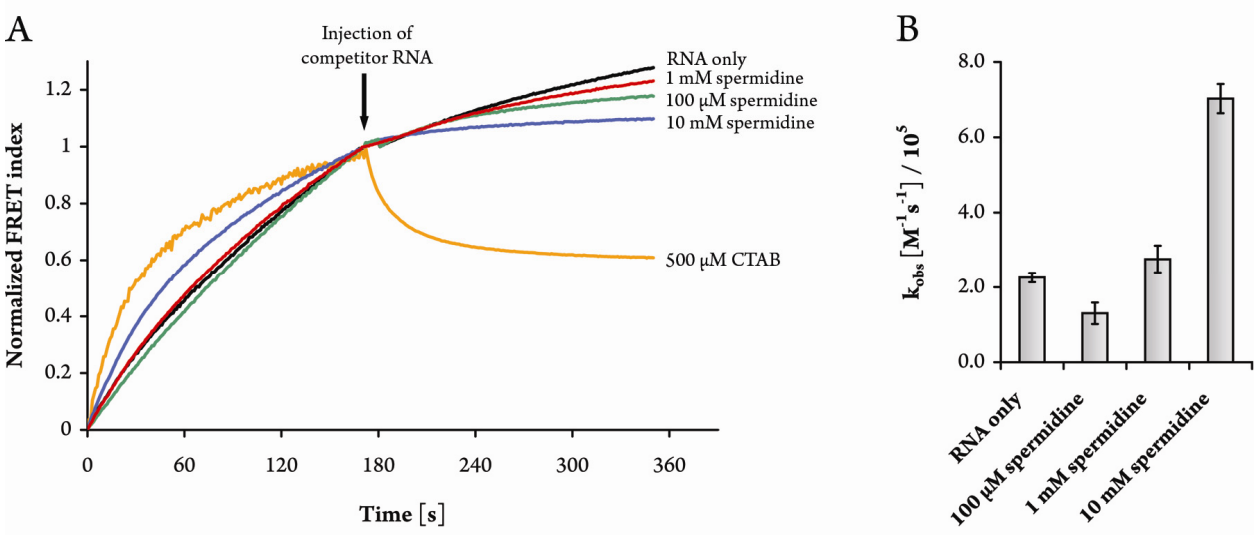

Figure 16. Spermidine enhances the annealing of JM1 RNA but does not promote strand-displacement. **(A)** Representation of data from the FRET-based annealing and strand-displacement assay. The FRET index (Cy5 signal / Cy3 signal) was normalized to 1 for clarity. Annealing is monitored in the first 180 seconds (phase I), the injection of competitor RNA starts the strand-displacement reaction (phase II). CTAB was used as a positive control for the strand-displacement reaction. **(B)** 10 mM spermidine enhances the annealing of JM1 RNA about 3-fold. 100 µM and 1 mM spermidine do not significantly alter or even slightly decrease the annealing rate constant. Error bars represent 2 x standard error of mean.

10 mM spermidine enhances the annealing of JM1 2 – 3-fold (table 6, figure 16). At lower concentrations of spermidine (100 µM and 1 mM), the annealing rate constant is unaltered or even seems to be slightly decreased compared to RNA only (figure 16). Interestingly, 1 mM spermidine effectively stabilizes the double-strand as shown in the UV-melting study (see 3. 1. 2.). Spermidine-mediated annealing enhancement is rather small considering that a 10^6-fold molar excess of metabolite to RNA is needed. In contrast, the 18 amino acid long basic peptide Tat(44-61) derived from the HIV-1 Tat protein accelerates annealing of the 21R duplex 7 – 8-fold at an only 15-fold molar excess in the same assay (Doetsch et al. 2011). This difference is unlikely due to a varying base-pair composition of the two RNA substrates since amines primarily interact with the sugar-phosphate backbone of RNA (Quigley et al. 1978). None of the other metabolites carrying a positive charge examined in this study such as amino acids, glycine betaine or TMAO show any effect on the annealing reaction. This may be explained by entropic effects upon RNA-metabolite interaction. Doetsch et. al. (2011) showed that the annealing-enhancement of Tat(44-61) is accompanied by a favourable

entropy term that may result from ion and water release upon peptide binding. Annealing enhancement is proposed to be a result from this favourable entropy and the conversion of the RNA strand into an annealing-competent conformation. A favourable entropy term was also shown for CTAB-mediated annealing enhancement (Nedbal et al. 1997). The replacement of one salt ion with a monovalent metabolite may leave the net-entropy unaltered. Spermidine carries three positive charges instead and more ions have to be released upon spermidine binding. This results in a favourable entropy term. The same may be true for CTAB assuming that CTAB forms aggregates by hydrophobic interactions of the alkane-tails as suggested by Nedbal et al. (1997).

Neither spermidine nor any other metabolite (data not shown) was found to enhance strand-exchange of 21R and JM1 at any concentration. Noteworthy, metabolites such as proline, glycine betaine and TMAO were shown to have a destabilizing effect on secondary structures at high metabolite-concentrations and in addition carry a positively charged group. Nevertheless, even at a 100 mM concentration of metabolite, no strand-displacement was detectable. It has to be considered, that the time frame of the measurement is short. In a later experiment, it was shown that strand-displacement between 21R and a competitor does occur at similar conditions over a time span of 30 minutes in the absence of enhancing metabolites (see section 3. 2. 2.). Such a small effect cannot be visualized in this assay due to a restricted time-span of the measurement and due to residual annealing of phase I. To exclude the possibility that the effect is covered by residual annealing, all metabolites were in addition tested in a FRET-based strand-displacement assay with a pre-annealed 21R double-strand (data not shown). Also in this assay, no cold-induced metabolite was found to be able to promote strand-displacement.

Screen of metabolite groups

Another possible explanation for the lack of activity is that the effect of one metabolite may not be sufficient to promote strand-displacement. This is in line with the finding that urea is unable to promote strand-exchange in the same assay even at concentrations that significantly destabilize secondary structures (Boris Fürtig, personal communication). For that reason, previously tested metabolites were combined and tested in groups. Metabolites containing the same functional group or metabolites predicted to have the same effect on RNA structural stability were combined to test for additive effects (table 7). However, most metabolites carry two or more functional

groups. This renders also cooperative effects possible. The metabolite groups contained equimolar concentrations of all metabolites.

None of the metabolite groups are able to enhance the annealing or strand-displacement of the JM1 substrate at any of the tested concentrations. Also metabolite groups consisting of RNA denaturants like glycine betaine, TMAO or proline in combination with metabolites that carry a positive charge were not able to do so. Since the destabilization of helices and the neutralization of the charge repulsion are not sufficient, it is likely that an additional functionality is crucial for the process of strand-displacement.

Table 7. Individual cold-shock metabolites were not able to promote annealing or strand-displacement of the 21R and the JM1 substrate. In order to test whether additive or cooperative effects of different metabolites are required for this activity, cold-shock metabolites were combined to arbitrary groups of metabolites that share common features and were tested for their ability to enhance the annealing or strand-displacement of the JM1 substrate. Since many metabolites carry more than one functional group, the grouping covers additive and cooperative effects. The points indicate that the respective metabolite was part of the group. (1) Two major cold-shock metabolites. (2) Amino acids. (3) Metabolites with a previously shown destabilizing effect on RNA secondary structure. (4) Metabolites that carry a COOH functional group. (5) Arbitrary group (6) Metabolites that carry an amino-group. (7) All metabolites that carry an OH group.

GROUP	ALLANTOIN	ASPARAGINE	GLYCINE BETAINE	ETHANOLAMINE	FRUCTOSE	GALACTINOL	GLUAMINE	GLYCEROL	*MYO*-INOSITOL	MALTOSE	PROLINE	RAFFINOSE	SUCROSE	TMAO
1						●					●			
2		●					●				●			
3			●								●		●	●
4		●					●				●			●
5				●			●	●		●	●	●		
6	●	●	●	●			●				●			●
7		●		●	●	●	●	●	●	●	●	●	●	

3. 2. CELL-EXTRACTS FROM COLD-SHOCK TREATED CELLS

In previous experiments, metabolites were grouped in order to cover additive or cooperative effects. To approximate physiological metabolite concentrations and combinations, polar metabolite extracts were produced from *Chlamydomonas reinhardtii* cells as previously described by Weckwerth et al. (2008). The metabolite profile of this monocellular alga changes drastically during cold-shock (figure 9) (Weckwerth laboratory, unpublished data, personal communication).
All experimental cultures were grown at 20 °C up to an OD_{750} = 1. Afterwards, cultures were incubated at 7 °C for 48 hours. Control cultures remained at 20 °C. Samples for metabolite extraction were drawn at 6 hours (CSE6) and at 48 hours (CSE48) after cold-induction. Kaplan et al. (2004) showed that *Arabidopsis* plants gain an enhanced freezing tolerance as early as 6 hours after cold-induction that proceeds to 96 hours after cold-induction. After the metabolite extraction procedure, the metabolite pellet was resuspended in the amount of water which was estimated to be the total cell volume of cells used for extraction in order to approximate cellular metabolite concentrations. It was not possible to avoid the presence of pigments within the polar cell extract without diminishing the quality of the extract. Since all extracts showed a high absorbance at the wavelength used for FRET measurements, a FRET-based assay could not be applied. A trans-splicing assay as well as strand-displacement gels were carried out instead.

3. 2. 1. Trans-Splicing is Equally Efficient in Cold-Shock Extracts and in Controls

To test the metabolite-extracts for their RNA chaperone activity, their ability to enhance the splicing reaction of a splicing-retarded group I intron was tested (Galloway Salvo et al. 1990; Coetzee et al. 1994) (figure 17). At a 0.5-fold estimated cellular concentration, no splicing is detectable in CSE6 or in extracts of control cells. The increase of the $MgCl_2$ concentration from 3 mM to 30 mM restores some of the splicing activity of the reaction in metabolite extracts. However, the reaction is still more efficient in the absence of small metabolites. It was considered that the metabolite extracts may inhibit splicing by destabilizing the intron too efficiently as it was previously shown for StpA on mutant group I introns (Grossberger et al. 2005). However, decreasing the reaction

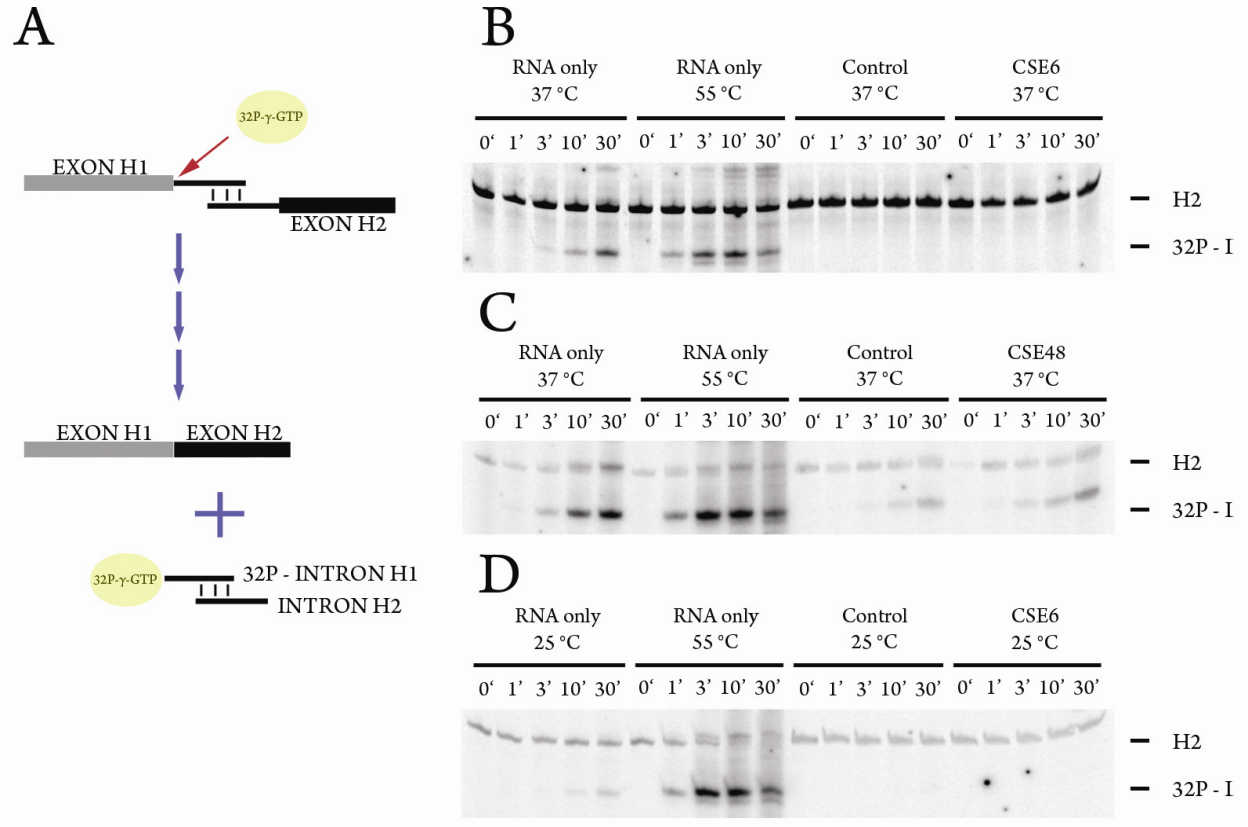

Figure 17. *In vitro trans*-splicing in the presence and absence of 0.5-fold the estimated cellular concentration of polar metabolite extracts of *Chlamydomonas reinhardtii* cells. The cells were cold-induced by lowering the temperature to 7 °C. Cell extracts of cells that were not cold-induced were used as controls. Trans-splicing is inefficient at 37 °C (negative control) but is enhanced at 55 °C (positive control) and in the presence of RNA chaperones. **(A)** Schematic representation of the splicing reaction. The *in vitro* transcribed RNA fragments H1 and H2 associate *in trans*. The addition of radiolabeled GTP as a splicing cofactor starts the reaction that results in the exclusion of the intron sequence. The intron is released with GTP covalently joined to its 5'end.
(B – D) The upper band corresponds to ^{35}S body labeled H2 RNA, the lower band to the H1 intron splice product with ^{32}P-γ-GTP covalently joined to its 5'end. **(B)** Splicing in 3 mM $MgCl_2$ in the presence of CSE6. The splicing activity in both extracts is below the detection limit. **(C)** The $MgCl_2$ concentration was increased to 30 mM. The increase restores some splicing activity in the control extract, in the cell extract of cold-shock treated cells 48 hours after cold-induction (CSE48) as well as in CSE6 (data not shown). Splicing is equally efficient in cold-shock extracts and control extracts and in both cases lower than splicing in the absence of extracts. **(D)** To increase the thermodynamic stability of the intron, the reaction temperature was lowered to 25 °C for the reaction in 30 mM $MgCl_2$. The splicing activity in both extracts is below the detection limit.

temperature to 25 °C (in order to counteract a too strong destabilizing effect) further inhibits the splicing reaction. Decreasing the concentration of the metabolite extract under the same experimental conditions again restores some of the splicing activity (figure 18). However, the reaction does not reach the activity of the intron in the absence of metabolites in any case. Therefore, the increased activity in higher Mg^{2+}

concentrations may not result from an Mg^{2+}-induced stabilization. Contrarily, higher Mg^{2+} concentrations seem to compensate for a reduced availability of Mg^{2+} in the presence of the metabolite extract. The reason for the low observed splicing-rate may be the presence of GTP in polar metabolite cell-extracts. Radiolabeled GTP is added to the splicing reaction as a splicing cofactor and marker. Additional unlabeled GTP would result in weaker bands due to unlabeled splicing products. Therefore, from these results it cannot be concluded that the metabolite extracts inhibit the splicing reaction.

Regardless of the overall splicing rate in metabolite extracts, the efficiency of splicing in the cold-shock extract always equalled the one in the control extract. Therefore, the splicing reaction is not enhanced in cold-shock extracts as compared to the control extract.

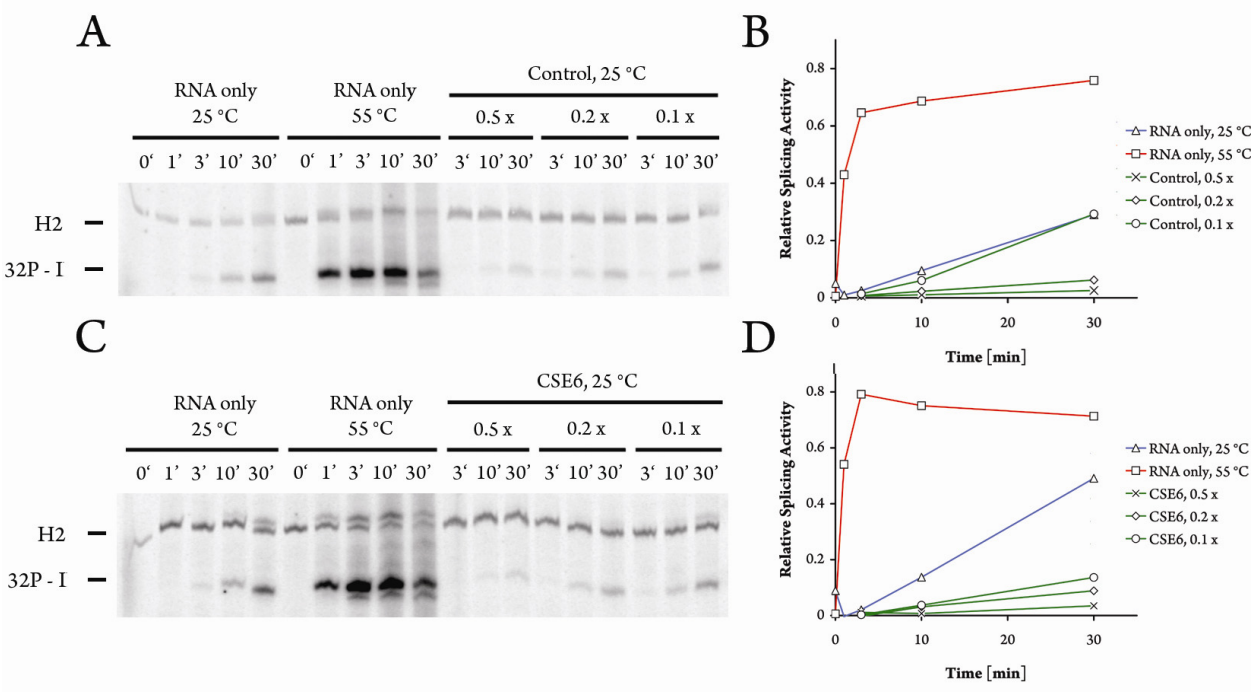

Figure 18. *In vitro trans*-splicing in the presence of decreasing concentrations of polar metabolite extracts of *Chlamydomonas reinhardtii* cells. A decrease in the concentration of the polar metabolite extract restores some splicing activity. **(A and C)** Splicing in the presence of 0.5-fold, 0.2-fold and 0.1-fold the estimated cellular concentration of the control extract and CSE6 in 30 mM $MgCl_2$ at 25 °C. 32P-I: H1 intron splice-product with ^{32}P-γ-GTP covalently joined to its 5'end. **(B and D)** The bands were quantified with ImageQuant®. The relative splicing activity is the ratio between the intensity of the splicing product (32P-I) and the combined intensities of the fragments H1 and H2 and the splicing product. The splicing activity increases with decreasing concentration of the extract but remains lower than the negative control. The ratio between the splicing activity in extracts and in RNA only samples at 37 °C is the same for control extracts and cold-shock extracts except for 0.1 x the control-extract.

3. 2. 2. Polar Metabolite-Extracts Enhance the Strand-Exchange Reaction

The ability of polar metabolite extracts to enhance the exchange between a 21R duplex and a 32mer competitor RNA with full complementarity was examined. Interestingly, the strand-displacement reaction is efficient in the absence of metabolites under experimental conditions (figure 19). After 30 minutes at 37 °C, 54 % ± 4 % of strands are present in a duplex with the 32mer competitor RNA. However, no strand-displacement between the same double-strand and a similar competing RNA ($21R^-$) can be detected in the FRET-based annealing and strand-displacement assay at similar buffer conditions. This can be attributed to the much smaller time-frame of the measurements as well as to the lower concentration of competitor used in the FRET-based assay.

At a 0.5-fold estimated cellular metabolite concentration, the fraction of the displaced strand increases to 66 % for the control extract and to 72 % for CSE6 (figure 19). Interestingly, CSE6 also enhances the strand-exchange reaction to a similar extent at a 0.15-fold metabolite concentration, whereas the strand-exchange was slightly inhibited at this concentration in the control extract. This has only been tested once for two biological replicates each. These results indicate that the change of the metabolite profile in the cell can have an influence on the folding reaction *in vitro*. However, a difference is seen only at a fraction of the estimated cellular concentration. Whether this is of biological relevance still has to be elucidated.

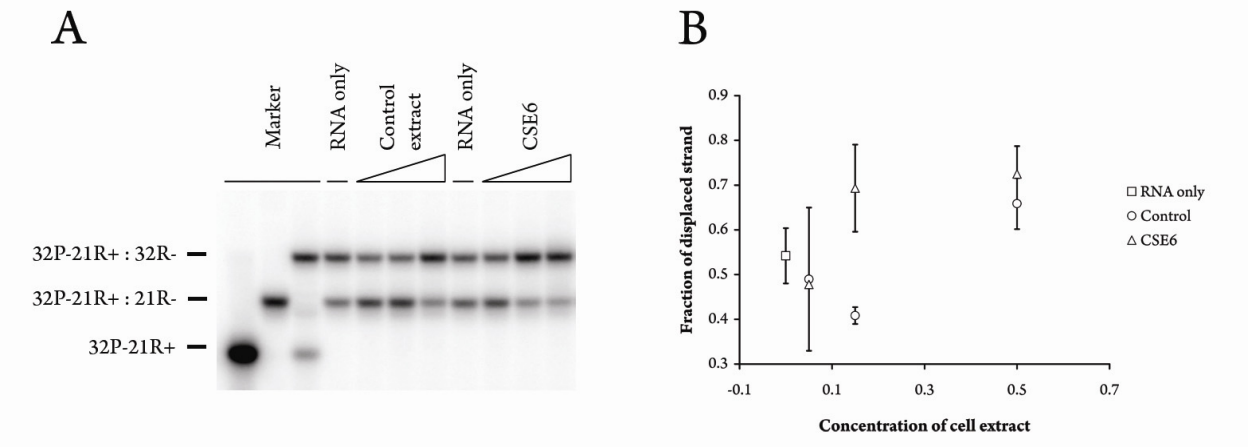

Figure 19. Strand-displacement between a 21R duplex RNA ($^{32}P\text{-}21R^+$:$21R^-$) and a 32mer fully complementary competitor RNA. **(A)** The RNA was incubated for 30 min at 37 °C in the absence (RNA only) or in the presence of increasing concentrations (0.05 x, 1.5 x, 0.5 x) of polar metabolite extracts from *Chlamydomonas reinhardtii*. Control extract: extract from cells without cold-treatment. **(B)** Quantification with ImageQuant®. After 30 minutes, about 55 %

of the strands are displaced in the absence of metabolites. Cold-shock extracts and control extracts enhance the strand-displacement reaction at a 0.5-fold estimated cellular concentration to 72 % and 66 %, respectively. In CSE6, also 0.15 x the estimated cellular concentration enhance the reaction to a similar extent whereas the reaction is slower at this concentration in the control extract compared to RNA only. Error bars represent 2 x standard error of mean.

3. 3. DEVELOPMENT OF A PROTEIN PURIFICATION STRATEGY FOR GRP7

The concentration of the small metabolites glutamine and proline was shown to increase upon cold-shock in *Arabidopsis thaliana* (Wienkoop et al. 2008). In the study presented here, the two metabolites were shown not to be sufficient to promote strand-displacement in the FRET-based annealing and strand-displacement assay. Interestingly, the concentrations of glutamine and proline correlate with the one of protein GRP7 (At2g21660) during the cold-shock response in *Arabidopsis thaliana* (Wienkoop et al. 2008). GRP7 was suggested to act as an RNA chaperone due to its ability to complement a cold-sensitive *E. coli* phenotype as well as its ability to increase the susceptibility of RNA to RNAse T_1 cleavage. The protein also has a DNA melting activity (Kim et al. 2007). However, an RNA strand-exchange activity was not explicitly shown so far. For future experiments, it would be of interest to verify the RNA chaperone activity of GRP7 in the FRET-based annealing and strand-displacement assay discussed earlier. This assay can also be used to study the activity of the protein in the presence of glutamine and proline.

Protein GRP7 was overexpressed in *E.coli* strain *ER2566* and purified without a tag using the IMPACT™ TWIN system. Two other proteins were considered possible candidates to act as RNA chaperones, namely At2g37220 and At3g53460. Both proteins contain at least one RRM as well as a glycine-rich region and are strongly induced upon cold-shock (Wienkoop et al. 2008). The proteins could not be purified. The on-column cleavage reaction of the *CBD-intein-At37220* fusion protein was not successful for all conditions tested. For the protein At3g53460, different cDNAs did not result in a clone with a 100 % identity to one of the published sequences.

4. CONCLUSION

The ability of cold-shock metabolites are able to act as RNA chaperones was investigated. Individual cold-shock metabolites as well as metabolite combinations were tested in a FRET-based annealing and strand-displacement assay. The metabolites were shown not to fulfill the requirements to enhance annealing or strand-displacement at any concentration (400 nM – 100 mM) or in any combination studied. Neither a destabilizing effect of metabolites nor positive functional groups neutralizing the charge repulsion between strands nor both is sufficient. This indicates that a further function is needed for the process of strand-displacement. It is possible that strand-exchange is not achieved by a competitor strand catching a single-strand of a partially opened helix but rather by the formation of another ternary complex. Such a ternary complex may be a triple helix. The formation of triple helices is usually dependent on helical regions where the regular A-form geometry is perturbed by mismatches. Factors that induce such a perturbation may favour strand-exchange. This idea is supported by the finding that CspE loses its nucleic acid melting activity when the intercalating amino-acids of the interacting surface are removed (Phadtare et al. 2002). Moreover, tetramethylammonium chloride, a metabolite that is equal to the head-group of CTAB, was shown to induce structural changes in DNA (Marky et al. 1981). CTAB effectively enhances annealing and strand-displacement. It may be worth testing whether metabolites that enhance annealing are able to promote strand-displacement of JM1 in combination with metabolites that perturb the helical geometry or of an RNA substrate containing mismatched bases.

Spermidine is able to enhance the annealing but not the stand-displacement reaction. Interaction of spermidine with the RNA backbone may result in a favourable entropy upon ion release and the convert the RNA into an annealing-competent conformation as was hypothesized for the annealing enhancement by the basic peptide Tat(44-61) (Doetsch et al. 2011).

Thermal melting studies were carried out in order to examine the effects of approximately physiological concentrations of cold-shock metabolites on RNA structural stability. The melting temperature as well as the shape of the melting transition of a small hairpin RNA is unaltered in the presence of cold-shock metabolites.

In order to approximate physiological combinations of metabolites, polar metabolite extracts of *Chlamydomonas reinhardtii* cells were prepared and it was tested whether the extracts are able to promote the functional fold of a splicing-retarded group I intron as well as to enhance strand-exchange. *Trans*-splicing is equally efficient in cold-shock extracts as in non-cold-shock extracts. In general, the assay was found to be not suited to test polar metabolite cell extracts, most likely due to remaining GTP in the extract. Strand-exchange was monitored between a 21R duplex and a fully complementary 32mer competitor strand. Metabolite extracts of cold-shock treated cells as well as control-extracts were able to enhance the strand-displacement reaction at a 0.5-fold estimated cellular concentration. At lower concentrations, the cold-shock extract but not the non-cold-shock extract is able to do so.

A protein purification protocol for a tag-free protein GRP7 was developed. GRP7 is a proposed RNA-chaperone that is upregulated upon cold-stress in *Arabidopsis thaliana*. During the cold adaption process, the concentration of GRP7 correlates with the cold-shock metabolites proline and glutamine (Wienkoop et al. 2008). In future experiments it would be worth to verify the RNA chaperone activity of GRP7 in the FRET-based annealing and strand-displacement assay as well as to study its activity in combination with the cold-shock metabolites proline and glutamine.

In conclusion, cold-shock metabolites were not found to influence RNA folding. However, the change in the metabolite profile upon cold-shock can have an influence on RNA *in vitro* as shown in the strand-displacement assay. Whether this influence is of biological relevance cannot be concluded.

5. REFERENCES

Atienza SG, Faccioli P, Perrotta G, Dalfino G, Zschiesche W, Humbeck K, Stanca AM, Cattivelli L. 2004. Large scale analysis of transcripts abundance in barley subjected to several single and combined abiotic stress conditions. *Plant Science* **167**(6): 1359-1365.

Barone G, DelVecchio P, Esposito D, Fessas D, Graziano G. 1996. Effect of osmoregulatory solutes on the thermal stability of calf-thymus DNA. *Journal of the Chemical Society-Faraday Transactions* **92**(8): 1361-1367.

Bolen DW, Baskakov IV. 2001. The osmophobic effect: Natural selection of a thermodynamic force in protein folding. *Journal of Molecular Biology* **310**(5): 955-963.

Bradford MM. 1976. A rapid and sensitive method for the quantitation of microgram quantities of protein utilizing the principle of protein-dye binding. *Anal Biochem* **72**: 248-254.

Brigotti M, Petronini PG, Carnicelli D, Alfieri RR, Bonelli MA, Borghetti AF, Wheeler KP. 2003. Effects of osmolarity, ions and compatible osmolytes on cell-free protein synthesis. *Biochemical Journal* **369**: 369-374.

Brion P, Westhof E. 1997. Hierarchy and dynamics of RNA folding. *Annu Rev Biophys Biomol Struct* **26**: 113-137.

Capp MW, Pegram LM, Saecker RM, Kratz M, Riccardi D, Wendorff T, Cannon JG, Record MT. 2009. Interactions of the Osmolyte Glycine Betaine with Molecular Surfaces in Water: Thermodynamics, Structural Interpretation, and Prediction of m-Values. *Biochemistry* **48**(43): 10372-10379.

Cate JH, Gooding AR, Podell E, Zhou K, Golden BL, Kundrot CE, Cech TR, Doudna JA. 1996. Crystal structure of a group I ribozyme domain: principles of RNA packing. *Science* **273**(5282): 1678-1685.

Chen SJ. 2008. RNA folding: Conformational statistics, folding kinetics, and ion electrostatics. *Annual Review of Biophysics* **37**: 197-214.

Chen WP, Li PH. 2002. *Attenuation of reactive oxygen production during chilling in ABA-treated maize.cultured cells*. Kluwer Academic/Plenum Publ, New York.

Coetzee T, Herschlag D, Belfort M. 1994. Escherichia coli proteins, including ribosomal protein S12, facilitate in vitro splicing of phage T4 introns by acting as RNA chaperones. *Genes Dev* **8**(13): 1575-1588.

Cook D, Fowler S, Fiehn O, Thomashow MF. 2004. A prominent role for the CBF cold response pathway in configuring the low-temperature metabolome of Arabidopsis. *Proceedings of the National Academy of Sciences of the United States of America* **101**(42): 15243-15248.

Costa M, Michel F. 1995. Frequent use of the same tertiary motif by self-folding RNAs. *EMBO J* **14**(6): 1276-1285.

Cristofari G, Darlix JL. 2002. The ubiquitous nature of RNA chaperone proteins. In *Progress in Nucleic Acid Research and Molecular Biology, Vol 72*, Vol 72, pp. 223-268. Academic Press Inc, San Diego.

Crothers DM, Cole PE, Hilbers CW, Shulman RG. 1974. The molecular mechanism of thermal unfolding of Escherichia coli formylmethionine transfer RNA. *J Mol Biol* **87**(1): 63-88.

Doetsch M, Fürtig B, Gstrein T, Stampfl S, Schroeder R. 2011. The RNA annealing mechanism of the HIV-1 Tat peptide: conversion of the RNA into an annealing-competent conformation. *Nucleic Acids Res*.

Draper DE. 2008. RNA Folding: Thermodynamic and Molecular Descriptions of the Roles of Ions. *Biophysical Journal* **95**(12): 5489-5495.

Dyson HJ, Wright PE. 2005. Intrinsically unstructured proteins and their functions. *Nature Reviews Molecular Cell Biology* **6**(3): 197-208.

Ferré-D'Amaré AR, Zhou K, Doudna JA. 1998. Crystal structure of a hepatitis delta virus ribozyme. *Nature* **395**(6702): 567-574.

Fowler S, Thomashow MF. 2002. Arabidopsis transcriptome profiling indicates that multiple regulatory pathways are activated during cold acclimation in addition to the CBF cold response pathway. *Plant Cell* **14**(8): 1675-1690.

Freier SM, Kierzek R, Jaeger JA, Sugimoto N, Caruthers MH, Neilson T, Turner DH. 1986. Improved free-energy parameters for predictions of RNA duplex stability. *Proc Natl Acad Sci U S A* **83**(24): 9373-9377.

Fuertig B, Wenter P, Reymond L, Richter C, Pitsch S, Schwalbe H. 2007. Conformational dynamics of bistable RNAs studied by time-resolved NMR spectroscopy. *Journal of the American Chemical Society* **129**(51): 16222-16229.

Furtig B, Wenter P, Pitsch S, Schwalbe H. 2010. Probing Mechanism and Transition State of RNA Refolding. *Acs Chemical Biology* **5**(8): 753-765.

Galloway Salvo JL, Coetzee T, Belfort M. 1990. Deletion-tolerance and trans-splicing of the bacteriophage T4 td intron. Analysis of the P6-L6a region. *J Mol Biol* **211**(3): 537-549.

Garg AK, Kim JK, Owens TG, Ranwala AP, Do Choi Y, Kochian LV, Wu RJ. 2002. Trehalose accumulation in rice plants confers high tolerance levels to different abiotic stresses. *Proceedings of the National Academy of Sciences of the United States of America* **99**(25): 15898-15903.

Gautheret D, Konings D, Gutell RR. 1994. A major family of motifs involving G.A mismatches in ribosomal RNA. *J Mol Biol* **242**(1): 1-8.

Giuliodori AM, Di Pietro F, Marzi S, Masquida B, Wagner R, Romby P, Gualerzi CO, Pon CL. 2010. The cspA mRNA Is a Thermosensor that Modulates Translation of the Cold-Shock Protein CspA. *Molecular Cell* **37**(1): 21-33.

Granot J, Kearns DR. 1982. Interactions of DNA with divalent metal ions. II. Proton relaxation enhancement studies. *Biopolymers* **21**(1): 203-218.

Graumann PL, Marahiel MA. 1998. A superfamily of proteins that contain the cold-shock domain. *Trends in Biochemical Sciences* **23**(8): 286-290.

Grossberger R, Mayer O, Waldsich C, Semrad K, Urschitz S, Schroeder R. 2005. Influence of RNA structural stability on the RNA chaperone activity of the Escherichia coli protein StpA. *Nucleic Acids Research* **33**(7): 2280-2289.

Guy C, Kaplan F, Kopka J, Selbig J, Hincha DK. 2008. Metabolomics of temperature stress. *Physiologia Plantarum* **132**(2): 220-235.

Hannah MA, Wiese D, Freund S, Fiehn O, Heyer AG, Hincha DK. 2006. Natural genetic variation of freezing tolerance in arabidopsis. *Plant Physiology* **142**(1): 98-112.

Hawkins ER, Chang SH, Mattice WL. 1977. Kinetics of the renaturation of yeast tRNA3 leu. *Biopolymers* **16**(7): 1557-1566.

Heilman-Miller SL, Pan J, Thirumalai D, Woodson SA. 2001a. Role of counterion condensation in folding of the Tetrahymena ribozyme. II. Counterion-dependence of folding kinetics. *J Mol Biol* **309**(1): 57-68.

Heilman-Miller SL, Thirumalai D, Woodson SA. 2001b. Role of counterion condensation in folding of the Tetrahymena ribozyme. I. Equilibrium stabilization by cations. *J Mol Biol* **306**(5): 1157-1166.

Hermann T, Patel DJ. 1999. Stitching together RNA tertiary architectures. *J Mol Biol* **294**(4): 829-849.

Herschlag D. 1995. RNA chaperones and the RNA folding problem. *J Biol Chem* **270**(36): 20871-20874.

Hilbers CW, Robillard GT, Shulamn RG, Blake RD, Webb PK, Fresco R, Riesner D. 1976. Thermal unfolding of yeast glycine transfer RNA. *Biochemistry* **15**(9): 1874-1882.

Holmes DS, Quigley M. 1981. A rapid boiling method for the preparation of bacterial plasmids. *Anal Biochem* **114**(1): 193-197.

Homann M, Nedbal W, Sczakiel G. 1996. Dissociation of long-chain duplex RNA can occur via strand displacement in vitro: Biological implications. *Nucleic Acids Research* **24**(22): 4395-4400.

Hong J, Capp MW, Anderson CF, Saecker RM, Felitsky DJ, Anderson MW, Record MT. 2004. Preferential interactions of glycine betaine and of urea with DNA: Implications for DNA hydration and for effects of these solutes on DNA stability. *Biochemistry* **43**(46): 14744-14758.

Jackson SA, Koduvayur S, Woodson SA. 2006. Self-splicing of a group I intron reveals partitioning of native and misfolded RNA populations in yeast. *RNA* **12**(12): 2149-2159.

Janska A, Marsik P, Zelenkova S, Ovesna J. 2010. Cold stress and acclimation - what is important for metabolic adjustment? *Plant Biology* **12**(3): 395-405.

Kaplan F, Kopka J, Haskell DW, Zhao W, Schiller KC, Gatzke N, Sung DY, Guy CL. 2004. Exploring the temperature-stress metabolome of Arabidopsis. *Plant Physiology* **136**(4): 4159-4168.

Kaplan F, Kopka J, Sung DY, Zhao W, Popp M, Porat R, Guy CL. 2007. Transcript and metabolite profiling during cold acclimation of Arabidopsis reveals an intricate relationship of cold-regulated gene expression with modifications in metabolite content. *Plant Journal* **50**(6): 967-981.

Kaplan F, Sung DY, Guy CL. 2006. Roles of beta-amylase and starch breakdown during temperatures stress. *Physiologia Plantarum* **126**(1): 120-128.

Kim JS, Park SJ, Kwak KJ, Kim YO, Kim JY, Song J, Jang B, Jung CH, Kang H. 2007. Cold shock domain proteins and glycine-rich RNA-binding proteins from Arabidopsis thaliana can promote the cold adaptation process in Escherichia coli. *Nucleic Acids Research* **35**(2): 506-516.

Kim YO, Kim JS, Kang H. 2005. Cold-inducible zinc finger-containing glycine-rich RNA-binding protein contributes to the enhancement of freezing tolerance in Arabidopsis thaliana. *Plant Journal* **42**(6): 890-900.

Klein DJ, Moore PB, Steitz TA. 2004. The contribution of metal ions to the structural stability of the large ribosomal subunit. *Rna-a Publication of the Rna Society* **10**(9): 1366-1379.

Klump H, Burkart W. 1977. Calorimetric measurements of the transition enthalpy of DNA in aqueous urea solutions. *Biochim Biophys Acta* **475**(4): 601-604.

Koculi E, Lee NK, Thirumalai D, Woodson SA. 2004. Folding of the Tetrahymena ribozyme by polyamines: Importance of counterion valence and size. *Journal of Molecular Biology* **341**(1): 27-36.

Korn M, Peterek S, Mock HP, Heyer AG, Hincha DK. 2008. Heterosis in the freezing tolerance, and sugar and flavonoid contents of crosses between Arabidopsis thaliana accessions of widely varying freezing tolerance. *Plant Cell and Environment* **31**(6): 813-827.

Kusama-Eguchi K, Watanabe S, Irisawa M, Watanabe K, Igarashi K. 1991. Correlation between spermine stimulation of rat liver Ile-tRNA formation and structural change of the acceptor stem by spermine. *Biochem Biophys Res Commun* **177**(2): 745-750.

Lambert D, Draper DE. 2007. Effects of osmolytes on RNA secondary and tertiary structure stabilities and RNA-Mg2+ interactions. *Journal of Molecular Biology* **370**(5): 993-1005.

Lambert D, Leipply D, Draper DE. 2010. The Osmolyte TMAO Stabilizes Native RNA Tertiary Structures in the Absence of Mg2+: Evidence for a Large Barrier to Folding from Phosphate Dehydration. *Journal of Molecular Biology* **404**(1): 138-157.

Leipply D, Lambert D, Draper DE. 2009. Ion-RNA interactions thermodynamic analysis of the effects of mono- and divalent ions on RNA conformational equilibria. *Methods Enzymol* **469**: 433-463.

Lescoute A, Westhof E. 2006. The interaction networks of structured RNAs. *Nucleic Acids Res* **34**(22): 6587-6604.

Lewis IA, Schommer SC, Hodis B, Robb KA, Tonelli M, Westler WM, Suissman MR, Markley JL. 2007. Method for determining molar concentrations of metabolites in complex solutions from two-dimensional H-1-C-13 NMR spectra. *Analytical Chemistry* **79**(24): 9385-9390.

Lin TY, Timasheff SN. 1994. Why do some organisms use a urea-methylamine mixture as osmolyte? Thermodynamic compensation of urea and trimethylamine N-oxide interactions with protein. *Biochemistry* **33**(42): 12695-12701.

Liu Y, Bolen DW. 1995. The peptide backbone plays a dominant role in protein stabilization by naturally occurring osmolytes. *Biochemistry* **34**(39): 12884-12891.

Love JJ, Li X, Chung J, Dyson HJ, Wright PE. 2004. The LEF-1 high-mobility group domain undergoes a disorder-to-order transition upon formation of a complex with cognate DNA. *Biochemistry* **43**(27): 8725-8734.

Mahen EM, Watson PY, Cottrell JW, Fedor MJ. 2010. mRNA Secondary Structures Fold Sequentially But Exchange Rapidly In Vivo. *Plos Biology* **8**(2): 14.

Marky LA, Patel D, Breslauer KJ. 1981. Effect of tetramethylammonium ion on the helix-to-coil transition of poly(deoxyadenylylthymidine): a nuclear magnetic resonance and calorimetric investigation. *Biochemistry* **20**(6): 1427-1431.

Maruyama K, Sato N, Ohta N. 1999. Conservation of structure and cold-regulation of RNA-binding proteins in cyanobacteria: probable convergent evolution with eukaryotic glycine-rich RNA-binding proteins. *Nucleic Acids Research* **27**(9): 2029-2036.

Mayer O, Rajkowitsch L, Lorenz C, Konrat R, Schroeder R. 2007. RNA chaperone activity and RNA-binding properties of the E-coli protein StpA. *Nucleic Acids Research* **35**(4): 1257-1269.

McKown R, Kuroki G, Warren G. 1996. Cold responses of Arabidopsis mutants impaired in freezing tolerance. *Journal of Experimental Botany* **47**(305): 1919-1925.

Mergny JL, Lacroix L. 2003. Analysis of thermal melting curves. *Oligonucleotides* **13**(6): 515-537.

Misra VK, Draper DE. 2000. Mg2+ binding to tRNA revisited: The nonlinear Poisson-Boltzmann model. *Journal of Molecular Biology* **299**(3): 813-825.

Mittler R. 2002. Oxidative stress, antioxidants and stress tolerance. *Trends in Plant Science* **7**(9): 405-410.

Moghaddam S, Caliskan G, Chauhan S, Hyeon C, Briber RM, Thirumalai D, Woodson SA. 2009. Metal Ion Dependence of Cooperative Collapse Transitions in RNA. *Journal of Molecular Biology* **393**(3): 753-764.

Nakaminami K, Karlson DT, Imai R. 2006. Functional conservation of cold shock domains in bacteria and higher plants. *Proceedings of the National Academy of Sciences of the United States of America* **103**(26): 10122-10127.

Nakayama K, Okawa K, Kakizaki T, Inaba T. 2008. Evaluation of the protective activities of a late embryogenesis abundant (LEA) related protein, Cor15am, during various stresses in vitro. *Bioscience Biotechnology and Biochemistry* **72**(6): 1642-1645.

Nedbal W, Homann M, Sczakiel G. 1997. The association of complementary ribonucleic acids can be strongly increased without lowering arrhenius activation energies or significantly altering structures. *Biochemistry* **36**(44): 13552-13557.

Noto R, Marorana V, Emanuele A, Fornili S. 1995. Comparison of the water perturbations induced by two small organic solutes: *ab initio* calculations and molecular dynamics simulation. *Journal of the Chemical Society, Faraday Transactions* **91**(21): 3803-3808.

Pan J, Thirumalai D, Woodson SA. 1997. Folding of RNA involves parallel pathways. *Journal of Molecular Biology* **273**(1): 7-13.

Pearce RS, Dunn MA, Rixon JE, Harrison P, Hughes MA. 1996. Expression of cold-inducible genes and frost hardiness in the crown meristem of young barley (Hordeum vulgare L cv Igri) plants grown in different environments. *Plant Cell and Environment* **19**(3): 275-290.

Phadtare S, Tyagi S, Inouye M, Severinov K. 2002. Three amino acids in Escherichia coli CspE surface-exposed aromatic patch are critical for nucleic acid melting activity leading to transcription antitermination and cold acclimation of cells. *Journal of Biological Chemistry* **277**(48): 46706-46711.

Pleij CW, Rietveld K, Bosch L. 1985. A new principle of RNA folding based on pseudoknotting. *Nucleic Acids Res* **13**(5): 1717-1731.

Puglisi JD, Wyatt JR, Tinoco I. 1988. A pseudoknotted RNA oligonucleotide. *Nature* **331**(6153): 283-286.

Pörschke D. 1976. Thermodynamic and kinetic parameters of ion condensation to polynucleotides. Outer sphere complex formed by Mg++ions. *Biophys Chem* **4**(4): 383-394.

Quigley GJ, Rich A. 1976. Structural domains of transfer RNA molecules. *Science* **194**(4267): 796-806.

Quigley GJ, Teeter MM, Rich A. 1978. Structural analysis of spermine and magnesium ion binding to yeast phenylalanine transfer RNA. *Proc Natl Acad Sci U S A* **75**(1): 64-68.

Rajkowitsch L, Chen D, Stampfl S, Semrad K, Waldsich C, Mayer O, Jantsch MF, Konrat R, Bläsi U, Schroeder R. 2007. RNA chaperones, RNA annealers and RNA helicases. *RNA Biol* **4**(3): 118-130.

Rajkowitsch L, Schroeder R. 2007. Coupling RNA annealing and strand displacement: a FRET-based microplate reader assay for RNA chaperone activity (vol 43, pg 304, 2007). *BioTechniques* **43**(5): 573.

Rees WA, Yager TD, Korte J, von Hippel PH. 1993. Betaine can eliminate the base pair composition dependence of DNA melting. *Biochemistry* **32**(1): 137-144.

Renaut J, Hausman JF, Wisniewski ME. 2006. Proteomics and low-temperature studies: bridging the gap between gene expression and metabolism. *Physiologia Plantarum* **126**(1): 97-109.

Rist M, Marino J. 2001. Association of an RNA kissing complex analyzed using 2-aminopurine fluorescence. *Nucleic Acids Res* **29**(11): 2401-2408.

Rook MS, Treiber DK, Williamson JR. 1998. Fast folding mutants of the Tetrahymena group I ribozyme reveal a rugged folding energy landscape. *Journal of Molecular Biology* **281**(4): 609-620.

Rubin RL. 1977. Spermidine-Deoxyribonucleic acid interaction in vitro and in Escherichia coli. *J Bacteriol* **129**(2): 916-925.

Russell R. 2008. RNA misfolding and the action of chaperones. *Front Biosci* **13**: 1-20.

Sachetto-Martins G, Franco LO, de Oliveira DE. 2000. Plant glycine-rich proteins: a family or just proteins with a common motif? *Biochimica Et Biophysica Acta-Gene Structure and Expression* **1492**(1): 1-14.

Santoro MM, Liu Y, Khan SM, Hou LX, Bolen DW. 1992. Increased thermal stability of proteins in the presence of naturally occurring osmolytes. *Biochemistry* **31**(23): 5278-5283.

Schwinefus JJ, Kuprian MJ, Lamppa JW, Merker WE, Dorn KN, Muth GW. 2007. Human telomerase RNA pseudoknot and hairpin thermal stability with glycine betaine and urea:

Preferential interactions with RNA secondary and tertiary structures. *Biochemistry* **46**(31): 9068-9079.
Semrad K, Green R. 2002. Osmolytes stimulate the reconstitution of functional 50S ribosomes from in vitro transcripts of Escherichia coli 23S rRNA. *Rna-a Publication of the Rna Society* **8**(4): 401-411.
Shelton VM, Sosnick TR, Pan T. 1999. Applicability of urea in the thermodynamic analysis of secondary and tertiary RNA folding. *Biochemistry* **38**(51): 16831-16839.
Soto AM, Misra V, Draper DE. 2007. Tertiary structure of an RNA pseudoknot is stabilized by "diffuse" Mg2+ ions. *Biochemistry* **46**(11): 2973-2983.
Strobel SA. 2002. Biochemical identification of A-minor motifs within RNA tertiary structure by interference analysis. *Biochem Soc Trans* **30**(Pt 6): 1126-1131.
Strobel SA, Doudna JA. 1997. RNA seeing double: close-packing of helices in RNA tertiary structure. *Trends Biochem Sci* **22**(7): 262-266.
Su L, Chen L, Egli M, Berger JM, Rich A. 1999. Minor groove RNA triplex in the crystal structure of a ribosomal frameshifting viral pseudoknot. *Nat Struct Biol* **6**(3): 285-292.
Thirumalai D, Lee N, Woodson SA, Klimov DK. 2001. Early events in RNA folding. *Annual Review of Physical Chemistry* **52**: 751-762.
Thirumalai D, Woodson SA. 1996. Kinetics of folding of proteins and RNA. *Accounts of Chemical Research* **29**(9): 433-439.
Timperio AM, Egidi MG, Zolla L. 2008. Proteomics applied on plant abiotic stresses: Role of heat shock proteins (HSP). *Journal of Proteomics* **71**(4): 391-411.
Tinoco I, Bustamante C. 1999. How RNA folds. *Journal of Molecular Biology* **293**(2): 271-281.
Tompa P, Csermely P. 2004. The role of structural disorder in the function of RNA and protein chaperones. *Faseb Journal* **18**(11): 1169-1175.
Tsuchihashi Z, Brown PO. 1994. DNA strand exchange and selective DNA annealing promoted by the human immunodeficiency virus type 1 nucleocapsid protein. *J Virol* **68**(9): 5863-5870.
Uhlenbeck OC. 1995. Keeping RNA happy. *RNA* **1**(1): 4-6.
Usadel B, Blasing OE, Gibon Y, Poree F, Hohne M, Gunter M, Trethewey R, Kamlage B, Poorter H, Stitt M. 2008. Multilevel genomic analysis of the response of transcripts, enzyme activities and metabolites in Arabidopsis rosettes to a progressive decrease of temperature in the non-freezing range. *Plant Cell and Environment* **31**(4): 518-547.
Valluru R, Van den Ende W. 2008. Plant fructans in stress environments: emerging concepts and future prospects. *Journal of Experimental Botany* **59**(11): 2905-2916.
Varani G, McClain WH. 2000. The G x U wobble base pair. A fundamental building block of RNA structure crucial to RNA function in diverse biological systems. *EMBO Rep* **1**(1): 18-23.
Waldsich C, Masquida B, Westhof E, Schroeder R. 2002. Monitoring intermediate folding states of the td group I intron in vivo. *EMBO J* **21**(19): 5281-5291.
Weckwerth W, Fiehn O. 2002. Can we discover novel pathways using metabolomic analysis? *Current Opinion in Biotechnology* **13**(2): 156-160.
Weckwerth W, Wenzel K, Fiehn O. 2004. Process for the integrated extraction, identification and quantification of metabolites, proteins and RNA to reveal their co-regulation in biochemical networks. *Proteomics* **4**(1): 78-83.
Weeks KM. 1997. Protein-facilitated RNA folding. *Current Opinion in Structural Biology* **7**(3): 336-342.
Weeks KM, Crothers DM. 1993. Major groove accessibility of RNA. *Science* **261**(5128): 1574-1577.

Wienkoop S, Morgenthal K, Wolschin F, Scholz M, Selbig J, Weckwerth W. 2008. Integration of metabolomic and proteomic phenotypes. *Molecular & Cellular Proteomics* **7**(9): 1725-1736.

Williams LJ, Barnett GR, Ristow JL, Pitkin J, Perriere M, Davis RH. 1992. Ornithine decarboxylase gene of Neurospora crassa: isolation, sequence, and polyamine-mediated regulation of its mRNA. *Mol Cell Biol* **12**(1): 347-359.

Woese CR, Winker S, Gutell RR. 1990. Architecture of ribosomal RNA: constraints on the sequence of "tetra-loops". *Proc Natl Acad Sci U S A* **87**(21): 8467-8471.

Woodson SA. 2010. Compact intermediates in RNA folding. *Annu Rev Biophys* **39**: 61-77.

Wu M, Tinoco I. 1998. RNA folding causes secondary structure rearrangement. *Proc Natl Acad Sci U S A* **95**(20): 11555-11560.

Xin ZG, Browse J. 1998. eskimo1 mutants of Arabidopsis are constitutively freezing-tolerant. *Proceedings of the National Academy of Sciences of the United States of America* **95**(13): 7799-7804.

Yancey PH. 2005. Organic osmolytes as compatible, metabolic and counteracting cytoprotectants in high osmolarity and other stresses. *Journal of Experimental Biology* **208**(15): 2819-2830.

Yancey PH, Clark ME, Hand SC, Bowlus RD, Somero GN. 1982. Living with water stress: evolution of osmolyte systems. *Science* **217**(4566): 1214-1222.

Zhang A, Derbyshire V, Salvo JL, Belfort M. 1995. Escherichia coli protein StpA stimulates self-splicing by promoting RNA assembly in vitro. *RNA* **1**(8): 783-793.

Zuker M. 1989. Computer prediction of RNA structure. *Methods Enzymol* **180**: 262-288.

-. 2003. Mfold web server for nucleic acid folding and hybridization prediction. *Nucleic Acids Res* **31**(13): 3406-3415.

Zuther E, Buchel K, Hundertmark M, Stitt M, Hincha DK, Heyer AG. 2004. The role of raffinose in the cold acclimation response of Arabidopsis thaliana. *Febs Letters* **576**(1-2): 169-173.

6. ACKNOWLEDGEMENTS

I would like to thank …

Renée Schröder
for giving me the opportunity to work in this laboratory, for supporting and encouraging me, for the help and patience and for the creativity and never-ending optimism that became an ideal for me and my future work as a scientist.

Martina Dötsch
for being a great supervisor, for instant help when ever I needed it and for giving me the freedom to work autonomously at the same time, for good advice, helpful discussions and constructive comments on my thesis.

Univ.-Prof. Dr. Wolfram Weckwerth
for the collaboration, for the opportunity to conduct metabolite extractions in his laboratory and for helpful discussions.

Lena Fragner and Anne-Mette Hanak
for the cultivation of Chlamydomonas cells, for the patient help with the metabolite extracts and for helpful discussions.

Dr. Takeshi Furuhashi and Dr. Luis Valledor
for kindly providing the GC-MS chromatograms of cold-shock treated and non cold-shock treated Chlamydomonas cells.

Armin Fuchs and Roman Bayer
for generously providing Arabidopsis cDNA.

Andrea Mair
for generously providing competent cells.

all members of the Schröder-laboratory

for the support and motivation, for helping me through desperate times with “THE TECAN”, for being so humorous, interesting and pleasant people and for making this lab a place I enjoyed working in every day.

Thank you Jen for constructive comments on my thesis, for the Wurst and for being such a refreshingly cheerful person. Thanks Bob for providing “geh blau”, it will help me in every future situation. Thanks to you Ivana I will always be a student. Thank you Boris for your help and fruitful ideas during our telephone conferences. Thank you Kasia for the general “of course” to every request I had and for introducing me into the secret of “the plums”. Thank you Johanna for always being the first aid for my mess even if you were drowning in work. Thank you, new generation of lab members, for carrying on the good mood of this laboratory.

my parents

for the warm and supporting environment I was allowed to grow up in, for their enthusiasm for science I inherited, for helping me in every situation possible and for their effort to offer me the best education possible.

my sister and my brother

for being so lovable, supporting, interested, interesting and good-humoured, for the help and for the occasional kick up the backside when I needed it.

my friends

Of all the people I would like to mention …

Thank you Armin for being my prototype for how to enjoy life. Thank you Klaus for bringing me back to earth when my head is in clouds. Thank you Lukas for permanently guarding me against becoming a science nerd. Thank you Mani for being a constant source of motivation. Thank you Philipp for always giving me a “Maß” for my “Ziel”. Thank you Rhea for being a point of reference independent of location and of (clock) time.

7. APPENDIX

7. 1. PUBLICATIONS

Doetsch M, **Gstrein T**, Schroeder R, Fuertig B. 2010. Mechanisms of StpA-mediated RNA remodeling. *RNA Biology* **7**(6): 735-743.

Doetsch M, Fuertig B, **Gstrein T**, Stampfl S, Schroeder R. 2011. The RNA annealing mechanism of the HIV-1 Tat peptide: conversion of the RNA into an annealing-competent conformation. *Nucleic Acid Res.* [in process]

REVIEW

RNA Biology 7:6, 735-743; November/December 2010; © 2010 Landes Bioscience

Mechanisms of StpA-mediated RNA remodeling

Martina Doetsch, Thomas Gstrein, Renée Schroeder and Boris Fürtig*

Max F. Perutz Laboratories; Vienna, Austria

Key words: StpA, RNA chaperones, RNA folding, folding mechanism, RNA-protein interaction

In bacteria, transcription, translation and gene regulation are highly coupled processes. The achievement of a certain functional structure at a distinct temporal and spatial position is therefore essential for RNA molecules. Proteins that facilitate this proper folding of RNA molecules are called RNA chaperones. Here a prominent example from *E. coli* is reviewed: the nucleoid associated protein StpA. Based on its various RNA remodeling functions, we propose a mechanistic model that explains how StpA promotes RNA folding. Through transient interactions via the RNA backbone, thereby shielding repelling charges in RNA, it pre-positions the RNA molecules for the successful formation of transition states from encounter complexes.

Introduction

Soon after catalytic RNAs were discovered, it was realized that, very much like proteins, RNAs fold into complex three-dimensional structures that are essential for their activities. Several catalytic RNAs like self-splicing introns are active in vitro without the help of proteins; however, many of these RNAs require non-physiological ionic conditions or are clearly dependent on proteins for optimal activity. Therefore the search for proteinaceous splicing factors accompanied the studies on self-splicing intron catalysis from the very beginning. Genetic screens were the most common approach to explore proteins that promote the activity of catalytic RNAs. Two main strategies were employed: screens for trans-acting mutants that result in splicing deficiency or screens for suppressors of splicing deficient intron mutants.[1-6] A screen using splicing-deficient mutants of the T4 phage derived thymidylate synthase (td) group I intron was performed to search for *E. coli* proteins that could restore splicing. It resulted in the discovery of StpA, "suppressor of the td$^-$ phenotype".[7] StpA is not a specific splicing factor like the maturases or Cyt-18 and CBP2. In contrast, it interacts with RNA non-specifically and promotes splicing by acting as an RNA chaperone. In this review, we will discuss the properties of this interesting protein, which reveal many of the most important characteristics of this class of proteins.

*Correspondence to: Boris Fürtig; Email: boris.fuertig@univie.ac.at
Submitted: 08/03/10; Revised: 10/05/10; Accepted: 10/06/10
Previously published online:
www.landesbioscience.com/journals/rnabiology/article/13882
DOI: 10.4161/rna.7.6.13882

Functions of StpA in gene-regulation. StpA-like genes have so far been found in several Gram negative bacteria while Gram positive bacteria do not seem to express homologs of this protein.[8] StpA's paralogy and overlapping function of the well-studied histone-like nucleoid structuring protein (H-NS) were recognized immediately.[9,10] In the form of a homo- or hetero-dimer with StpA or other proteins H-NS shapes the structure and organization of the *E. coli* genome by bending and bridging DNA[11] and both H-NS and StpA restrain DNA supercoils in vitro. Thus, H-NS and StpA exert the role of pleiotropic regulators and influence transcription of certain genes in an either positive or negative way.[10]

In full medium, StpA is not abundant and its expression is only induced during a very concise period in mid-exponential growth phase. Expression of StpA can be enhanced through osmolytic stress or elevated temperatures and a more pronounced induction of StpA expression can be achieved in minimal growth medium.[12] Apart from negative auto-regulation of both H-NS and StpA genes, both proteins cross-regulate their homologue's expression in a negative way indicating that they have partially overlapping functions.[10] Some H-NS regulated genes have indeed been found to be regulated by StpA, while others remain unaffected. So far, no genes have been identified which are regulated by StpA only.[8] Consistently, while mutation of the *hns* gene has noticeable effects on growth and cell structure, single *stpA*-knockouts do not show a specific phenotype. However, growth of double *hns*/*stpA* mutants is strongly impaired under normal growth temperatures as well as under cold or heat shock. For those reasons, StpA is sometimes considered a 'molecular back-up' of H-NS. However, the ability of H-NS to dimerize with StpA and other H-NS like proteins hints at the establishment of fine-tuning mechanisms in response to changing growth conditions as opposed to simple H-NS substitution by StpA or other H-NS like proteins.[11]

Like H-NS, StpA is a histone-like protein that binds and bends DNA,[10] and therefore, it was surprising when StpA was isolated as a suppressor of an RNA-based phenotype. The ability of StpA to refold RNA molecules has been studied extensively. StpA has been shown to stimulate group I intron splicing by accelerating folding of the intron RNA both in vitro and in vivo.[7,13] While specific splicing factors stabilize the structure of RNAs by recognizing and binding a particular RNA sequence, StpA, being an RNA chaperone loosens the structure by non-specific interactions with RNA.[13,14] Most important for distinguishing specific splicing factors from RNA chaperones is the observation that RNA chaperones are only needed during folding and as soon as the RNA is in its native conformation, the chaperones are no longer required.[15] StpA can interact with many different

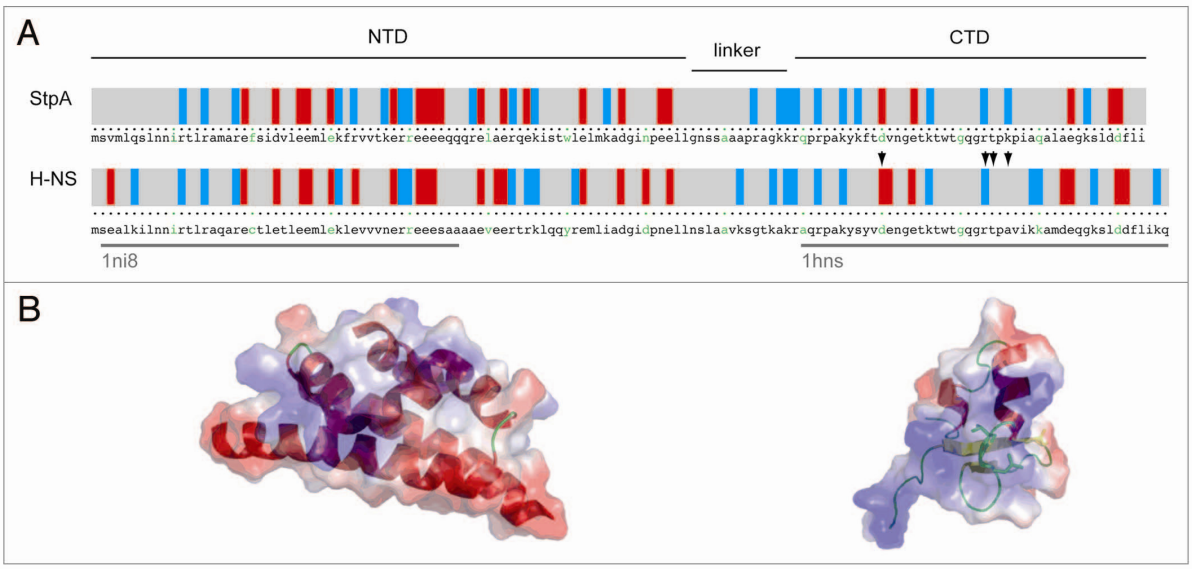

Figure 1. Domain architecture of StpA in comparison to H-NS: (A) displays the primary structure of both proteins; in a color-coded scheme the distribution of charged amino-acids is displayed, blue and red bars indicate positively (R and K) and negatively (D and E) charged amino-acids, respectively; the green letters separate every ten amino-acids; the over-bars indicate the domain structure of StpA as discussed in the text and the grey under-bars show the domains of H-NS for which high-resolution structures (pdb-codes: 1ni8 and 1 hns) are available; residues involved in H-NS DNA binding are highlighted by arrow heads; in (B) the three-dimensional structures are displayed in cartoon representation; the color-coding on the surface representation equates the electrostatic potential; residues involved in H-NS DNA binding are highlighted by stick representation.

RNA molecules and has no sequence preference.[16] It accelerates annealing and strand displacement of many different RNAs. In an RNA recombination assay, StpA was able to enhance copy-choice recombination during reverse transcription of HIV leading to higher reshuffling of genetic markers.[17] Additionally, StpA's simultaneous action on DNA and RNA could be explained by the spatial-temporal coupling of transcription and translation in bacteria. This has also been shown for the *E. coli* cold shock protein, CspA which also has RNA chaperone activity and regulates transcription and translation.[18] Recently, it was noticed that mRNAs in *E. coli* stay at their site of transcription attached to the chromosome during their lifetime. Thus StpA and other nucleic acid chaperones could easily act on both DNA and RNA substrates to regulate gene expression.[19]

Structure of StpA. StpA is a modular protein with remarkable similarities to the chromatin-associated protein H-NS, sharing a 58% identity over all residues.[20] The protein can be subdivided into two domains (**Fig. 1**). The N-terminal domain comprising residues 1–76, has a lower identity to the respective H-NS domain (51%) and functions as the site for homo-[16] and heterodimerization with H-NS.[21] The C-terminal domain (residues 90–134) shows a higher degree of similarity to H-NS (73% identity) and forms a stable 6 kDa product after restricted proteolysis. Both domains are connected by a flexible linker (residues 76–90) that is prone to proteolysis. According to Cusick et al.[20] StpA's RNA chaperone activity resides in the basic C-terminal domain (CTD) of StpA, which is also responsible for RNA/DNA binding. The CTD contains 5 lysine and 3 arginine residues in a total of 46 residues. In contrast, the StpA N-terminal domain does not exhibit activity in either the annealing or the trans-splicing assays, although in the cis-splicing assay, RNA chaperone activity was also found for the N-terminal domain. Bio-informatics predictions made for several RNA chaperones indicate a high propensity of disorder within the proteins, which may be a universal property of this class of proteins and mechanistically important for their function.[22] Calculations using the PONDR-algorithm[23] to determine the overall disorder score indicate that StpA has an overall disorder of 73% and is therefore a largely unstructured protein.[24] A study using the meta-structure approach[25] resulted in the prediction of certain secondary structure elements: α-helical structures in the N-terminal domain (residues 115 to 134) and at the very C-terminal end, and a stretch of β-sheets for residue 90 to 115. Moreover, the overall compactness for StpA CTD is lower in these calculations than for folded proteins with an $ARC^{\text{folded proteins}}$ (average residue compactness) around 300. Interestingly, the linker-region that is most sensitive to limited proteolysis shows no clear propensity for a certain secondary structure but a rather high measure of compactness, compared to the rest of the sequence.[16]

Contrasting the rigorous results of the PONDR prediction is the considerably strong homology to highly structured H-NS, for which three-dimensional structures of certain domains could be determined.[26,27] This suggests that StpA might also exhibit folded domains. Furthermore, the stabilities of the homo- and heterodimers with H-NS are remarkable.[21] Therefore, we assume that StpA exhibits well-defined structured domains.

It is interesting that although both proteins harbor the same amount of basic amino acids (each with 23 arginines and lysines), H-NS is less active than StpA in the applied chaperone assays,

indicating a possible structure-function relationship.[20] The difference could be either attributed to the compensation of the positive charges by the presence of acidic residues or to the spatial distribution of the charged amino acids. The positive net-charge is lower in H-NS (H-NS-pI 5.44) than in StpA (StpA-pI 6.41; calculated using ExPASy). The spatial distribution of charged residues over the surface of the proteins shows a higher difference for the nucleic acids binding C-terminal domain harboring the RNA chaperone activity when compared to the NTD (**Fig. 1**). Moreover, the H-NS DNA binding site was mapped by NMR spectroscopic methods to a mostly positive charged surface region of the CTD of the protein. Most affected residues upon DNA binding are D101, T109, R113, T114 and A116 (see arrow marks in **Fig. 1**).[28] If the homologous region of StpA is involved in nucleic acid binding, a net of two positive charges is added to the interaction surface.

Table 1. The table summarizes the results of various in vitro chaperone assays for WT StpA, the N terminal domain (NTD) and the C terminal domain (CTD) of StpA as well as two StpA mutants G126V and L30P

	Annealing	Strand displacement	cis-splicing	trans-splicing
WT	(+)[7,10,20]	(+)[7](-)[20]	(+)[31]	(+)[7,10,20]
CTD	(+)[7]/(-)[30]	(+)[30]/(-)[20]	(+)[16]	(+)[20]
NTD	(-)[20,30]	(-)[30]	(+)[16]	(-)[20]
G126V	n.d.	n.d.	(+)[16]	n.d.
L30P	(-)[30]	(+)[30]	n.d.	n.d.

(+) and (-) indicate activity or no activity, respectively, n.d. indicates that the respective assay was not applied, numbers refer to publications in the reference section. Mutant G126V was shown to have a decreased RNA binding efficiency but an increased cis-splicing activity when compared to WT StpA. Mutant L30P lacks the ability to dimerize. The assays varied in substrate RNA and experimental setup as described in the text for the respective assays. Contradicting results are discussed in the annealing section.

Assays for RNA Chaperone Activity

The diversity of the assays that have been used is key to the understanding of the mode of action of proteins with RNA chaperone activity. Here all assays in which StpA has been tested, as well as its performance in these assays, are summarized. Besides full-length StpA, two mutant variants of the protein as well as the CTD and NTD were tested (**Table 1**). The NTD is responsible for dimerization and the CTD has been implicated in nucleic acid interaction. The RNA chaperone activity of StpA was shown in different in vitro and in vivo assays, comprising mono- and bimolecular reactions.

RNA Annealing and RNA Strand Displacement. The two basic activities an RNA chaperone is expected to accomplish are the acceleration of hybridization (annealing) and the dissociation (displacement) of complementary RNA strands. Assays to monitor annealing or strand displacement are usually carried out with radioactively labeled RNAs and visualized via gel electrophoresis. In addition, complementary RNAs can be end-labeled with fluorophores and the fraction of double-stranded RNAs can be monitored via FRET. Using a pair of unstructured 21mer RNAs that self-anneal with a rate constant of $k_{ann} = 10^6\ M^{-1}sec^{-1}$, StpA was shown to accelerate the rate constant of annealing about 4-fold.[16] Using longer complementary RNAs of 96 nt and 92 nt, that are capable of forming a 86 bp duplex, but do not self-anneal due to intramolecular structures, StpA accelerates the initial rate of annealing >130-fold at 37°C.[7] StpA shows the highest activity at about 1.8 μM. Due to the length of the substrate RNA, it is likely that the assay monitors not only the annealing reaction but also an unwinding step which is required because of secondary structures.[29] The use of short unstructured RNA substrates allows the discrimination between strand annealing and unfolding of pre-existing secondary structures in the complementary oligonucleotides.

In addition to annealing, StpA also stimulates strand displacement without the addition of ATP.[7,30] In a combined FRET-based assay, a pair of complementary 21mer long RNAs anneals in the presence or absence of StpA (phase I). The addition of a non-labelled fully complementary competitor 21mer RNA initiates strand displacement (phase II). In the absence of StpA, phase II is dominated by the annealing activity, however in the presence of StpA, strand displacement is catalyzed with a rate constant of $k_{SD} = 4 \times 10^6\ M^{-1}sec^{-1}$.

T4 *td* Intron Splicing. The group I intron derived from the T4 bacteriophage thymidylate synthase (*td*) gene self splices in vivo and in vitro. The splicing reaction is initiated by the nucleophilic attack of guanosine at the 5' splice site and followed by two transesterfication reactions. Splicing of the *td* intron is strongly dependent on the correct three-dimensional fold of the RNA. In vivo, the process is probably promoted by different trans-acting factors and is therefore fast and efficient, whereas in vitro, misfolding of the RNA renders the process slow and inefficient. Overexpression of StpA in *E. coli* cells expressing the *td* pre-mRNA leads to a 3.0-fold increase of the pre-mRNA level and a 7.4-fold increase of the mRNA level. Thus, the mRNA-to-pre-mRNA ratio was increased 2.5-fold.[7]

Group I intron splicing in cis. In vitro transcribed *td* intron pre-mRNA is very inefficient in folding, probably due to stable misfolded intermediates. In a non-renatured sample of *td* intron pre-mRNA over 90% of the molecule are not able to splice efficiently. RNA chaperones can resolve the misfolded structures and thereby elevate the fraction of fast-reacting molecules. At a concentration of 1.4 μM, StpA was shown to accelerate splicing of the *td* intron 30–45-fold compared to splicing of the RNA alone, leaving only a small fraction of RNA molecules in the slow reacting conformation.[16,31]

Group I intron splicing in trans. The *td* intron RNA structure is modular and can thereby be partitioned into pieces, which can refold and assemble into an active intron ribozyme.[32] However, assembly of the RNA is inefficient at 37°C, whereas at 55°C or in the presence of an RNA chaperone, a splicing-competent conformation is restored and effective trans splicing can occur.[15] StpA strongly promotes trans-splicing in vitro, with a peak activity at about 2 μM protein.[7]

In vivo folding trap. Splicing of the *td* intron in vivo is strongly dependent on translation of the pre-mRNA, probably due to a

folding trap consisting of a 9 bp interaction between exon and intron sequences. The ribosome disrupts this interaction during translation enabling a splicing competent intron conformation. A stop-codon directly upstream of the folding trap prevents its resolution by the ribosome and traps the intron in a slow reacting conformation with a splicing efficiency of less than 1%. StpA rescues the stop codon mutant but not the intronic mutants, disrupting the thermal stability of the three-dimensional structure of the intron. This distinguishes it from proteins like CYT-18 which specifically recognize and stabilize the intron structure, thereby rescuing activity of both mutants.[33]

Mechanisms

From assays towards the understanding of mechanisms. Annealing and strand displacement refer to different events in the folding of an RNA molecule and are therefore discussed individually in this review. It has to be kept in mind, that the rate-limiting step in RNA folding is the dissociation of formed base pairs. Depending on the structural context of the RNA interaction (e.g., domain architecture, structure of the transition state, large or many extended regions etc.,), annealing becomes a second important step in the folding reaction, and both functionalities must coincide. StpA has been tested in various assays using a large variety of different substrates resulting in more or less complex reactions, making it difficult to distinguish between strand annealing, strand dissociation and the influence of StpA on tertiary interactions. Moreover, it is probable that the two processes of annealing and displacement affect each other to a certain extent. Not only might the strand displacement activity of a chaperone support annealing by the opening of mispaired nucleotides, but the displacement of one strand by a competitor might also be strongly dependent on annealing. Even further, annealing and strand displacement may be part of one and the same process (see the discussion in the last section with the generalized model).

In order to discuss possible mechanisms of how StpA chaperones RNA folding, a closer look into the mechanisms of RNA folding itself is necessary. Within milliseconds after synthesis, significant amounts of the RNA molecule fold to form various possible secondary structures. In many regions, the structure may initially consist primarily of small base-paired elements. Over time, ranging from microseconds to minutes,[34-37] parts of the molecule will continue to fold into compact structures stabilized by tertiary interactions. Via such folding routes, RNA is prone to adopt non-native stable conformations which may act as folding traps.[38,39] To overcome these folding traps, the RNA molecules have to partially unfold and refold to reach the final functional state. Furthermore, many ribonucleic acids are able to adopt more than one single three-dimensional structure.[40,41] These alternative structures have again very similar thermodynamic stabilities but show substantially different dynamics and function. Structural transitions between a single or several different metastable RNA states and the final functional state often constitute the rate-limiting steps on the folding pathway towards a functional RNA fold.[38] The mechanisms by which RNA molecules refold consist of three distinct steps: (a) the strand displacement that disrupts stabilizing interactions in the starting state, (b) formation of a transition state and (c) strand association to form the final state.[30,42] Depending on the RNA sequence, strand dissociation and association can occur simultaneously or sequentially.[35] As mentioned above these processes are rate limiting and therefore catalysis of the folding process is required, as the RNA folding problem is not only an in vitro artifact but also occurs in vivo.[33,43] There are various mechanisms under discussion as to how proteins facilitate the remodeling of RNA conformations. The proposed models, which are not mutually exclusive, can be grouped into two main classes: (i) RNA-binding proteins act as cofactors, bind tightly to the RNA and become part of the native RNA-protein complex or (ii) proteins that interact only transiently with the RNA (most probably with the transition state) and thereby lower the activation energy in the remodeling reaction (**Fig. 2**).[44] In general, RNA chaperones are defined as polypeptidic modulators of RNA conformations and molecular associations (referring to Gething et al.[45]). The mode of action of these chaperones seems to be as manifold as the interactions that shape RNAs. Here we will discuss the mechanistic properties of the RNA chaperone StpA, from its RNA binding properties to its ability to accelerate annealing and strand displacement of RNAs.

RNA binding properties of StpA. No specific RNA recognition sequence is known for StpA. In a Genomic SELEX screen[16] no binding motifs could be significantly enriched suggesting that StpA does not exhibit any sequence-dependent RNA-binding. StpA rather has a broad specificity to RNA molecules of any sequence. The dissociation constants measured for different target molecules are in the low μM range. Interestingly, for unstructured RNAs (intronless mRNA) or small ssRNA oligonucleotides the dissociation constant is lower than that for more structured RNAs (short exons carrying a folded intron), K_D = 0.58 μM vs. K_D = 0.73 μM, respectively. Furthermore, in a filter-binding assay the retention is dramatically reduced by a factor of 8, if a highly structured and compact RNA is tested in comparison to the more unstructured mRNA. The same low binding affinity is monitored for structured short RNAs such as small stable duplexes and hairpins.[16] In all assays the optimal concentration for the action of StpA is close to but above the determined dissociation constants (between 1.4 μM and 8 μM).[7,10,20] Similar results were also reported for other proteins with RNA chaperone activity (e.g., Ncp7), in which an inhibitory effect is shown for concentrations beyond this optimum.[14]

Dissociation constants for the interaction between StpA and DNA are in the same range as between StpA and RNA (K_D = 0.7 μM, for the H-NS/DNA interaction the dissociation constant is determined to be K_D = 2.8 μM). Other proteins with RNA chaperone activity (e.g., Nucleolin) have been shown to be both RNA[46] and DNA[47] chaperones. Since StpA interacts with both RNA and DNA with comparable dissociation constants the most probable interaction occurs at the phosphate-backbone interface of the nucleic acid. In line with the proposed interaction via the phosphate-backbone, the potency of interaction between StpA and RNA is highly dependent on the ionic strength of the

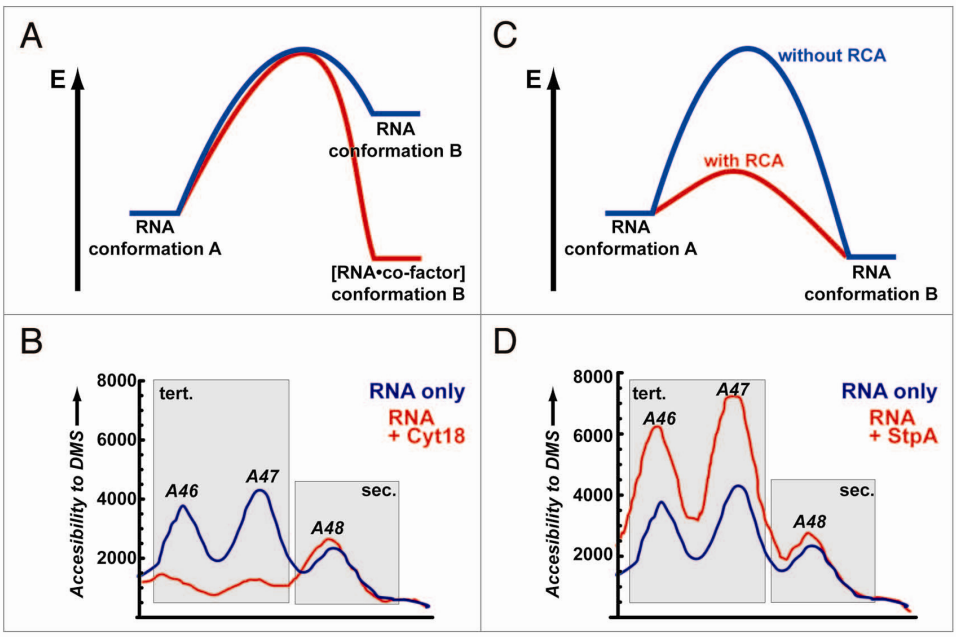

Figure 2. Two simplistic models of how proteins facilitate the remodeling of RNA conformations. (A) Energy landscape for a tight binding protein that acts as a co-factor for RNA and through binding induces a conformational change that is more stable (red) then the respective RNA conformation in the absence of the protein (blue). (B) As an experimental example for such a scenario the changes in the *td* intron structure upon binding of Cyt-18 are shown. Without the protein residues, A46 and A47 are moderately accessible to DMS modifications (blue line). In the presence of Cyt-18 these residues become involved in a stable tertiary interaction and are protected (red line). No apparent changes are monitored for A48 which is part of a secondary structure element. (C) Energy landscape for proteins that interact only transiently with the transition state of an RNA and thereby lowers the activation energy in the remodeling reaction (blue versus red reaction path, for RNA alone and RNA/protein, respectively). (D) As an experimental example for this scenario the changes in the *td* intron structure upon interaction with StpA are shown. Without the protein residues A46 and A47 are moderately accessible to DMS modifications. In the presence of StpA these residues sample more open conformations and are easier to access by DMS (red lines). No apparent changes are monitored for A48 as it is involved in a secondary structure interaction; (B and C) are adapted from reference (Waldsich et al.).[13]

solution. Mono- as well as divalent-ions can compete for the RNA's interaction with the protein and can also induce similar changes on the protein structure as RNA (Fürtig B, unpublished).[16] The increase of magnesium ion concentration reduces the efficient binding of RNA to StpA by a factor of ~4. When increasing the concentration of magnesium from 0.1 mM to 0.5 mM, the same behavior is observed as during an increase in concentration of monovalent ions from 25 mM to 250 mM.[16] Assuming that the interaction with the phosphate backbone is the dominant recognition mode, then shielding the charge of the phosphate backbone could contribute to the RNA annealing and displacement activities by reducing either inter- or/and intramolecular repulsions.[48]

From a dual binding assay, which probes the interaction of StpA with two non-complementary 21mer RNAs[16,30] it can be deduced that the protein is able to interact with two different strands of RNA at the same time. The dual binding assay further suggests an additional interesting fact: although the amplitudes of the annealing reaction and the dual binding reaction differ strongly, the rate constants for both reactions are identical ($k_{obs,ann} = k_{obs,bind} = 4 \times 10^6\ M^{-1}s^{-1}$). This suggests that the rate-limiting step for StpA catalyzed RNA annealing is the binding step. In other words, binding of the RNA to protein induces a structural change in the RNA that makes it favorable for annealing (for further discussion see the generalized model section).

Aside from the low dissociation constant and the broad specificity of StpA, the concept that the interactions between protein and RNA are only of transient nature is founded on the observation that the protein does not need to stay bound, when the folding reaction of the RNA is completed. It can be digested without changing the reaction dynamics or 'un-folding' the chaperoned RNA.[7] This also implies that in ribozyme-based assays the physical folding steps are affected but the functional steps are not. Furthermore, a mutant of StpA (G126V), which has a dramatically reduced binding affinity to RNA (K_D >10 μM), harbors an increased RNA chaperone activity.[16] This implies that the tighter the binding strength of a protein is to RNA, the more reduced is its ability to promote RNA folding as an RNA chaperone. This correlation between RNA chaperone activity and weak RNA binding[16,49-51] gives strong evidence that the transient nature of RNA-protein interaction is a necessity for RNA structure remodelling. In fact, the nature of the StpA-RNA interaction fits well with the notion that 'transient complexes' are dominated by long-range electrostatic interactions.[52]

RNA annealing. So far, three different, but not necessarily mutually exclusive, mechanisms for the acceleration of complementary RNA annealing have been proposed: (a) the active attraction of RNA molecules to increase the encounter frequency between them, (b) stabilization of the annealing transition state by shielding the negative RNA backbone charges (often referred to as 'matchmaker activity') and (c) 'conversion' of the RNA into an annealing-prone conformation.[53-55] Studies of annealing acceleration that used different proteins suggest not a general applicability of one of the above mentioned scenarios, but instead the co-existence of several (mixed) mechanisms.

In all the applied annealing assays the protein was used in a 25- to 200- fold molar excess over RNA single strands. Furthermore, a threshold StpA concentration of 0.6 μM was found in a mixed annealing and strand displacement assay below which no reaction acceleration could be detected.[7] It is generally assumed for RNA annealers (as well as for chaperones) that several molecules of protein bind one RNA molecule. This 'RNA coating' is presumed to be a necessity for acceleration of annealing (and strand displacement).

Several authors described the importance of positively charged amino acids for nucleic acid annealing activity.[55-59] In fact, the CTD of StpA is rich in basic residues and carries a net charge of +3. We analyzed RNA annealing acceleration by the short HIV-1 Tat protein-derived peptide Tat(44–61) (Doetsch et al. paper in preparation). Our results stress not only the importance of the overall charge of the protein, but also suggest a distinct spatial arrangement of basic residues within the peptide. The same relation between positive charges and annealing activity may also apply to StpA: Interestingly, H-NS is less active than StpA in annealing assays,[20] which could be explained by the different distributions of positive amino acids within their sequence (**Fig. 1**). RNA annealing activity is sometimes connected to the ability of proteins to actively increase the encounter frequency between complementary RNA molecules.[29] One potential mechanism for the StpA-catalyzed annealing reaction is an increase of local concentration of the RNA molecules, as proposed by Mayer et al.[16] and Rajkowitsch et al.[30] It was suggested that for simultaneous RNA binding and thus RNA annealing acceleration, dimerization of the protein is indispensable. This hypothesis is supported by the dimerization-deficient StpA L30P mutant that is inactive in annealing assays. These results oppose those from the Belfort lab, reporting that both CTD and NTD individually are inactive in annealing assays.[30] The CTD's lack of annealing activity was explained by its inability to bind two RNAs simultaneously. Since StpA dimerization is attributed to the NTD, the CTD alone may have only one RNA binding platform. However, more recent experiments show that the CTD is active in annealing (Fürtig B, et al. unpublished results). The contradicting performance of the CTD might be explained with different protein preparations resulting in different concentrations of active protein, as well as with the use of different salt concentrations in the applied annealing assays. StpA's activity, like that of other RNA chaperones, is inhibited by low amounts of $MgCl_2$ and NaCl. Therefore, the hypothesis that annealing activity is conferred by simultaneous RNA binding needs further confirmation.

RNA displacement. As indicated above, the opening of stretches of base-paired nucleotides and subsequent exchange of one of the pairing partners are fundamental steps in RNA folding. Most often, the opening process is energetically disfavored and characterized with a low rate constant, that decreases exponentially with the length of the stretch that has to be opened.[60] Catalysis of this process is beneficial in order to increase the overall folding rate of RNAs and is therefore an important feature of RNA chaperones.[61] Using a FRET assay, an orders-of-magnitude increase in strand displacement activity could be monitored for StpA.[30]

Mechanistically, strand exchange has to involve open or at least partially open RNA conformations as intermediate or transition states. This reduction in the extent of structure is necessary to speed up the zippering process.[49] In the open states, nucleotides are exposed and subsequently available for new interactions. This effect was seen for StpA. Upon interaction with StpA the *td* group I intron showed a higher accessibility to modifying agents, such as DMS, for tertiary structure elements and a reduced compactness of the overall fold (**Fig. 2**).[13,31] Interestingly, the sensitivity of an RNA towards StpA correlates with the three dimensional structural stability of the RNA.[62] Intron mutants with lower thermal stability showed a decreased splicing efficiency in the presence of StpA. This effect could be reverted by dropping the temperature from 37°C to 25°C, indicating that the opening of RNA structures by StpA is only beneficial for folding up to a certain degree.[62] This result is consistent with the notion that there is an optimal concentration for StpA beyond which folding efficiency is again decreased. Even so, it is also notable that StpA can not unfold stable RNAs completely.[62] These results show a clear difference between StpA and specific binding proteins such as tRNA synthetase Cyt-18, which acts in an opposite way, by binding to the RNA and stabilizing tertiary elements in the RNA (**Fig. 2**).[13]

A Generalized Model for StpA Activities

All these findings can be used to define a generalized mechanism for StpA promoting RNA annealing and strand displacement.

The astounding identity of rate constants. The rate constants of the StpA catalyzed annealing, strand displacement and dual binding reactions hint at which step StpA influences RNA folding.[16,30] Strikingly, all three rate constants are identical within error, namely about 4×10^6 $M^{-1}sec^{-1}$, suggesting that all three activities are subject to the same rate-limiting step in the presence of StpA.

The RNA-only folding scenario. To explain this phenomenon, we first consider the RNA folding reaction simplified as the annealing of two complementary RNA molecules (**Fig. 3A**). On their way to the formation of the thermodynamically most stable complex, the RNA molecules form a first encounter complex, which might either proceed into a transition state or fall apart. While the encounter complex is characterized by long-range (mainly electrostatic) interactions, the transition state contains RNAs that have already formed initial base pairs.[52] The formation of the final duplex evolving from the transition state is assumed to be very fast.[63-65] The annealing rate constants of complementary RNAs are very small and in the conformationally-controlled

regime. This means that the reaction velocity is restricted by necessary RNA refolding events which have to take place before the transition state formation.[52] For example, long 69mer RNAs with some degree of internal secondary structures anneal with a rate of 3.4 x 10^3 $M^{-1}sec^{-1}$ and a 21mer unstructured RNA anneals with a rate of 10^6 $M^{-1}sec^{-1}$ in the absence of RNA chaperones.[30,54] We therefore assume that the rate-limiting step of the folding reaction is the conversion from encounter complex to transition state. We suggest that the restricting processes are conformational changes in both RNA molecules that are necessary for base pair formation. Apart from folding into the most stable conformation, the RNAs have the propensity to form other more or less stable duplexes. Thus, RNA molecules might either get trapped in alternative folds or they might form duplexes that fall apart due to low stability (**Fig. 3A**).

The effect of StpA on RNA annealing. In the presence of StpA (**Fig. 3B**) colliding RNA molecules are most probably not 'naked' but instead coated with one or more StpA molecules. Due to electrostatic attraction between RNA and StpA and the strong molar excess of protein over RNA, it is very likely that most RNAs are in an StpA-bound state. Thus, the encounter complex contains, besides the two RNAs, additional StpA molecules. The rate constants for annealing and strand displacement lie within the diffusion-controlled regime, meaning that StpA changes the rate limiting step of RNA folding. Thus, we assume that StpA acts on the conversion between encounter and transition state. Considering the role of basic amino acid residues in StpA's chaperone activity, we suggest that the protein alters RNA conformation in such way that the probability of progression into the transition state is increased and less encounter complexes fall apart. In addition to its conformational influence on the RNA, StpA could also act through shielding of negative RNA backbone charges and thus stabilize the first encounter complex. In summary, StpA induces conformational changes in the RNA that overcome structural barriers that prohibit base pair formation and thus render the RNA strands prone for annealing.

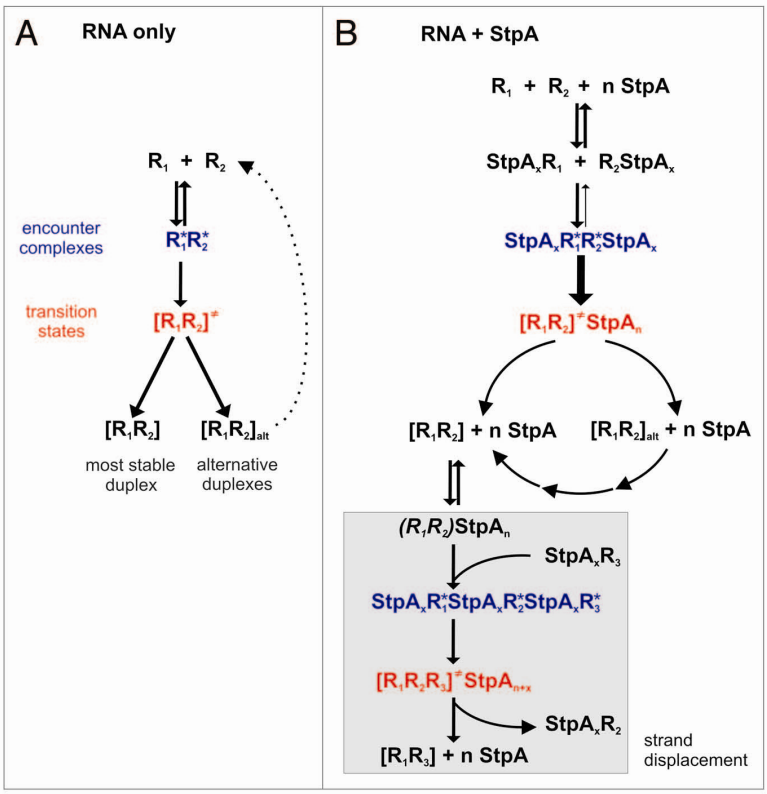

Figure 3. A Generalized Model for StpA Activities. (A) Two annealing RNAs (R_1 and R_2 with complementary sequences) run through different states before they form a duplex. In addition to the most stable double-strand, alternative duplexes (indicated by the subfix 'alt') can form and, depending on their thermodynamic stability, eventually fall apart again. (B) Proposed mechanisms for StpA-facilitated RNA-RNA annealing and strand displacement. Partial opening of the R_1R_2 duplex (indicated through parentheses) allows the R_1-complementary R_3 RNA to invade the double-strand.

The catalysis of strand displacement by StpA and its connection with RNA annealing. Another difference from the 'RNA only' scenario is the propensity of StpA to open up stable duplexes (**Fig. 3B**). This results in the refolding of the alternative duplexes so that the most prominent product of annealing will be the thermodynamically most stable structure. Since StpA works in a sequence unspecific way, one has to keep in mind that all base paired regions are susceptible to being opened up, including the thermodynamically most stable duplex. This is the basis for strand displacement: when a competing RNA strand is present (especially when it is in molar excess) it will be able to invade a just partly opened duplex and thus replace one of the strands. Thus, the strand displacement reaction is strongly coupled to an annealing process.

The connection of annealing, strand displacement and dual binding. In the presence of StpA both reactions, annealing and strand displacement, become diffusion-controlled while steps subsequent to encounter complex/transition state formation are very fast and thus not rate-limiting anymore. This means, the reactions are only dependent on the velocity with which RNA molecules collide. The process of StpA-coated RNA molecules meeting each other is what is measured with the dual binding assay. That annealing, strand displacement and dual binding share the same rate-limiting step is the reason for their identical rate constants. In summary, we propose that StpA does not accelerate diffusion of RNA molecules towards each other but instead pre-positions RNAs and stabilizes the encounter complex and thus increases the probability of successful RNA remodeling.

Acknowledgements

We would like to thank all members of the Schroeder Lab for helpful discussions on the topic of RNA chaperones. We are indebted to Jennifer L. Boots and Bob Zimmermann for critical reading of the manuscript and helpful comments. This work is supported by F.W.F. through a Lise Meitner-Position (M1157-B12) to B.F. and grant F1703 to R.S. and by the European Community (EU-NMR, Contract # RII3-026145). M.D. is funded by the University of Vienna.

References

1. Akins RA, Lambowitz AM. A protein required for splicing group I introns in Neurospora mitochondria is mitochondrial tyrosyl-tRNA synthetase or a derivative thereof. Cell 1987; 50:331-45.
2. Dujardin G, Jacq C, Slonimski PP. Single base substitution in an intron of oxidase gene compensates splicing defects of the cytochrome b gene. Nature 1982; 298:628-32.
3. Labouesse M, Netter P, Schroeder R. Molecular basis of the 'box effect', A maturase deficiency leading to the absence of splicing of two introns located in two split genes of yeast mitochondrial DNA. European journal of biochemistry/FEBS 1984; 144:85-93.
4. Lazowska J, Jacq C, Slonimski PP. Sequence of introns and flanking exons in wild-type and box3 mutants of cytochrome b reveals an interlaced splicing protein coded by an intron. Cell 1980; 22:333-48.
5. Seraphin B, Simon M, Faye G. MSS18, a yeast nuclear gene involved in the splicing of intron aI5 beta of the mitochondrial cox1 transcript. EMBO J 1988; 7:1455-64.
6. De la Salle H, Jacq C, Slonimski PP. Critical sequences within mitochontrial introns: pleiotropic mRNA maturase and cis-dominant signals of the box intron controlling reductase and oxidase. Cell 1982; 721-32.
7. Zhang A, Derbyshire V, Salvo JL, Belfort M. *Escherichia coli* protein StpA stimulates self-splicing by promoting RNA assembly in vitro. RNA 1995; 1:783-93.
8. Dorman CJ, Hinton JC, Free A. Domain organization and oligomerization among H-NS-like nucleoid-associated proteins in bacteria. Trends Microbiol 1999; 7:124-8.
9. Zhang A, Belfort M. Nucleotide sequence of a newly-identified *Escherichia coli* gene, stpA, encoding an H-NS-like protein. Nucleic Acids Res 1992; 20:6735.
10. Zhang A, Rimsky S, Reaban ME, Buc H, Belfort M. *Escherichia coli* protein analogs StpA and H-NS: regulatory loops, similar and disparate effects on nucleic acid dynamics. EMBO J 1996; 15:1340-9.
11. Muller CM, Schneider G, Dobrindt U, Emody L, Hacker J, Uhlin BE. Differential effects and interactions of endogenous and horizontally acquired H-NS-like proteins in pathogenic *Escherichia coli*. Mol Microbiol 75:280-93.
12. Free A, Dorman CJ. The *Escherichia coli* stpA gene is transiently expressed during growth in rich medium and is induced in minimal medium and by stress conditions. Journal of bacteriology 1997; 179:909-18.
13. Waldsich C, Grossberger R, Schroeder R. RNA chaperone StpA loosens interactions of the tertiary structure in the td group I intron in vivo. Genes and Dev 2002; 16:2300-12.
14. Herschlag D, Khosla M, Tsuchihashi Z, Karpel RL. An RNA chaperone activity of non-specific RNA binding proteins in hammerhead ribozyme catalysis. EMBO J 1994; 13:2913-24.
15. Coetzee T, Herschlag D, Belfort M. *Escherichia coli* proteins, including ribosomal protein S12, facilitate in vitro splicing of phage T4 introns by acting as RNA chaperones. Genes Dev 1994; 8:1575-88.
16. Mayer O, Rajkowitsch L, Lorenz C, Konrat R, Schroeder R. RNA chaperone activity and RNA-binding properties of the *E. coli* protein StpA. Nucleic Acids Res 2007; 35:1257-69.
17. Negroni M, Buc H. Copy-choice recombination by reverse transcriptases: reshuffling of genetic markers mediated by RNA chaperones. Proc Natl Acad Sci USA 2000; 97:6385-90.
18. Jiang W, Hou Y, Inouye M. CspA, the major cold-shock protein of *Escherichia coli*, is an RNA chaperone. J Biol Chem 1997; 272:196-202.
19. Llopis PM, Jackson AF, Sliusarenko O, Surovtsev I, Heinritz J, Emonet T, et al. Spatial organization of the flow of genetic information in bacteria. Nature 2010; 466:77-81.
20. Cusick ME, Belfort M. Domain structure and RNA annealing activity of the *Escherichia coli* regulatory protein StpA. Mol Microbiol 1998; 28:847-57.
21. Leonard PG, Ono S, Gor J, Perkins SJ, Ladbury JE. Investigation of the self-association and hetero-association interactions of H-NS and StpA from Enterobacteria. Mol Microbiol 2009; 73:165-79.
22. Dyson HJ, Wright PE. Intrinsically unstructured proteins and their functions. Nat Rev Mol Cell Biol 2005; 6:197-208.
23. Garner E, Romero P, Dunker AK, Brown C, Obradovic Z. Predicting Binding Regions within Disordered Proteins. Genome informatics 1999; 10:41-50.
24. Tompa P, Csermely P. The role of structural disorder in the function of RNA and protein chaperones. FASEB J 2004; 18:1169-75.
25. Konrat R. The protein meta-structure: a novel concept for chemical and molecular biology. Cell Mol Life Sci 2009; 66:3625-39.
26. Bloch V, Yang Y, Margeat E, Chavanieu A, Auge MT, Robert B, et al. The H-NS dimerization domain defines a new fold contributing to DNA recognition. Nat Struct Biol 2003; 10:212-8.
27. Shindo H, Iwaki T, Ieda R, Kurumizaka H, Ueguchi C, Mizuno T, et al. Solution structure of the DNA binding domain of a nucleoid-associated protein, H-NS, from *Escherichia coli*. FEBS letters 1995; 360:125-31.
28. Sette M, Spurio R, Trotta E, Brandizi C, Brandi A, Pon CL, et al. Sequence-specific recognition of DNA by the C-terminal domain of nucleoid-associated protein H-NS. J Biol Chem 2009; 284:30453-62.
29. Cristofari G, Darlix JL. The ubiquitous nature of RNA chaperone proteins. Prog Nucleic Acid Res Mol Biol 2002; 72:223-68.
30. Rajkowitsch L, Schroeder R. Dissecting RNA chaperone activity. RNA 2007; 13:2053-60.
31. Mayer O, Waldsich C, Grossberger R, Schroeder R. Folding of the td pre-RNA with the help of the RNA chaperone StpA. Biochem Soc Trans 2002; 30:1175-80.
32. Salvo JL, Coetzee T, Belfort M. Deletion-tolerance and trans-splicing of the bacteriophage T4 td intron. Analysis of the P6-L6a region. J Mol Biol 1990; 211:537-49.
33. Clodi E, Semrad K, Schroeder R. Assaying RNA chaperone activity in vivo using a novel RNA folding trap. EMBO J 1999; 18:3776-82.
34. Webb AE, Weeks KM. A collapsed state functions to self-chaperone RNA folding into a native ribonucleoprotein complex. Nat Struct Biol 2001; 8:135-40.
35. Furtig B, Buck J, Manoharan V, Bermel W, Jaschke A, Wenter P, et al. Time-resolved NMR studies of RNA folding. Biopolymers 2007; 86:360-83.
36. Woodson SA. RNA folding and ribosome assembly. Current opinion in chemical biology 2008; 12:667-73.
37. Williamson JR. Biophysical studies of bacterial ribosome assembly. Current opinion in structural biology 2008; 18:299-304.
38. Zarrinkar PP, Williamson JR. Kinetic intermediates in RNA folding. Science 1994; 265:918-24.
39. Treiber DK, Rook MS, Zarrinkar PP, Williamson JR. Kinetic intermediates trapped by native interactions in RNA folding. Science 1998; 279:1943-6.
40. Mayer O, Windbichler N, Wank H, Schroeder R. Protein-induced RNA Switches in Nature. In: Silvermann SK, Ed. Nucleic Acid Switches and Sensors: Landes Bioscience 2005.
41. Schwalbe H, Buck J, Furtig B, Noeske J, Wohnert J. Structures of RNA switches: insight into molecular recognition and tertiary structure. Angewandte Chemie (International ed) 2007; 46:1212-9.
42. Wong CH, Hendrix M, Priestley ES, Greenberg WA. Specificity of aminoglycoside antibiotics for the A-site of the decoding region of ribosomal RNA. Chem Biol 1998; 5:397-406.
43. Semrad K, Schroeder R. A ribosomal function is necessary for efficient splicing of the T4 phage *thymidylate synthase* intron in vivo. Genes Dev 1998; 12:1327-37.
44. Duncan CD, Weeks KM. Nonhierarchical ribonucleoprotein assembly suggests a strain-propagation model for protein-facilitated RNA folding. Biochemistry 49:5418-25.
45. Gething MJ, Sambrook J. Protein folding in the cell. Nature 1992; 355:33-45.
46. Ghisolfi L, Joseph G, Amalric F, Erard M. The glycine-rich domain of nucleolin has an unusual supersecondary structure responsible for its RNA-helix-destabilizing properties. J Biol Chem 1992; 267:2955-9.
47. Sapp M, Knippers R, Richter A. DNA binding properties of a 110 kDa nucleolar protein. Nucleic Acids Res 1986; 14:6803-20.
48. Portman DS, Dreyfuss G. RNA annealing activities in HeLa nuclei. EMBO J 1994; 13:213-21.
49. Munroe SH, Dong XF. Heterogeneous nuclear ribonucleoprotein A1 catalyzes RNA.RNA annealing. Proc Natl Acad Sci USA 1992; 89:895-9.
50. Cobianchi F, Calvio C, Stoppini M, Buvoli M, Riva S. Phosphorylation of human hnRNP protein A1 abrogates in vitro strand annealing activity. Nucleic Acids Res 1993; 21:949-55.
51. Ammerman ML, Fisk JC, Read LK. gRNA/pre-mRNA annealing and RNA chaperone activities of RBP16. RNA 2008; 14:1069-80.
52. Schreiber G, Haran G, Zhou HX. Fundamental aspects of protein-protein association kinetics. Chem Rev 2009; 109:839-60.
53. Nedbal W, Frey M, Willemann B, Zentgraf H, Sczakiel G. Mechanistic insights into p53-promoted RNA-RNA annealing. J Mol Biol 1997; 266:677-87.
54. Nedbal W, Homann M, Sczakiel G. The association of complementary ribonucleic acids can be strongly increased without lowering Arrhenius activation energies or significantly altering structures. Biochemistry 1997; 36:13552-7.
55. Muller UF, Goringer HU. Mechanism of the gBP21-mediated RNA/RNA annealing reaction: matchmaking and charge reduction. Nucleic Acids Res 2002; 30:447-55.
56. Hitti E, Neunteufel A, Jantsch MF. The double-stranded RNA-binding protein X1rbpa promotes RNA strand annealing. Nucleic Acids Res 1998; 26:4382-8.
57. Lee CG, Zamore PD, Green MR, Hurwitz J. RNA annealing activity is intrinsically associated with U2AF. J Biol Chem 1993; 268:13472-8.
58. Muller UF, Lambert L, Goringer HU. Annealing of RNA editing substrates facilitated by guide RNA-binding protein gBP21. EMBO J 2001; 20:1394-404.
59. Schumacher MA, Karamooz E, Zikova A, Trantirek L, Lukes J. Crystal structures of *T. brucei* MRP1/MRP2 guide-RNA binding complex reveal RNA matchmaking mechanism. Cell 2006; 126:701-11.

60. Furtig B, Wenter P, Reymond L, Richter C, Pitsch S, Schwalbe H. Conformational dynamics of bistable RNAs studied by time-resolved NMR spectroscopy. Journal of the American Chemical Society 2007; 129:16222-9.
61. Rajkowitsch L, Chen D, Stampfl S, Semrad K, Waldsich C, Mayer O, et al. RNA chaperones, RNA annealers and RNA helicases. RNA Biol 2007; 4:118-30.
62. Grossberger R, Mayer O, Waldsich C, Semrad K, Schroeder R. Influence of RNA structural stability on the RNA chaperone activity of the *E. coli* portein StpA. Nuc Acids Res 2005; 33:2280-9.
63. Mohan S, Hsiao C, VanDeusen H, Gallagher R, Krohn E, Kalahar B, et al. Mechanism of RNA double helix-propagation at atomic resolution. The journal of physical chemistry 2009; 113:2614-23.
64. Porschke D. A direct measurement of the unzippering rate of a nucleic acid double helix. Biophysical chemistry 1974; 2:97-101.
65. Porschke D. Model calculations on the kinetics of oligonucleotide double helix coil transitions. Evidence for a fast chain sliding reaction. Biophysical chemistry 1974; 2:83-96.

Published online 4 February 2011

Nucleic Acids Research, 2011, Vol. 39, No. 10 ***4405–4418***
doi:10.1093/nar/gkq1339

The RNA annealing mechanism of the HIV-1 Tat peptide: conversion of the RNA into an annealing-competent conformation

Martina Doetsch, Boris Fürtig, Thomas Gstrein, Sabine Stampfl and Renée Schroeder*

Max F. Perutz Laboratories, Dr Bohrgasse 9/5, 1030 Vienna, Austria

Received October 12, 2010; Revised December 17, 2010; Accepted December 19, 2010

ABSTRACT

The annealing of nucleic acids to (partly) complementary RNA or DNA strands is involved in important cellular processes. A variety of proteins have been shown to accelerate RNA/RNA annealing but their mode of action is still mainly uncertain. In order to study the mechanism of protein-facilitated acceleration of annealing we selected a short peptide, HIV-1 Tat(44–61), which accelerates the reaction efficiently. The activity of the peptide is strongly regulated by mono- and divalent cations which hints at the importance of electrostatic interactions between RNA and peptide. Mutagenesis of the peptide illustrated the dominant role of positively charged amino acids in RNA annealing—both the overall charge of the molecule and a precise distribution of basic amino acids within the peptide are important. Additionally, we found that Tat(44–61) drives the RNA annealing reaction via entropic rather than enthalpic terms. One-dimensional-NMR data suggest that the peptide changes the population distribution of possible RNA structures to favor an annealing-prone RNA conformation, thereby increasing the fraction of colliding RNA molecules that successfully anneal.

INTRODUCTION

As with proteins, the folding of RNA molecules into their native and functional structure is a non-trivial problem (1,2). These folding problems are not only *in vitro* artefacts but do also exist *in vivo* (3,4). It is assumed that certain proteins assist refolding events *in vivo* in a non-specific and ATP-independent manner and thereby support RNA molecules in the process of obtaining their native structure. These proteins have been defined as 'RNA chaperones'; proteins 'that resolve misfolded structures' (1,5). Although most proteins that were shown experimentally to assist nucleic acid folding in a non-specific way were named nucleic acid chaperones (1,6), we recently demonstrated the necessity of discriminating between the mere acceleration of annealing and actual unfolding of RNA structures (7). As proteins can have either only one or both of these two activities, we suggested the following nomenclature: (i) 'nucleic acid annealers' are proteins that, with no sequence-specificity, accelerate annealing of complementary nucleic acids but are not able to dissolve RNA structures. (ii) 'RNA chaperones' destabilize RNA double-stranded nucleic acid regions (and might in addition accelerate annealing). The necessity of this discrimination is supported by the finding that some DEAD-box RNA helicases exert strand displacement activity in the presence of ATP but are not able to dissolve RNA structures in the absence of ATP, while still retaining their ability to accelerate annealing. For the human RNA helicase II/Gu protein even the physical separation of RNA unwinding and annealing activities was shown (8,9). RNA annealers and chaperones are extremely diverse and do not share a common amino acid motif (5). It is thus not clear which sequence or structural features determine whether a protein exhibits only one or both of the mentioned activities.

Proteins with nucleic acid annealing activity have been found in viruses (10 12), bacteria (13 15) and eukaryotes (6,16 28). The biological role of proteins with annealing activity ranges from bacterial translational regulation to the maturation of eukaryotic transcripts and RNA editing in kinetoplastid organisms. Due to the complexity and difficulty of *in situ* annealing assays, the potential role of nucleic acid annealers has so far only been assayed in *in vitro* experiments. Thus, the question whether they also exert the characterized activity on the described substrates *in vivo* remains unanswered.

All groups that studied protein-accelerated annealing in greater detail concordantly found basic amino acids to be

*To whom correspondence should be addressed. Tel: +43 1 4277 54690; Fax: +43 1 4277 9546; Email: renee.schroeder@univie.ac.at

crucial for, and high salt concentrations to be detrimental to, the annealing activity (18,20,26,27). The proposed mechanisms for annealing acceleration are: (i) active increase of local RNA concentration, (ii) stabilization of the annealing transition state by shielding the negative RNA backbone charges, (iii) 'conversion' of the RNA into an annealing-prone conformation (17,19,29). However, the following questions remain unanswered: do amino acids other than positively charged ones play a role for the annealing activity? Do nucleic acid annealers share a common mechanism or distinct features? Is there a more precise definition of amino acid composition and arrangement in nucleic acid annealers? Here, we used a model RNA annealer protein to address these questions.

The HIV-1 transactivator of transcription (Tat) is one of the early regulators of the viral life cycle. By binding to the TAR RNA, a structure formed by the nascent viral transcript, Tat recruits cellular factors to the HIV-1 promoter and indirectly stimulates viral transcription. (30,31) Tat was also suggested to play a role in other cellular and viral processes including translation (32), interaction with the RNAi machinery (33 35), PKR regulation (36,37), viral mRNA capping (38) and reverse transcription (39 41).

More recently, the Tat protein as well as its fragment Tat(44 61) were found to exhibit nucleic acid chaperone activity (42). In Tat(44 61), which comprises the basic domain and part of the core domain of the full-length protein, the authors claimed to have found the smallest known RNA chaperone to date. Due to its small size we selected Tat(44 61) as a model peptide for our studies on proteins that assist RNA folding.

Although we could not reproduce the protein's RNA strand displacement activity, the full-length Tat protein and its fragment Tat(44 61) are potent nucleic acid annealers. We subjected Tat(44 61) to a detailed mutational analysis to identify the amino acids that are crucial for the annealing activity of the peptide. We confirmed the essential role of basic amino acids, but also found evidence for the contribution of polar amino acids that can potentially hydrogen bond with the RNA backbone. We found the peptide's overall charge and the arrangement of basic amino acids within the peptide important for RNA annealing acceleration. Furthermore, we demonstrated that the acceleration of annealing is conferred by an increase in transition state entropy. One-dimensional (1D) ^{1}H NMR data show that the population of possible RNA structures is changed in the presence of Tat(44 61). Thus, either the peptide selectively binds a preexisting RNA conformation and thereby shifts the equilibrium or it changes the structure of the RNA molecule upon binding. In either case the abundance of annealing-prone RNA conformations is increased which raises the fraction of colliding RNA molecules that efficiently anneal with each other.

MATERIALS AND METHODS

RNAs and peptides

All RNAs used were synthesized on solid phase (Eurogentech). Lyophilized RNAs were dissolved in DEPC water and stored at −20 or at −80°C (for long-term storage). The nucleic acid substrates used for the FRET-based assay in this study are listed in Supplementary Table S1.

Synthetic peptides were provided by ThermoFischer Scientific, peptides scr1-3, K7A R13A and K7A R9A R13A were a generous gift of Peter Steinlein, Research Institute for Molecular Pathology Vienna, Austria. The peptides were dissolved in DEPC water, aliquoted, freeze-dried and stored at −20°C. Shortly before use they were dissolved and diluted in 30 mM Tris HCl pH 7, 30 mM NaCl and 1 mM DTT. Mass spectrometry results confirmed the sequence identity and integrity of Tat(44 61) that had been stored lyophilized at −20°C for several months. Although modifications (such as hydrolysis) of the peptide upon short-time storage in solution are unlikely, we cannot completely exclude this possibility. The fact that the peptide can accelerate annealing of two complementary sequences, however, hints at it being active. The recombinant full-length Tat protein was delivered in a freeze-dried form by Jena Bioscience and dissolved in degassed 100 mM Tris HCl pH 7.5, 150 mM NaCl and 10 mM DTT. The full-length Tat protein is very sensitive to inactivation through oxidation and aggregation (43) and is thus difficult to handle. We excluded degradation of the protein on SDS PAGE and confirmed the correct protein sequence by mass spectrometry. Furthermore, we took precautions to avoid oxidation of the protein such as degassing all solutions.

FRET-based annealing and strand displacement assays

Combined nucleic acid annealing and strand displacement assays as well as annealing assays were carried out as described by Rajkowitsch and Schroeder (2007) (44), at 30°C if not indicated otherwise, and using the following concentrations: 10 nM of each RNA strand, 50 mM Tris HCl in the pH range of 6.5 8, 2 mM DTT and salt concentrations as indicated in the text. Annealing curves were fitted by non-linear regression to the following second-order reaction equation using GraphPadPrism® (with Y being the normalized FRET index and the time X):

$$Y = \text{amplitude} \times \left(1 - \frac{1}{k_{\text{obs}} \times X + 1}\right). \quad (1)$$

Filter binding assays

Filter binding assays were conducted according to ref. (45) with the following changes: the reaction buffer contained 50 mM Tris HCl pH 7, 2 mM DTT and 6% glycerol. Reactions were incubated for 5 min at room temperature before filtering. Binding curves were fitted to a Hill equation [Equation (2)] using GraphPadPrism®. (Y, relative amount of filter-bound RNA; $B_{\max}$, maximally bound RNA; h, Hill coefficient; K_D, binding constant; X, peptide concentration)

$$Y = \frac{B_{\max} \times Y^h}{K_D^h + X^h}. \quad (2)$$

Due to reproducibility problems of absolute K_D values and Hill coefficients which have also been faced by other groups (Michael F. Jantsch, personal communication), we moved on to recording binding curves for the mutant of interest (or the wild-type peptide under the salt condition of interest) in parallel with the wild-type mutant under no salt conditions. We thus obtained relative K_D values and Hill coefficients. Other common techniques to determine binding constants, like mobility shift assays, quenching methods and ITC, were not applicable to our system due to their specific limitations.

Aggregation assays

Aggregation through proteins was measured on the basis of the sedimentation assay described by Vo *et al.* (46). Ten nanomolar ^{32}P-labeled single-stranded 21R$^+$ RNA or double-stranded 21R RNA were incubated at 30°C for 3 min in aggregation buffer (50 mM Tris HCl pH 7, 2 mM DTT, NaCl and $MgCl_2$ concentrations as indicated in each single experiment) in the presence or absence of 100 300 nM Tat(44 61) or ~0.1 μg/μl BSA (NEB), total volume 40 μl. After a 10 min centrifugation at 13.4 × g at room temperature, 5 μl of the supernatant were removed carefully and subjected to Scintillation analysis.

Gel annealing and strand displacement assays

Due to temperature limitations of the multiplate reader, the rate constants' temperature dependence was measured using gel annealing assays: 10 nM Cy5-labeled 21R$^+$ were pre-incubated with or without 300 nM peptide in 50 mM Tris HCl pH 7, 0.5 mM $MgCl_2$ and 2 mM DTT final concentrations at the temperature of interest. The annealing reaction was started by adding 10 nM final concentration of Cy3-labeled 21R$^-$. Ten microliter-aliquots were taken after the indicated time points, mixed with 2.5 μl 5× stop buffer (3 μM 21R$^+$, 2% SDS, 150 mM EDTA, 15% sucrose, 12.5% ficoll) and directly loaded onto a running 15% native PAGE (1× TBE). Fluorescent signals of both Cy5 and Cy3 were scanned with a Typhoon™ 9400 (GE Healthcare), quantified with ImageQuant™ and annealing curves were fitted to Equation (1) using GraphPadPrism®.

The full-length Tat protein is susceptible to aggregation (43) which disturbed the fluorescent signal in the FRET-based assay so that an evaluation of the resulting curves was not possible. We thus carried out gel strand displacement assays. Strand displacement gel assays were conducted in a similar way to the annealing gels, apart from the following changes: to start the reaction a 10-fold excess of competitor was added to an already formed double-stranded substrate. The reaction was stopped using a 2.5× stop buffer containing 60 mM EDTA, 0.5 mg/ml yeast tRNA, 0.6% SDS, 30% sucrose and 12.5% ficoll.

Calculations of kinetic parameters

The reaction constants k_{obs}, determined at different temperatures, were divided by the RNA concentration used in the gel annealing assay. From these normalized rate constants, k, an Arrhenius plot was derived (17,47). The slope of the Arrhenius plot yielded the activation energy E_a of the annealing reaction (R gas constant):

$$E_a = \text{slope} \times (-R). \quad (3)$$

The free activation energy $\Delta G^{\neq}$ was derived according to the Eyring Polyani relation (48) from the normalized rate constant k at a specific temperature T:

$$\Delta G^{\neq} = -RT \ln\left(\frac{k \times h}{k_B \times T}\right) \quad (4)$$

(h Planck's constant equivalent to 6.626×10^{-34} Js, k_B Boltzmann's constant equivalent to 1.381×10^{-23} JK^{-1}).

Based on E_a and $\Delta G^{\neq}$, the thermodynamic parameter enthalpy $\Delta H^{\neq}$ and entropy $\Delta S^{\neq}$ were calculated using Equations (5) and (6).

$$\Delta H^{\neq} = E_a - RT, \quad (5)$$

$$\Delta S^{\neq} = -\frac{1}{T} \times \left(\Delta G^{\neq} - \Delta H^{\neq}\right). \quad (6)$$

Interaction between RNA and peptide: NMR spectroscopy

To probe the interaction between RNA and peptide, a series of titration NMR experiments were recorded. Spectra were measured at temperatures between 273 and 320 K on either a Varian 600 MHz spectrometer equipped with a z-grad HCN probe or a Bruker 700 MHz spectrometer equipped with a cryogenic z-grad HCN probe. In all samples H_2O was exchanged with D_2O by multiple cycles of freeze-drying and resolvation in 99.999% D_2O (Sigma Aldrich). ^{1}H pulses were applied at the resonance of the water frequency with field strength of 15.6 kHz. One hundred and twenty-eight transients were averaged, the relaxation delay was set to 1.5 s and the spectral width was 10 ppm. Hard power pulses were applied at the water frequency, 16 kpts were recorded for t_1. Spectra were processed and analyzed using NMRpipe and NMRdraw (49). For processing, an exponential window function with a LB factor of 1.5 Hz was applied.

Starting from an idealized A-form helical 21R$^+$ RNA (the structure was calculated with CNS using a restrained TAD simulated annealing protocol starting from an extended structure and applying canonical A-form restraints) the chemical shifts were calculated using the program NUCHEMICS (50,51) and were subsequently translated into NMR spectra with the NMRSIM module of TOPSPIN. ^{1}H chemical shifts are referenced directly to TSP as an external reference. Notably, upon addition of peptide to the RNA sample a white precipitate appeared which we assumed to be a fraction of the RNA peptide complex. Precipitation was probably caused by high working concentrations (400 μM RNA and 400 or 800 μM peptide). Thus, the concentration of peptide and RNA in solution was somewhat smaller than intended.

RESULTS AND DISCUSSIONS

Tat and its fragment Tat(44–61) have nucleic acid annealing activity, but no strand displacement activity

The assays conducted and described by Kuciak *et al.* (42) implied that the HIV-1 Tat protein possesses two distinct activities: namely acceleration of annealing and destabilization of nucleic acid structures. Although some of these assays made use of potential natural substrates of Tat, both the RNA ribozyme and the RNA *trans*-splicing assay suggested that the protein has sequence non-specific RNA chaperone activity.

In order to confirm the described activities we used Tat(44–61) in a two-phase FRET-based assay (Figure 1A) that has previously been described and used for several potential RNA chaperone proteins (14,44). As anticipated, Tat(44–61) considerably accelerated annealing of the 21R substrate (Supplementary Table S1), a 21 base-pair long, blunt-ended, artificial RNA duplex [T_m = 72.4°C, calculated using the DINAMelt server (52)] (Figure 1B, phase I). The peptide was however not active in the second (strand displacement) phase of the assay while the positive control StpA efficiently catalyzed strand displacement. Remarkably, Tat(44–61) also accelerated annealing of the DNA substrate 21D while not catalyzing strand displacement by a competitor DNA (Supplementary Figure S1). To exclude the possibility of the 21R double-stranded substrate being too stable for peptide mediated unfolding we used the jm1 substrate which has a lower GC content (T_m = 49.3°C), with the same result (Supplementary Table S1 and Figure S2C). Some proteins are known to need a single-stranded or helical binding platform to perform double-strand unwinding (8). To test this possibility for Tat(44–61) we used a 46 nt RNA, which forms a short hairpin at the 3′-end, together with a partly complementary 21-mer in the combined FRET-based assay (jm1heli substrate). Annealing of this substrate was accelerated by the peptide, whereas no strand displacement was detected (Supplementary Figure S2D). Other variations of the assay included using different temperatures (30 and 37°C), testing several peptide to nucleotide ratios (10 nM to 1 mM peptide per 10 nM RNA), changing the concentrations of $MgCl_2$ and NaCl, using exactly the same buffer composition as described by ref. (42) (buffer A) as well as testing peptide buffers with different $ZnCl_2$ concentrations. While we could always detect an acceleration of annealing, the peptide did not catalyze strand displacement under any of the applied conditions (Supplementary Figure S2A, B, E and F).

To test the full-length Tat protein's ability to promote strand displacement we conducted polyacrylamide gel assays using the 21R substrate, with CsdA as a positive control (Supplementary Figure S3). Again, we could not detect an RNA chaperone activity.

To ensure that the contradiction in results were not caused by a limitation in our assay we carried out the DNA strand displacement assay as described by Kuciak *et al.* (42) (Supplementary Figure S4) and the *trans*-splicing assay (53) (Supplementary Figure S5).

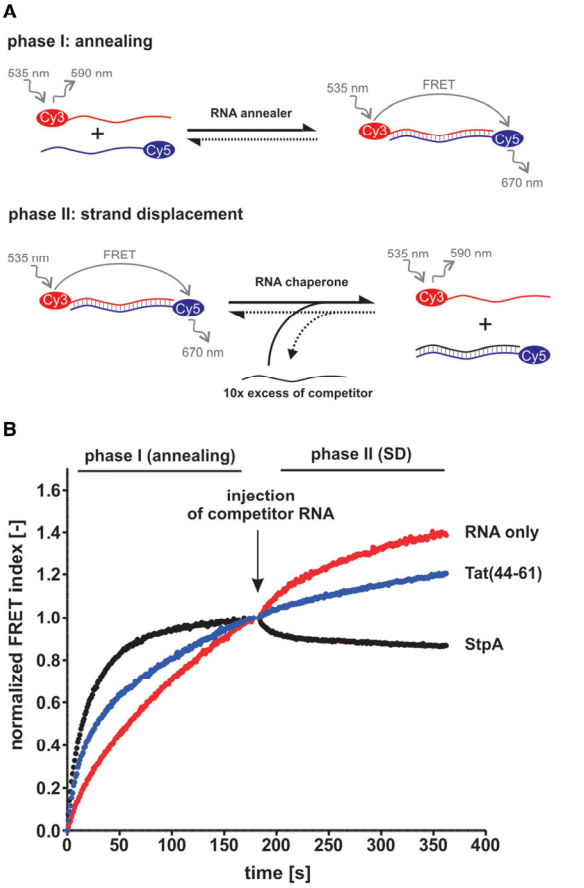

Figure 1. Tat(44–61) accelerates annealing of two complementary RNAs but does not promote strand displacement. (**A**) Scheme of the FRET-based combined annealing and strand displacement (SD) assay according to Rajkowitsch and Schroeder (44). Two short complementary RNAs, labeled with a Cy3- (donor) and a Cy5-dye (acceptor), respectively, are annealed in a microplate (phase I). The close proximity of the two dyes results in a fluorescence resonance energy transfer (FRET) when the donor dye is excited. Both fluorescent emission signals are measured at 1 s intervals using a microplate reader, and the FRET index is calculated as the ratio of the FRET to the Cy3-signal. Strand displacement is detected in phase II of the assay which is started through the addition of an unlabeled competitor RNA and results in a decrease of the FRET signal. (**B**) The assay was conducted with 21R RNA in the absence or presence of 1 μM Tat peptide and at 30°C. *E. coli* StpA (1 μM) was used as a positive control. For clarity, the FRET index was normalized to 1 (phase I and II) and 0 (only phase I).

Despite all positive controls showing activity, we could not reproduce the reported activities of the full-length Tat protein and Tat(44–61) in these RNA chaperone assays.

We therefore conclude that Tat and its fragment are facilitators of annealing but not RNA chaperones. Due to its strong annealing activity, the small size, good availability and easy handling of Tat(44–61) we used it as a model RNA annealer and studied its annealing activity in greater detail.

The annealing activity of Tat(44–61) is dependent on the concentration of mono- and divalent cations

Tat(44–61) accelerated annealing with very similar k_{obs} between pH 6.5 and 7.5 (Supplementary Figure S6). We thus measured acceleration of annealing at pH 7. We also tested the influence of mono- and divalent cations on the peptide's activity (Figure 2). Consistent with the kinetic salt effect, the reaction constant of the 'RNA only' reaction increased with rising NaCl or $MgCl_2$ concentration (47). In comparison to 'no salt' conditions 100 mM NaCl and 10 mM $MgCl_2$ accelerated annealing 1.5- and 3-fold, respectively (data not shown). Tat(44–61) does not require any cations for its annealing activity: the peptide accelerated annealing ~7- to 8-fold when no or only low amounts of ions were present. These k_{acc} values [with $k_{acc} = k_{obs}(peptide)/k_{obs}(RNA\ only)$] are in good agreement with the calculated acceleration of annealing measured with gel annealing assays (k_{acc} = 6 and 9.5 at 10 or 20°C, respectively, as derived from the k_{obs} values in Figure 6).

Acceleration of annealing by Tat(44–61) was strongly impaired at $MgCl_2$ concentrations >2 mM and NaCl concentrations above 60 mM (Figure 2). Similar dependences on $MgCl_2$ concentrations have been reported for HIV-1 NCp7 although the nucleocapsid protein was tolerant for NaCl concentrations of up to 90 mM (10). Both Na^+ and Mg^{2+} ions have been shown to compete with positively charged peptides for the interaction with RNA (54,55). Thus, the dependence of the peptide's activity on the ion concentration hints at the importance of ionic interactions between the peptide's basic amino acids and the negatively charged RNA backbone for the acceleration of annealing by Tat(44–61).

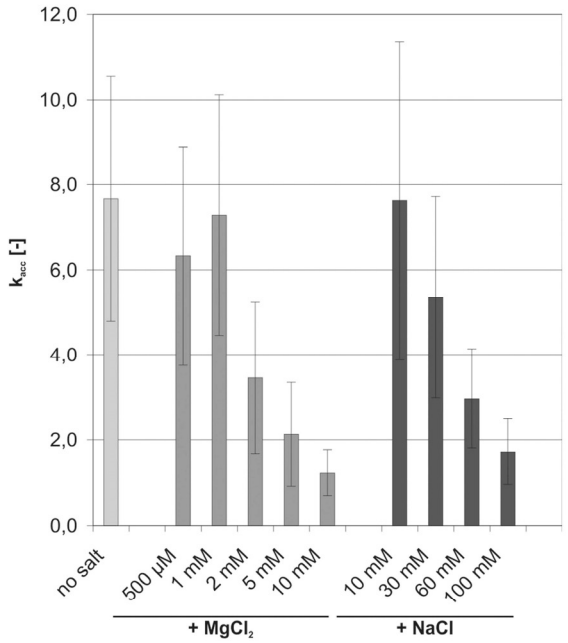

Figure 2. Mono- and divalent cations are detrimental to the peptide's annealing activity. FRET-based annealing assays with 21R RNA were carried out in the absence or presence of 300 nM Tat(44–61), and at different $MgCl_2$ and NaCl concentrations. The reaction constants (k_{obs}) of the reaction in the presence of peptide were divided by the k_{obs} of the 'RNA only' reaction, yielding k_{acc}. Acceleration of annealing by the peptide was strongly impaired at $MgCl_2$ concentrations above 2 mM and NaCl concentrations >60 mM.

All basic amino acids are similarly important for the annealing activity of Tat(44–61)

The importance of basic amino acid stretches in nucleic acid annealing was reported by several groups (10,17–20,26,56,57) and is now generally accepted, although the specific role of the positive charges during the annealing process is under debate and might differ for each protein. The presence of eight basic residues in the 18 amino acid long sequence of Tat(44–61) supports the hypothesis of a mainly charge driven annealing acceleration process. The small size of the Tat peptide prompted us to explore the contribution of individual amino acids to its activity.

A set of peptides with single amino acid substitutions was therefore tested for their annealing activity in our FRET-based annealing assay (Figure 3, Supplementary Figure S7). Figure 3B shows the mutants' k_{obs} normalized to the wild-type k_{obs}. Relative k_{obs} values were confirmed for a few selected mutants using gel annealing assays (data not shown).

Strikingly, each time a basic amino acid was replaced by an alanine the peptide's activity was decreased by a factor of three. The position of the exchanged residue within the primary sequence did not seem to be important at all. Furthermore, the Y4R mutant in which a charge was added to the peptide was more active than the wild-type peptide while the Y4Q mutant did not accelerate annealing any different from Tat(44–61). The double and triple mutants (K7A R13A and K7A R9A R13A) did not accelerate annealing under the tested conditions. Only when we added mutant peptide amounts in the 10 µM range could we detect an activity similar to the activity of 300 nM wild-type peptide (Supplementary Figure S8).

The mutation of the polar amino acids serine (at position 3) and glutamine (position 11) that could theoretically interact with the RNA via hydrogen bonds or Van der Waals interactions did not show an effect. However, the exchange of isoleucine (position 2) for a threonine increased the peptide's annealing activity. The additional threonine might either enhance the activity indirectly, for example by increasing the peptide's stability and/or solubility. Alternatively, it might act directly by interacting with the RNA. Threonine has indeed often been shown to make contacts with phosphates of the nucleic acid backbone (58).

Together, these results demonstrate that the presence of a certain amount of basic residues is indispensable for the peptide to confer RNA annealing acceleration. Amino acids with the ability to hydrogen bond might support the annealing activity. This observation further bolsters the hypothesis of backbone phosphate charges conferring peptide/RNA binding. These (mainly ionic) interactions would explain the promiscuity of the peptide's annealing

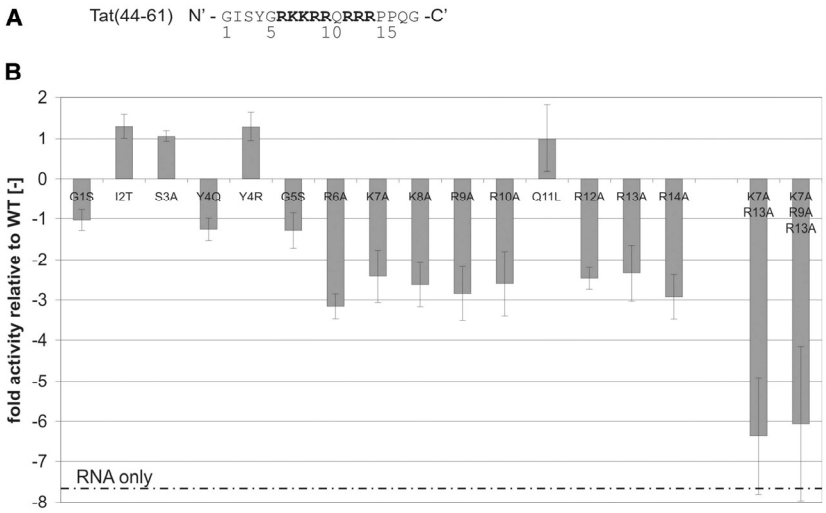

Figure 3. The peptide's basic amino acids are crucial for the acceleration of annealing. (**A**) Amino acid sequence of Tat(44–61) with the positively charged amino acids in bold. (**B**) Different single amino acid mutants and a double and triple amino acid mutant of Tat(44–61) were tested in our FRET-based annealing assay with the 21R RNA pair at 30°C (using 300 nM peptide). Normalized FRET-values were fitted to the monophasic second-order reaction equation yielding the k_{obs} for each peptide mutant. The obtained k_{obs} were used to calculate the mutant activities relative to the WT as follows. In case the k_{obs}(mutant) was higher than the k_{obs}(WT), k_{obs}(mutant) was divided by k_{obs}(WT) and plotted as a positive value. In case of a decreased mutant k_{obs} relative to the WT k_{obs}, k_{obs}(WT) was divided by k_{obs}(mutant) and plotted as a negative value. This calculation method was used in order to emphasize specifically k_{obs} decreases. Notably, the activity of all peptides in which a basic arginine or lysine was exchanged against alanine was reduced by a factor of 2.5–3 relative to the wild-type peptide. The double and triple mutant 'K7A R13A' and 'K7A R9A R13A' did not accelerate annealing detectably at the applied conditions. Two peptide mutants (I2T and Y4R) showed a higher annealing activity than Tat(44–61).

activity towards different RNA substrates as well as DNA. The importance of the overall peptide charge can be partly explained by the peptide screening the nucleic acid surface similarly to metal ions. It is a well known fact that Na^+ and Mg^{2+} stabilize RNA double strands thermodynamically by reducing the electrostatic stress arising from the small distances of the RNA backbone phosphates, with ions that have a higher charge density being more effective stabilizers (59). Thus, they accelerate annealing to a certain degree, especially at higher concentrations. Similarly, the multivalent Tat peptide might accelerate annealing partly because of this screening effect. However, as the magnitude of acceleration of annealing by Tat(44–61) can not be achieved by a simple increase of the salt concentration, there must be a different mechanism that is beyond charge neutralization.

The spatial arrangement of the amino acids in the Tat peptide is important for its activity

The results discussed in the previous section imply that the most important factor that confers annealing activity is the overall charge of the peptide. This could mean that the peptide acts as an octovalent ion. To assess the question as to whether a specific spatial arrangement of basic amino acids within the peptide is important we scrambled the peptide in three different ways (Figure 4A): (i) in the mutant scr1 the eight basic amino acids are distributed evenly over the peptide; (ii) scr3 contains two stretches of basic residues, as does the WT peptide, however these are separated by a larger amount of uncharged amino acids; (iii) scr2 contains only one basic stretch while the other basic residues are more distributed.

Interestingly, all three scrambled peptides are less active than the wild-type peptide in our RNA annealing assay with scr1 being more active than scr2 and scr3 (Figure 4B). Thus, the overall charge [which is the same for scr1-3 and Tat(44–61)] alone is not sufficient to account for the extent of RNA annealing activity. In every charged molecule only a limited number of the charged amino acids can participate in the interaction with the binding partner due to structural reasons. Quantitatively, this is expressed by the effective charge Z_{eff} as opposed to the overall charge (55). Changing Z_{eff} by scrambling the Tat peptide sequence is likely, even though we expect a peptide of only 18 amino acids length to be extremely flexible which might result in a similar mean Z_{eff} in the WT and scr1-3. We hypothesize that, apart from maintaining a certain effective charge, an annealing competent protein positions its positively charged residues in a well-defined (but still unknown) manner in space in order to facilitate rather defined interactions between amino acids and nucleic acids.

Binding strength and annealing activity do not correlate

We tested RNA binding of two different peptide mutants as well as of the wild-type peptide using filter binding assays. The RNA of interest was the single-stranded $21R^+$, one of the RNA strands used for the FRET-based annealing assay. We always recorded binding curves for the mutant peptide of interest in parallel with the wild-type. We thus obtained relative K_D values and

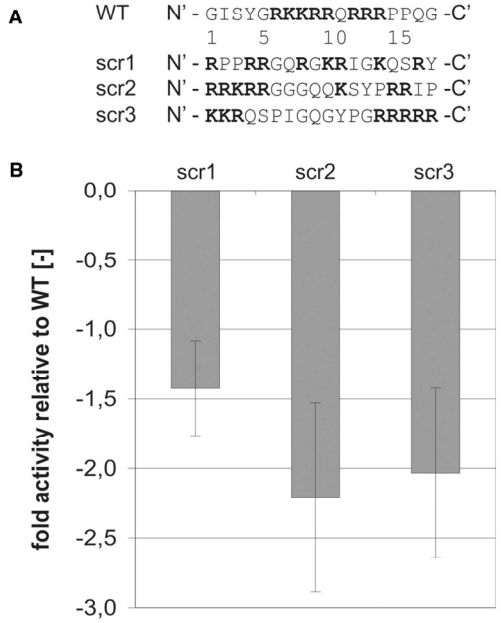

Figure 4. The spatial arrangement of basic amino acids within the peptide is important for annealing activity. (**A**) Primary sequences of scrambled peptides with the same amino acid composition as the WT Tat(44–61) peptide. (**B**) The FRET-based annealing assay using 21R RNA was carried out at 30°C. The obtained reaction constant k_{obs} of each peptide mutant was normalized to the WT k_{obs}, yielding the 'fold activity relative to the WT'. Interestingly, all scrambled peptides containing the same amount of basic amino acids as Tat(44–61) were less active than the WT.

relative Hill coefficients (Table 1). The wild-type K_D as measured in 16 independent experiments was 1110 ± 434 nM. The R13A mutant's K_D is slightly higher than the wild-type's K_D while the Hill factor remains unchanged. The K7A R13A mutant's K_D is double that of the wild-type's binding constant. The different RNA binding strength of this mutant is also reflected in a slightly lower Hill coefficient. The loss of annealing activity of these two mutants is ~70% (R13A) or complete (K7A R13A) at a peptide concentration of 300 nM (see Figure 3B). Thus, the mutants' loss of activity is not reflected in their binding constants.

We could therefore confirm the missing correlation between RNA annealing activity and RNA binding as described by several other groups (14,26,60–62). The results suggest that, besides RNA/peptide binding, another process (such as an RNA conformation change) occurs for which a certain amount of basic amino acids is necessary. Considering that the removal of one or two basic amino acids from Tat(44–61) will probably change the peptide's conformation, the spatial arrangement of positive charges might also play a role in this process.

Tat(44–61) does not accelerate annealing through aggregation

One of the suggested mechanisms for protein accelerated annealing is the increase of the local nucleic acid concentration. Several studies have shown that HIV-1 nucleocapsid protein Ncp7 induces the sequence non-specific aggregation of nucleic acids which is considered to be a major element of its chaperone activity (46,63–67). Besides proteins, different multivalent cations such as spermidine and spermine compact and aggregate nucleic acids via electrostatic interactions (68,69) and thus it was suggested that highly positively charged annealing competent proteins in general accelerate annealing via this mechanism.

Table 1. Binding constants for peptide-RNA binding of two different peptide mutants relative to the WT peptide

	R13A	K7A R13A
k_{obs} (mutant): k_{obs} (WT) [–]	0.43 ± 0.10	0.16 ± 0.04
K_D (mutant): K_D (WT) [–]	1.23 ± 0.13	2.27 ± 0.31
h (mutant): h (WT) [–]	1.07 ± 0.16	0.87 ± 0.10

Relative K_D values and Hill factors h were calculated from three independent sets of filter binding experiments. For comparison, the k_{obs} for mutant peptide accelerated annealing relative to the wild-type reaction constant is additionally listed.

To address this hypothesis, we tested whether Tat(44–61) aggregates RNA with a simple centrifugation assay (46). We found the peptide to be positive in this assay using single-stranded $21R^+$ (Figure 5A) and double-stranded 21R RNA (data not shown). However, the addition of BSA to the reaction prevented Tat(44–61) caused depletion of RNA from the solution almost completely. Interestingly, BSA had no influence on the annealing activity of Tat(44–61) as assayed with the FRET-based annealing assay (Figure 5B). We therefore assume that the observed 'aggregation' was due to non-specific binding of the Tat peptide to test tube walls and that in contrast to Ncp7 no aggregates were formed. Further experiments supported this conclusion. $MgCl_2$ and NaCl concentrations that inhibited annealing acceleration by the Tat peptide (Figure 2) did not affect the outcome of the aggregation assay (Figure 5C and D). In contrast, mono- and divalent ions have been shown to strongly influence Ncp7 induced nucleic acid aggregation (63). We could not detect a difference in RNA depletion for the three different peptide concentrations 100, 200 and 300 nM, which showed different magnitudes of annealing activity as well. Shorter centrifugation times resulted in less 'aggregated' RNA for all three concentrations without showing any significant discrimination between the three concentrations (Supplementary Figure S9).

We therefore conclude that nucleic acid aggregation is not the basis for Tat peptide accelerated RNA annealing.

Tat(44–61) increases the entropy of the annealing transition state

To learn more about the mechanism of Tat(44–61)-facilitated annealing we collected annealing rate constants at different temperatures using gel annealing assays (Figure 6A–C). From the temperature dependence of the

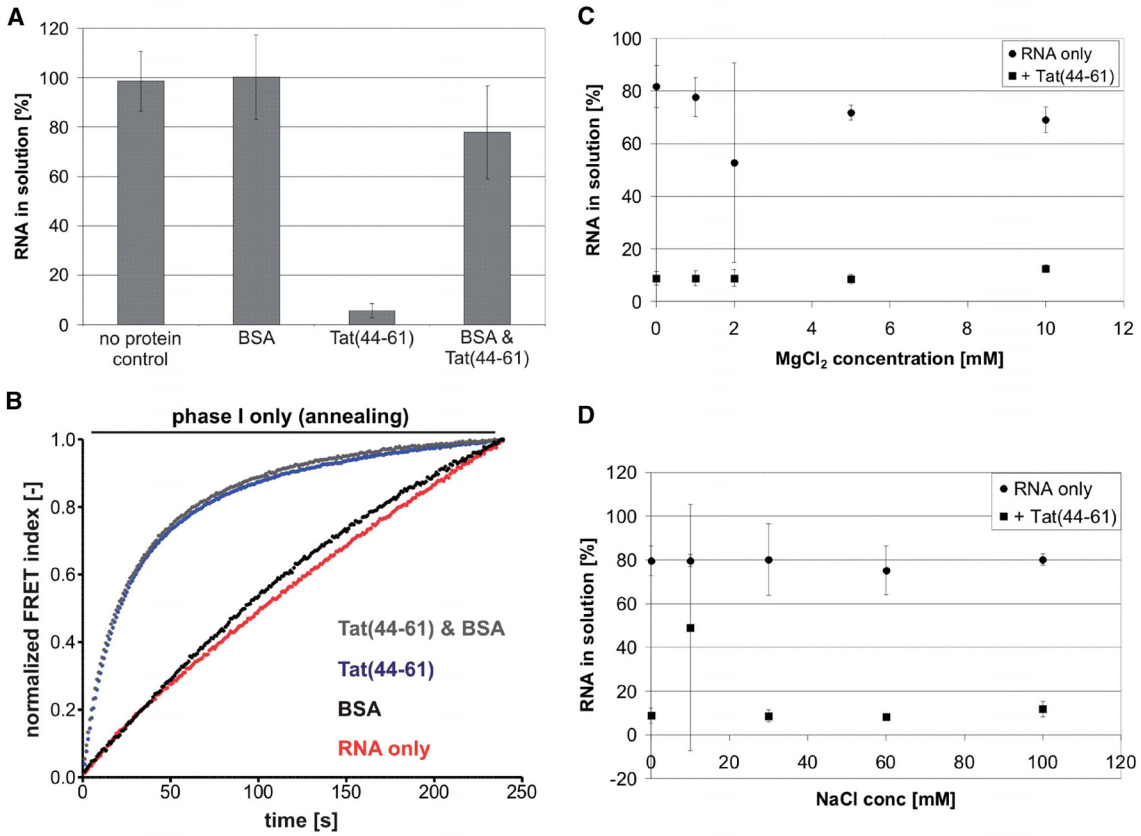

Figure 5. Aggregation and annealing acceleration by the Tat peptide do not correlate. (**A**) Aggregation assays with $21R^+$ ssRNA in the presence of 300 nM Tat(44–61), ~0.1 μg/μl BSA or both proteins were carried out. While BSA did not aggregate the RNA, Tat(44–61) depleted >90% RNA from the solution. In the presence of BSA, however, Tat(44–61) had only a minor aggregation effect. (**B**) Interestingly, the same amount of BSA did not influence the RNA annealing activity of 300 nM of the peptide as determined using the FRET-based annealing assay. (**C** and **D**) RNA aggregation by 300 nM Tat(44–61) was assayed under different $MgCl_2$ and NaCl concentrations that had been shown to inhibit the peptide's annealing activity to a greater or lesser extent. However, no significant difference in measured aggregation was detectable.

rate constant k an Arrhenius plot was drawn (Figure 6D) and thermodynamic parameters of the transition state of annealing (Table 2) were calculated as described previously (29).

The relation between Gibbs free energy, enthalpy and the entropy term are described by the following equation:

$$\Delta G^{\neq} = \Delta H^{\neq} - T \times \Delta S^{\neq}. \quad (7)$$

The Tat peptide increases the activation energy E_a from 40 to 70 kJ/mol and concomitantly the transition enthalpy $\Delta H^{\neq}$ of annealing by 30 kJ/mol which is detrimental to the reaction. Nevertheless, in the presence of the peptide the transition free energy $\Delta G^{\neq}$ is lowered from 40 to 35 kJ/mol. This is also reflected by the increase of the annealing reaction constant by a factor of 9.5 under these conditions. Thus, the peptide-induced $\Delta G^{\neq}$ decrease must be caused by entropic rather than enthalpic terms. Consistently, the transition entropy $\Delta S^{\neq}$ is increased significantly in the presence of Tat(44–61) (Table 2). A similar thermodynamic effect on RNA annealing has so far been shown only for the chemical CTAB (29) and (with a not as pronounced magnitude) for the tumor suppressor protein p53 (17). The interaction of positively charged peptides with nucleic acids is generally accompanied by a counterion and water release which results in a considerable entropy increase (55,70). This entropy increase is driven solely by the net charge of the peptide, and not the amino acid arrangement (54). A very recent study on thermodynamics of binding of the Tat fragment Tat(46–60) to the TAR RNA confirmed an entropy increase of the system through RNA–peptide interaction (71). The calculated entropy increase through non-specific binding at 80 mM NaCl $\Delta S^{\text{binding}}$ was determined to be 63 ± 4 J/(mol K), which is in the same range as our calculated entropy increase for the transition state. We speculate that, also in the case of RNA/RNA annealing, $\Delta S^{\neq}$ elevation is mainly driven by counterion and water release upon peptide binding. The question that remains unanswered is: What happens to the RNA upon peptide/RNA interaction that accelerates annealing? These processes might either support or counteract the entropic effect of counterion release.

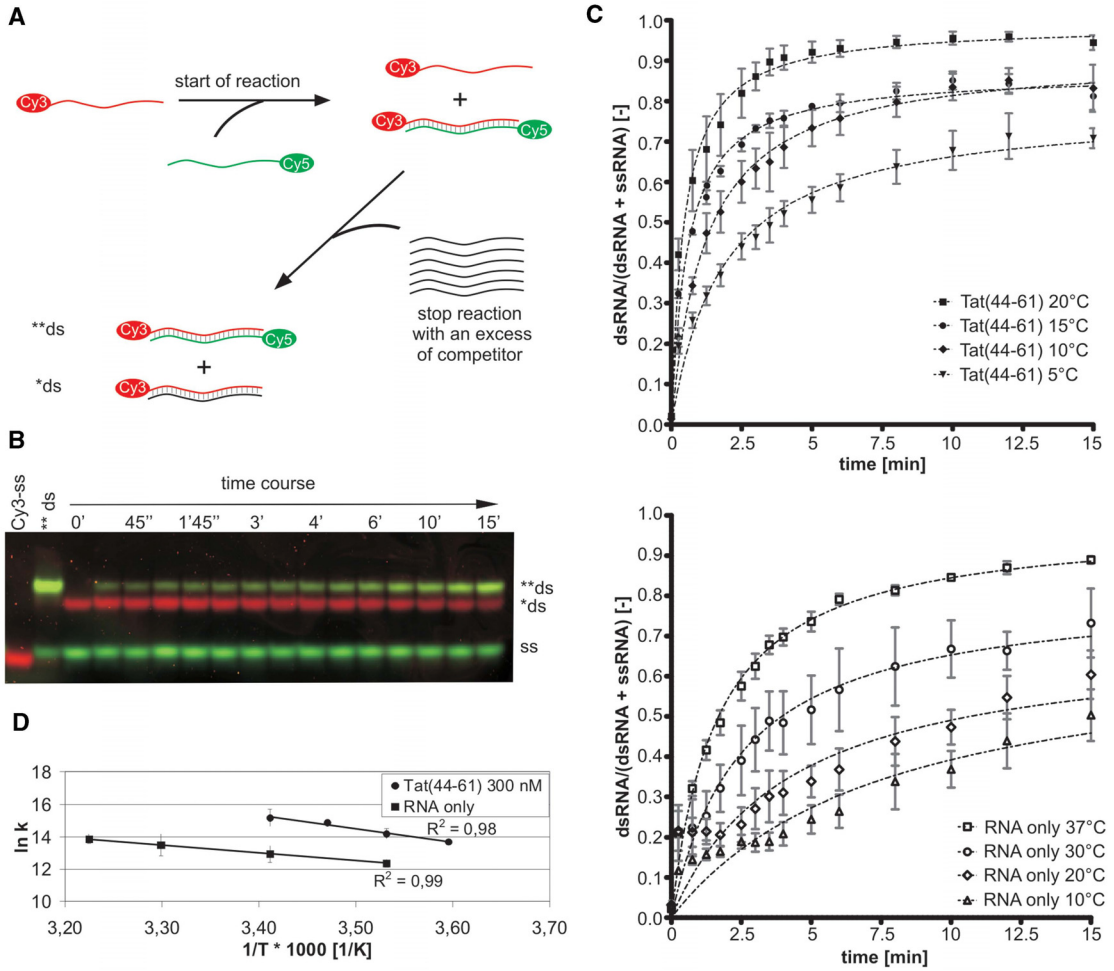

Figure 6. Tat(44–61) increases the transition state entropy of the annealing reaction. (**A**) RNA gel annealing assays were conducted in the absence or presence of protein and at different temperatures. To start the reaction a Cy3-labeled RNA strand was added to the Cy5-labeled complementary RNA. Aliquots were drawn after certain time points and the reaction was stopped with a 60× excess of non-labeled competitor strand. (**B**) The samples were applied directly onto a running native PAGE. Since the Cy5-dyes add 'size' to the RNAs the heteroduplex of two labeled strands (**ds) runs higher than the complex of the Cy3- and the unlabeled strands (*ds). The Cy5- and Cy3-fluorescent signals were scanned and the Cy5-signals from single and double strands were quantified. (**C**) Plotting the ratio of double-stranded RNA to total amount of RNA for each time point of a reaction yielded annealing curves which were fitted with a monophasic second-order reaction equation with equimolar initial reaction concentration. With rising temperature the k_{obs} of the annealing reaction in the presence or absence of 300 nM Tat(44–61) increased. The rate constants k, normalized to the RNA concentration, were as follows: Tat(44–61) 5°C $9.0 \times 10^5\,M^{-1}s^{-1}$ (filled inverted triangle), 10°C $14.5 \times 10^5\,M^{-1}s^{-1}$ (filled diamond), 15°C $29.0 \times 10^5\,M^{-1}s^{-1}$ (filled circle), 20°C $40.0 \times 10^5\,M^{-1}s^{-1}$ (filled square); RNA only 10°C $2.4 \times 10^5\,M^{-1}s^{-1}$ (open triangle), 20°C $4.2 \times 10^5\,M^{-1}s^{-1}$ (open diamond), 30°C $7.3 \times 10^5\,M^{-1}s^{-1}$ (open circle), 37°C $10.6 \times 10^5\,M^{-1}s^{-1}$ (open square). Means of curves and rate constants k were calculated from three to four independent experiments. (**D**) The natural logarithms of the normalized reaction constants k were plotted against the inverse temperature demonstrating the linear correlation between the two values in the measured temperature range (Arrhenius plot).

Tat(44–61) favors an annealing-competent RNA structure

In order to learn more about the structural influence of Tat(44–61) on its RNA substrate we recorded 1D ^{1}H spectra of the 21R + RNA in the absence or presence of different amounts of Tat peptide and at different temperatures (Figure 7).

The 1D ^{1}H NMR spectra of the 21R$^+$ RNA recorded in 9/1 H_2O/D_2O-buffer did not show any signals in the imino-proton region at a temperature range of 0–47°C (data not shown). Therefore we conclude that under our experimental conditions the RNA molecule does not exhibit any secondary-structure elements that involve base-pair interactions and truly represents an 'unfolded' RNA chain. Changing the solvent from H_2O to D_2O allows recording of the spectra without the deterring effect from water suppression. The same signal pattern of non-exchangeable protons is found, indicating that changing the solvent has no effect on the conformation of the RNA.

The NMR spectra of the 21R$^+$ RNA alone show a strong temperature-dependent behavior in the range between 0 and 47°C (Figure 7). At low temperatures,

Table 2. Thermodynamic data at 20°C derived from the Arrhenius plot in Figure 6

	K ($M^{-1}s^{-1}$)	E_a (kJ/mol)	$\Delta G^{\neq}$ (kJ/mol)	$\Delta H^{\neq}$ (kJ/mol)	$\Delta S^{\neq}$ [J/(mol·K)]
RNA only	4.2×10^5	40 ± 1	40 ± 1	38 ± 1	−8 ± 6
Tat(44–61) 300 nM	4.0×10^6	70 ± 6	35 ± 1	68 ± 6	112 ± 26

Parameters are as follows: k, RNA concentration corrected rate constant of the annealing reaction; E_a, Arrhenius activation energy; $\Delta G^{\neq}$, free activation energy; $\Delta H^{\neq}$, enthalpy; $\Delta S^{\neq}$, entropy.

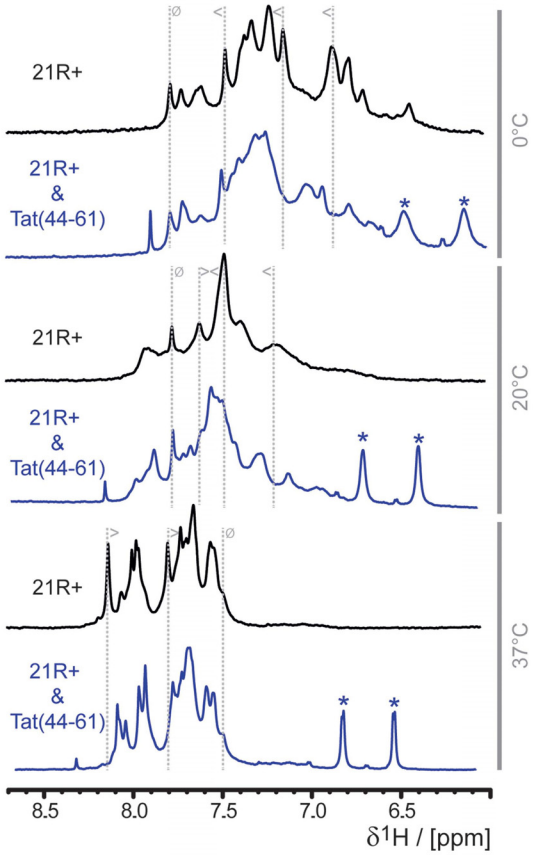

Figure 7. Tat(44–61) selects a specific RNA structure. ^{1}H 1D NMR spectra of 21R$^+$, a 21nt single stranded RNA, in the absence (black) or the presence (blue) of two equivalents of Tat(44–61) at different temperatures (indicated in gray at the right panel of the figure) were recorded. The chemical shifts of the aromatic protons did not overlap with the peptide chemical shifts and serve thus as an indicator for the peptide's influence on the RNA conformation: the only visible peaks of the peptide in this spectral region are stemming from the aromatic protons of Y47 and are marked with asterisks. To follow changes in the spectrum upon addition of peptide gray dotted lines are added exemplarily, the symbol indicate if peaks are shifting upon addition of the peptide (less than and greater than symbol) or show no change (struck through circle).

such as 0°C, distinct signals are detectable and show a reasonable chemical shift dispersion for an RNA void of any canonical structural elements. As displayed in Figure 7 (and Supplementary Figure S10), the peaks of the aromatic protons spread over a spectral region of ~1.3 ppm. As the temperature is increased the dispersion of the signals is lost and the spread of the aromatic protons is narrowed down to ~0.7 ppm at 37°C. Furthermore, the shape of the peaks shows a marked temperature dependence. At temperatures ~20–25°C, the peaks become broad but the line-shape narrows down again when the temperature is further increased to 37°C or higher (Supplementary Figure S10). This behavior is not only observed in the aromatic spectral region, but for all RNA peaks in the whole spectrum (the line-width of signals from buffer molecules stay constant within error over the whole temperature scale). The changes in the spectrum are reversible and multiple cycles of cooling and heating over the indicated temperature range always produces the same spectra. The integrity of the RNA was confirmed by biochemical methods before and after NMR measurements.

For a more analytical evaluation of the experimental spectra, simulated NMR spectra of the 21R$^+$ RNA were generated with the NUCHEMICS software. The simulations were based on two structures of the 21R$^+$ RNA: one representing the single strand in A-form conformation and a second representing a structurally randomized conformation. Although the exact experimental spectrum could not be reproduced by the simulation, the chemical shift dispersion behavior could be reproduced (Supplementary Figure S11). For the aromatic region, the simulated spectra show a dispersion of signals over ~1.8 ppm based on the A-form conformation, whereas the randomized conformation leads to a reduction of chemical shift dispersion down to ~0.8 ppm and an overlap of peaks. Generally, the dispersion in RNA spectra (especially for the aromatic protons in the nucleo-bases) derives from the stacking behavior of the RNA chain. Therefore, the absence of helicality in the RNA reduces the proportion of stacked nucleotides and the effect on the chemical shifts in the NMR spectrum is a reduced chemical shift dispersion.

We conclude that at low temperatures a distinct, probably helical conformation is adopted by the single-stranded 21R$^+$ RNA (Figure 8A). When the temperature is raised, this conformation starts to melt. Around 20–25°C the molecule is no longer best described by a single static conformation but by an ensemble of interconverting partially melted 'helices'. The temperature increase to 47°C converts the 21R$^+$ RNA into similar, unstructured (and most probably unstacked) conformations that give rise to the low dispersion but narrow line-shape signature of the peaks. This observation is in accordance with CD-spectroscopic melting experiments (Supplementary Figure S12). When the CD-temperature row is analyzed for a two-state unfolding process, the melting temperature is determined to be T_m = 38°C

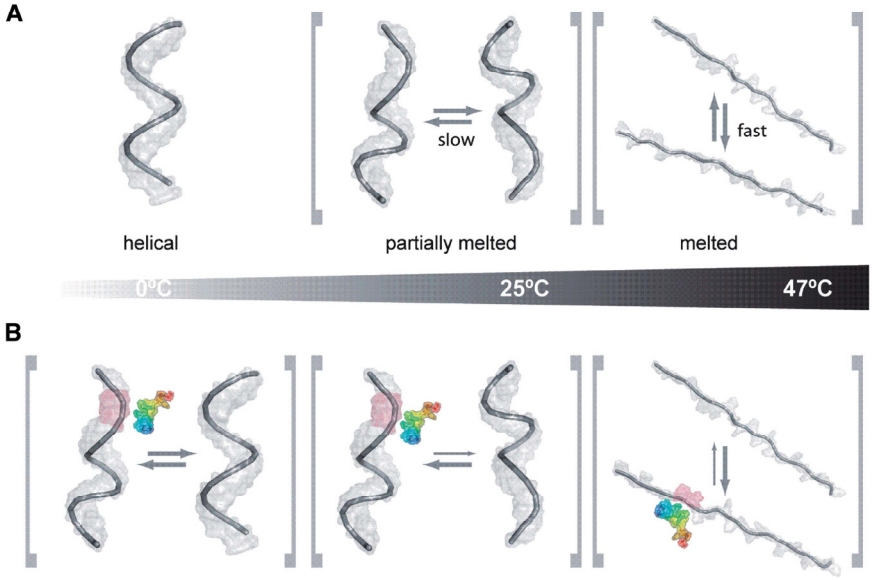

Figure 8. Schematic representation of peptide-induced RNA structural changes. (**A**) RNA only, (**B**) RNA in the presence of Tat(44–61) with its N-terminus in blue and its C-terminus in red. At low temperature, the interaction of the peptide with the RNA induces changes in the conformational equilibrium in a way that not only a single helical conformation is present but the helical-conformation is locally disrupted or partially melted. At intermediate temperatures (close to the 'melting point') the RNA is anyhow in a conformational equilibrium between helical and partially melted conformations. The addition of peptide to this pool of conformers results in a partial stabilization of the partially melted RNA conformations, which are probably the ones where RNA duplex formation initiates. At high temperatures, Tat(44–61) will stabilize not the completely randomized unfolded form of the RNA, but intermediates that are prone to interaction with a complementary strand of RNA.

meaning that at this particular temperature the RNA is in an equilibrium of 50% unfolded and folded conformations.

The addition of peptide to the $21R^+$ changed the RNA spectra in a temperature dependent way (Figure 7). A control spectrum of peptide alone demonstrated that RNA aromatic hydrogen shifts did not overlap with peptide peaks (Supplementary Figure S13). Thus, the chemical shift changes upon addition of peptide could be attributed directly to structural changes within the RNA, assuming that shift changes in the peptide do not lead to an overlap in the NMR spectra of the complex. The addition of peptide Tat(44–61) to the RNA induces chemical shift changes in the RNA and leads to a broadening of the signals at low (0°C) and high (37°C) temperatures. At these temperatures, the interaction of the RNA with Tat(44–61) leads to an equilibrium between the selected conformation and the ground-state conformation on a timescale turning the peaks in the spectrum broad. At intermediate temperatures (20°C) (when the signals are already broad and the chemical shift dispersion is limited), the spectrum gets more disperse and more distinct signals and are visible upon addition of peptide. This is due to the selection of a certain conformation from the pool of slowly interconverting RNA conformations (Figure 8).

This conformation selection might be achieved by true selective binding of already formed RNA conformations which relocates the equilibrium between different RNA structures. Another possible reason for the population change is the modulation of RNA structure upon peptide binding. Indeed, it has been shown by other groups that arginine/lysine oligopeptides are able to change DNA conformations by tilting the bases or altering the winding angle (70). Regarded on a molecular level, a lot of encounters between RNA molecules turn out to be fruitless due to unfavorable RNA conformations and/or orientations. Switching the RNA molecules to a favorable conformation and/or orientation would thus increase the probability of procession from an encounter to the transition state of duplex formation. At the level of the RNA molecule ensemble, this activity would have the propensity to accelerate the overall annealing reaction. Thus, we suggest that Tat(44–61) shifts the RNA structure into an annealing-competent form which might be a partly helical and partly melted conformation as indicated by our data.

CONCLUSIONS

HIV-1 Tat as well as its fragment Tat(44–61) have potent nucleic acid annealing activity but do not catalyze strand displacement and are thus nucleic acid annealers. The activity of the model peptide Tat(44–61) is based on ionic interactions between peptide and the RNA backbone. Therefore, positively charged amino acids play a dominant role in annealing acceleration while other amino acids are not important. Both the net charge of the peptide, as well as an exact arrangement of basic amino acids within the peptide, determine the magnitude of the annealing activity. Thermodynamically, Tat(44–61) increases the entropy of the annealing

transition state, thereby decreasing the Gibbs free energy. According to previous studies, the peptide-conferred entropy increase is caused by a counterion release upon peptide binding (55,70). The actual acceleration of annealing, however, is probably mainly caused by a conversion of the RNA into an annealing prone conformation. This RNA conformational change in the presence of peptide must be detrimental to the reaction's entropy but its contribution is apparently too small to compensate the counterion release effect. These findings also explain the equal importance of both the peptide's overall charge and the basic amino acid distribution: while the peptide net charge dictates RNA/peptide binding and entropy increase (54), the basic amino acid distribution probably mediates the RNA conformational change. We found no evidence for the contribution of the proposed annealing mechanism (A) (active increase of the local RNA concentration, see 'Introduction' section) to the annealing activity of the Tat peptide. The potential annealing mechanism (B) (stabilization of the annealing transition state by shielding the negative RNA backbone charges) can be excluded for Tat(44 61) since it would demand a decrease of the activation energy E_a. Considering the promiscuous annealing acceleration of RNAs with different sequences, it seems obvious that Tat(44 61) does not form strong complexes with its substrates. Thus, binding constants might not be of significance when discussing RNA annealers and chaperones. In fact, the interaction of Tat(44 61) and RNA are most probably of a very transient nature which we believe to be a key element to annealing acceleration (72). Although CTAB-, Ncp7- and p53-facilitated annealing apparently underlie different mechanisms, we think that our findings might apply to other facilitators of annealing that are rich in basic amino acids, such as *Escherichia coli* StpA, ribonucleoprotein hnRNP A1 and guideRNA binding protein gBP21. In each unique case other amino acids (like hydrogen bond-forming ones) might contribute to the activity.

SUPPLEMENTARY DATA

Supplementary Data are available at NAR Online.

ACKNOWLEDGEMENTS

We are grateful to Peter Steinlein for the fast synthesis of peptides and to Michael Jantsch for help concerning the conduction of the filter binding assays. We would like to thank all members of the Schroeder Lab for helpful discussions on the topic of RNA chaperones. We are indebted to Christina Waldsich, Brooke Morriswood and Jennifer L. Boots for critical reading of the article and helpful comments.

FUNDING

University of Vienna (to M.D.); Fonds zur Förderung der wissenschaftlichen Forschung (FWF) through a Lise Meitner-Position (M1157-B12 to B.F.), RNA Biology Doktoratskolleg (W1207 to M.D. and R.S.), (F1703 to R.S). Funding for open access charge: Austrian Science Fund FWF.

Conflict of interest statement. None declared.

REFERENCES

1. Herschlag,D. (1995) RNA chaperones and the RNA folding problem. *J. Biol. Chem.*, **270**, 20871–20874.
2. Uhlenbeck,O.C. (1995) Keeping RNA happy. *RNA*, **1**, 4–6.
3. Semrad,K. and Schroeder,R. (1998) A ribosomal function is necessary for efficient splicing of the T4 phage thymidylate synthase intron in vivo. *Genes Dev.*, **12**, 1327–1337.
4. Schroeder,R., Grossberger,R., Pichler,A. and Waldsich,C. (2002) RNA folding in vivo. *Curr. Opin. Struct. Biol.*, **12**, 296–300.
5. Rajkowitsch,L., Chen,D., Stampfl,S., Semrad,K., Waldsich,C., Mayer,O., Jantsch,M.F., Konrat,R., Bläsi,U. and Schroeder,R. (2007) RNA Chaperones, RNA Annealers and RNA Helicases. *RNA Biol.*, **4**, 118–130.
6. Cristofari,G. and Darlix,J.L. (2002) The ubiquitous nature of RNA chaperone proteins. *Prog. Nucleic Acid Res. Mol. Biol.*, **72**, 223–268.
7. Rajkowitsch,L. and Schroeder,R. (2007) Dissecting RNA chaperone activity. *RNA*, **13**, 2053–2060.
8. Cordin,O., Banroques,J., Tanner,N.K. and Linder,P. (2006) The DEAD-box protein family of RNA helicases. *Gene*, **367**, 17–37.
9. Valdez,B.C., Henning,D., Perumal,K. and Busch,H. (1997) RNA-unwinding and RNA-folding activities of RNA helicase II/Gu–two activities in separate domains of the same protein. *Eur. J. Biochem.*, **250**, 800–807.
10. Lapadat-Tapolsky,M., Pernelle,C., Borie,C. and Darlix,J.L. (1995) Analysis of the nucleic acid annealing activities of nucleocapsid protein from HIV-1. *Nucleic Acids Res.*, **23**, 2434–2441.
11. Huang,Z.S., Chen,A.Y. and Wu,H.N. (2004) Characterization and application of the selective strand annealing activity of the N terminal domain of hepatitis delta antigen. *FEBS Lett.*, **578**, 345–350.
12. Stewart-Maynard,K.M., Cruceanu,M., Wang,F., Vo,M.N., Gorelick,R.J., Williams,M.C., Rouzina,I. and Musier-Forsyth,K. (2008) Retroviral nucleocapsid proteins display nonequivalent levels of nucleic acid chaperone activity. *J. Virol.*, **82**, 10129–10142.
13. Hopkins,J.F., Panja,S., McNeil,S.A. and Woodson,S.A. (2009) Effect of salt and RNA structure on annealing and strand displacement by Hfq. *Nucleic Acids Res.*, **37**, 6205–6213.
14. Mayer,O., Rajkowitsch,L., Lorenz,C., Konrat,R. and Schroeder,R. (2007) RNA chaperone activity and RNA-binding properties of the E. coli protein StpA. *Nucleic Acids Res.*, **35**, 1257–1269.
15. Kim,S. and Marians,K.J. (1995) DNA and RNA-DNA annealing activity associated with the tau subunit of the Escherichia coli DNA polymerase III holoenzyme. *Nucleic Acids Res.*, **23**, 1374–1379.
16. Portman,D.S. and Dreyfuss,G. (1994) RNA annealing activities in HeLa nuclei. *EMBO J.*, **13**, 213–221.
17. Nedbal,W., Frey,M., Willemann,B., Zentgraf,H. and Sczakiel,G. (1997) Mechanistic insights into p53-promoted RNA-RNA annealing. *J. Mol. Biol.*, **266**, 677–687.
18. Muller,U.F., Lambert,L. and Goringer,H.U. (2001) Annealing of RNA editing substrates facilitated by guide RNA-binding protein gBP21. *EMBO J.*, **20**, 1394–1404.
19. Muller,U.F. and Goringer,H.U. (2002) Mechanism of the gBP21-mediated RNA/RNA annealing reaction: matchmaking and charge reduction. *Nucleic Acids Res.*, **30**, 447–455.
20. Lee,C.G., Zamore,P.D., Green,M.R. and Hurwitz,J. (1993) RNA annealing activity is intrinsically associated with U2AF. *J. Biol. Chem.*, **268**, 13472–13478.
21. Akhmedov,A.T., Bertrand,P., Corteggiani,E. and Lopez,B.S. (1995) Characterization of two nuclear mammalian homologous DNA-pairing activities that do not require associated exonuclease activity. *Proc. Natl Acad. Sci. USA*, **92**, 1729–1733.

22. Baechtold,H., Kuroda,M., Sok,J., Ron,D., Lopez,B.S. and Akhmedov,A.T. (1999) Human 75-kDa DNA-pairing protein is identical to the pro-oncoprotein TLS/FUS and is able to promote D-loop formation. *J. Biol. Chem.*, **274**, 34337–34342.
23. Altmann,M., Wittmer,B., Methot,N., Sonenberg,N. and Trachsel,H. (1995) The Saccharomyces cerevisiae translation initiation factor Tif3 and its mammalian homologue, eIF-4B, have RNA annealing activity. *EMBO J.*, **14**, 3820–3827.
24. Skabkin,M.A., Evdokimova,V., Thomas,A.A. and Ovchinnikov,L.P. (2001) The major messenger ribonucleoprotein particle protein p50 (YB-1) promotes nucleic acid strand annealing. *J. Biol. Chem.*, **276**, 44841–44847.
25. Kwon,S.H., Lee,I.H., Kim,N.Y., Choi,D.H., Oh,Y.M. and Bae,S.H. (2007) Translation initiation factor eIF1A possesses RNA annealing activity in its oligonucleotide-binding fold. *Biochem. Biophys. Res. Commun.*, **361**, 681–686.
26. Hitti,E., Neunteufl,A. and Jantsch,M.F. (1998) The double-stranded RNA-binding protein X1rbpa promotes RNA strand annealing. *Nucleic Acids Res.*, **26**, 4382–4388.
27. Schumacher,M.A., Karamooz,E., Zikova,A., Trantirek,L. and Lukes,J. (2006) Crystal structures of T. brucei MRP1/MRP2 guide-RNA binding complex reveal RNA matchmaking mechanism. *Cell*, **126**, 701–711.
28. Zikova,A., Kopecna,J., Schumacher,M.A., Stuart,K., Trantirek,L. and Lukes,J. (2008) Structure and function of the native and recombinant mitochondrial MRP1/MRP2 complex from Trypanosoma brucei. *Int. J. Parasitol.*, **38**, 901–912.
29. Nedbal,W., Homann,M. and Sczakiel,G. (1997) The association of complementary ribonucleic acids can be strongly increased without lowering Arrhenius activation energies or significantly altering structures. *Biochemistry*, **36**, 13552–13557.
30. Jones,K.A. and Peterlin,B.M. (1994) Control of RNA initiation and elongation at the HIV-1 promoter. *Annu. Rev. Biochem.*, **63**, 717–743.
31. Brigati,C., Giacca,M., Noonan,D.M. and Albini,A. (2003) HIV Tat, its TARgets and the control of viral gene expression. *FEMS Microbiol. Lett.*, **220**, 57–65.
32. SenGupta,D.N., Berkhout,B., Gatignol,A., Zhou,A.M. and Silverman,R.H. (1990) Direct evidence for translational regulation by leader RNA and Tat protein of human immunodeficiency virus type 1. *Proc. Natl Acad. Sci. USA*, **87**, 7492–7496.
33. Bennasser,Y. and Jeang,K.T. (2006) HIV-1 Tat interaction with Dicer: requirement for RNA. *Retrovirology*, **3**, 95.
34. Bennasser,Y., Le,S.Y., Benkirane,M. and Jeang,K.T. (2005) Evidence that HIV-1 encodes an siRNA and a suppressor of RNA silencing. *Immunity*, **22**, 607–619.
35. Lin,J. and Cullen,B.R. (2007) Analysis of the interaction of primate retroviruses with the human RNA interference machinery. *J. Virol.*, **81**, 12218–12226.
36. McMillan,N.A., Chun,R.F., Siderovski,D.P., Galabru,J., Toone,W.M., Samuel,C.E., Mak,T.W., Hovanessian,A.G., Jeang,K.T. and Williams,B.R. (1995) HIV-1 Tat directly interacts with the interferon-induced, double-stranded RNA-dependent kinase, PKR. *Virology*, **213**, 413–424.
37. Cai,R., Carpick,B., Chun,R.F., Jeang,K.T. and Williams,B.R. (2000) HIV-I TAT inhibits PKR activity by both RNA-dependent and RNA-independent mechanisms. *Arch. Biochem. Biophys.*, **373**, 361–367.
38. Chiu,Y.L., Ho,C.K., Saha,N., Schwer,B., Shuman,S. and Rana,T.M. (2002) Tat stimulates cotranscriptional capping of HIV mRNA. *Mol. Cell*, **10**, 585–597.
39. Harrich,D., Ulich,C., Garcia-Martinez,L.F. and Gaynor,R.B. (1997) Tat is required for efficient HIV-1 reverse transcription. *EMBO J.*, **16**, 1224–1235.
40. Kameoka,M., Morgan,M., Binette,M., Russell,R.S., Rong,L., Guo,X., Mouland,A., Kleiman,L., Liang,C. and Wainberg,M.A. (2002) The Tat protein of human immunodeficiency virus type 1 (HIV-1) can promote placement of tRNA primer onto viral RNA and suppress later DNA polymerization in HIV-1 reverse transcription. *J. Virol.*, **76**, 3637–3645.
41. Apolloni,A., Hooker,C.W., Mak,J. and Harrich,D. (2003) Human immunodeficiency virus type 1 protease regulation of tat activity is essential for efficient reverse transcription and replication. *J. Virol.*, **77**, 9912–9921.
42. Kuciak,M., Gabus,C., Ivanyi-Nagy,R., Semrad,K., Storchak,R., Chaloin,O., Muller,S., Mely,Y. and Darlix,J.L. (2008) The HIV-1 transcriptional activator Tat has potent nucleic acid chaperoning activities in vitro. *Nucleic Acids Res.*, **36**, 3389–3400.
43. Fanales-Belasio,E., Moretti,S., Nappi,F., Barillari,G., Micheletti,F., Cafaro,A. and Ensoli,B. (2002) Native HIV-1 Tat protein targets monocyte-derived dendritic cells and enhances their maturation, function, and antigen-specific T cell responses. *J. Immunol.*, **168**, 197–206.
44. Rajkowitsch,L. and Schroeder,R. (2007) Coupling RNA annealing and strand displacement: a FRET-based microplate reader assay for RNA chaperone activity. *Biotechniques*, **43**, 304, 306, 308 passim.
45. Hallegger,M., Taschner,A. and Jantsch,M.F. (2006) RNA aptamers binding the double-stranded RNA-binding domain. *RNA*, **12**, 1993–2004.
46. Vo,M.N., Barany,G., Rouzina,I. and Musier-Forsyth,K. (2009) Effect of Mg(2+) and Na(+) on the nucleic acid chaperone activity of HIV-1 nucleocapsid protein: implications for reverse transcription. *J. Mol. Biol.*, **386**, 773–788.
47. Atkins,P., Höpfner,A., Schleitzer,A. and Bär,M. (1996) *Physikalische Chemie*, VCH, Weinheim.
48. Laidler,K. and King,M. (1983) Development of transition-state theory. *J. Phys. Chem.*, **87**, 2657–2664.
49. Delaglio,F., Grzesiek,S., Vuister,G.W., Zhu,G., Pfeifer,J. and Bax,A. (1995) NMRPipe: a multidimensional spectral processing system based on UNIX pipes. *J. Biomol. NMR*, **6**, 277–293.
50. Wijmenga,S., Kruithof,M. and Hilbers,C. (1997) Analysis of 1 H chemical shifts in DNA: assessment of the reliability of 1 H chemical shift calculations for use in structure refinement. *J. Biomol. NMR*, **10**, 337–350.
51. Cromsigt,J.A., Hilbers,C.W. and Wijmenga,S.S. (2001) Prediction of proton chemical shifts in RNA. Their use in structure refinement and validation. *J. Biomol. NMR*, **21**, 11–29.
52. Markham,N.R. and Zuker,M. (2005) DINAMelt web server for nucleic acid melting prediction. *Nucleic Acids Res.*, **33**, W577–W581.
53. Semrad,K., Green,R. and Schroeder,R. (2004) RNA chaperone activity of large ribosomal subunit proteins from Escherichia coli. *RNA*, **10**, 1855–1860.
54. Mascotti,D.P. and Lohman,T.M. (1992) Thermodynamics of single-stranded RNA binding to oligolysines containing tryptophan. *Biochemistry*, **31**, 8932–8946.
55. Record,M.T. Jr, Lohman,M.L. and De Haseth,P. (1976) Ion effects on ligand-nucleic acid interactions. *J. Mol. Biol.*, **107**, 145–158.
56. Huang,Z.S. and Wu,H.N. (1998) Identification and characterization of the RNA chaperone activity of hepatitis delta antigen peptides. *J. Biol. Chem.*, **273**, 26455–26461.
57. Croitoru,V., Semrad,K., Prenninger,S., Rajkowitsch,L., Vejen,M., Laursen,B.S., Sperling-Petersen,H.U. and Isaksson,L.A. (2006) RNA chaperone activity of translation initiation factor IF1. *Biochimie*, **88**, 1875–1882.
58. Draper,D.E. (1999) Themes in RNA-protein recognition. *J. Mol. Biol.*, **293**, 255–270.
59. Draper,D.E. (2004) A guide to ions and RNA structure. *RNA*, **10**, 335–343.
60. Munroe,S.H. and Dong,X.F. (1992) Heterogeneous nuclear ribonucleoprotein A1 catalyzes RNA.RNA annealing. *Proc. Natl Acad. Sci. USA*, **89**, 895–899.
61. Cobianchi,F., Calvio,C., Stoppini,M., Buvoli,M. and Riva,S. (1993) Phosphorylation of human hnRNP protein A1 abrogates in vitro strand annealing activity. *Nucleic Acids Res.*, **21**, 949–955.
62. Ammerman,M.L., Fisk,J.C. and Read,L.K. (2008) gRNA/pre-mRNA annealing and RNA chaperone activities of RBP16. *RNA*, **14**, 1069–1080.
63. Le Cam,E., Coulaud,D., Delain,E., Petitjean,P., Roques,B.P., Gerard,D., Stoylova,E., Vuilleumier,C., Stoylov,S.P. and Mely,Y. (1998) Properties and growth mechanism of the ordered aggregation of a model RNA by the HIV-1 nucleocapsid protein: an electron microscopy investigation. *Biopolymers*, **45**, 217–229.
64. Tsuchihashi,Z. and Brown,P.O. (1994) DNA strand exchange and selective DNA annealing promoted by the human

immunodeficiency virus type 1 nucleocapsid protein. *J. Virol.*, **68**, 5863–5870.
65. Mely,Y., de Rocquigny,H., Sorinas-Jimeno,M., Keith,G., Roques,B.P., Marquet,R. and Gerard,D. (1995) Binding of the HIV-1 nucleocapsid protein to the primer tRNA(3Lys), in vitro, is essentially not specific. *J. Biol. Chem.*, **270**, 1650–1656.
66. al-Ghusein,H., Ball,H., Igloi,G.L., Gbewonyo,A., Coates,A.R., Mascagni,P. and Roberts,M.M. (1996) Chemically synthesised human immunodeficiency virus P7 nucleocapsid protein can self-assemble into particles and binds to a specific site on the tRNA(Lys,3) primer. *Biochem. Biophys. Res. Commun.*, **224**, 191–198.
67. Cruceanu,M., Urbaneja,M., Hixson,C., Johnson,D., Datta,S., Fivash,M., Stephen,A., Fisher,R., Gorelick,R. and Casas-Finet,J. (2006) Nucleic acid binding and chaperone properties of HIV-1 Gag and nucleocapsid proteins. *Nucleic Acids Res.*, **34**, 593.
68. Nguyen,T., Rouzina,I. and Shklovskii,B. (2000) Reentrant condensation of DNA induced by multivalent counterions. *J. Chem. Phys.*, **112**, 2562.
69. Raspaud,E., Olvera de la Cruz,M., Sikorav,J.L. and Livolant,F. (1998) Precipitation of DNA by polyamines: a polyelectrolyte behavior. *Biophys J.*, **74**, 381–393.
70. Helene,C. and Maurizot,J.C. (1981) Interactions of oligopeptides with nucleic acids. *CRC Crit. Rev. Biochem.*, **10**, 213–258.
71. Suryawanshi,H., Sabharwal,H. and Maiti,S. (2010) Thermodynamics of peptide-RNA recognition: the binding of a Tat peptide to TAR RNA. *J. Phys. Chem. B*, **114**, 11155–11163.
72. Schreiber,G., Haran,G. and Zhou,H.X. (2009) Fundamental aspects of protein-protein association kinetics. *Chem. Rev.*, **109**, 839–860.

7. 2. ABSTRACT

Low temperature is a major stress factor for plants. The plants response to this kind of stress involves a dramatic change in the metabolite and protein profile. Among other cold-inducible proteins, RNA chaperones are highly expressed. RNA chaperones are able to resolve RNA-RNA interactions and thereby help the cell to cope with the increased thermodynamic stability of non-native RNA structures at low temperature. The change in the metabolite profile is poorly understood. One major group of upregulated metabolites are “osmolytes”, a group of metabolites that maintain the cells osmolarity but do not show any interaction with macromolecules. However, many cold-inducible metabolites were shown to influence the thermodynamic stability of proteins and nucleic acids. This study tested whether these metabolites can help the plant cell during cold stress by acting as RNA chaperones.

Individual cold-shock metabolites as well as groups of cold-shock metabolites do not fulfill the requirements to enhance annealing or strand-displacement of short RNA oligonucleotides in a FRET-based assay. Approximately physiological concentrations of these metabolites also did not alter RNA stability nor the shape of the melting transition. In order to approximate physiological metabolite combinations, polar metabolites were extracted from cold-treated *Chlamydomonas reinhardtii* cells. The extracts were tested for their ability to promote the functional conformation of a folding retarded group I intron in a *trans*-splicing assay. The splicing was equally efficient in extracts from cold-treated cells and from not-cold-treated cells. Both extracts were found to enhance the strand-displacement reaction between a 21mer duplex RNA and a 32mer fully complementary competitor. The cold-shock extract enhanced the displacement-reaction already at lower concentrations. In addition, a protocol for a tag-free purification of the proposed RNA chaperone GRP7 was developed.

In conclusion, cold-shock metabolites were not found to influence RNA folding. However, the change in the metabolite profile upon cold-shock can have an influence on RNA *in vitro* as shown in the strand-displacement assay. Whether this influence is of biological relevance cannot be concluded.

7. 3. ZUSAMMENFASSUNG

Die Anpassung von Pflanzen an Kältestress beinhaltet eine drastische Änderung des Metabolit- und Proteinprofils. Neben anderen Proteinen werden auch RNA-Chaperone vermehrt exprimiert. RNA-Chaperone können RNA-RNA Interaktionen lösen und dadurch der Zelle helfen, die erhöhte thermodynamische Stabilität von RNA Strukturen bei niedriger Temperatur zu kompensieren. Dagegen ist über die Funktion von Metaboliten während der Kälteadaption wenig bekannt. Eine gut untersuchte Gruppe stress-induzierter Metaboliten sind Osmolyte. Osmolyte halten die Osmolarität der Zelle aufrecht, ohne jedoch mit Makromolekülen der Zelle zu interagieren. In hohen Konzentrationen verändern jedoch viele kälte-induzierte Metaboliten die Stabilität von Proteinen und Nukleinsäuren. In dieser Studie wurde getestet, ob diese Metaboliten als RNA-Chaperone fungieren können, indem sie den Austausch zwischen RNA-Strängen beschleunigen.

Weder individuelle kälte-induzierte Metaboliten noch Metabolitgruppen beschleunigen die Hybridisierung von oder den Austausch zwischen kurzen RNA Oligonukleotiden. Es konnte ebenfalls kein Einfluss auf die strukturelle Stabilität von RNA festgestellt werden. Um eine physiologische Metabolitzusammensetzung zu approximieren, wurden Metabolitextrakte von kältebehandelten und nicht-kältebahandelten *Chlamydomonas reinhardtii* Zellen hergestellt und verglichen. Beide Extrakte fördern die korrekte Faltung von RNA im selben Ausmaß und beschleunigen den Austausch zwischen kurzen RNA Oligonukeotiden. Allerdings ist diese Beschleunigung in Kälteschockextrakten, im Vergleich zu Kontrollextrakten schon bei niedrigeren Metabolitkonzentrationen zu beobachten.

Ein Protokoll für die Aufreinigung von GRP7, einem kälte-induzierten Protein welches vermutlich RNA-Chaperon Aktivität aufweist, wurde entwickelt.

Zusammenfassend konnte kein Einfluss von individuellen kälte-induzierten Metaboliten auf die RNA-Faltung festgestellt werden. Kälte-Schock Extrakte beschleunigen den Austausch zwischen RNA Strängen *in vitro*. Dies weist darauf hin, dass die Änderung des Metabolitprofils während Kälteschock einen Einfluss auf RNA haben könnte. Allerdings lassen diese Ergebnisse keine Schlussfolgerung zu, ob dieser Einfluss von biologischer Relevanz ist.

7. 4. CURRICULUM VITAE

PERSONAL DATA

Name	Thomas Gstrein
Birth	03/02/1987 in Rum, Austria
Nationality	Austria

EDUCATION

1993 – 1997	**Elementary school**, Hall in Tirol, Austria
1997 – 2005	**Humanities-oriented Gymnasium**, Hall in Tirol, Austria
2005 – 2008	**Bachelor studies in Biology,** University of Innsbruck, Austria
07/2006 – 01/2007	**Military service**, training as combat medic
Since 10/2008	**Master studies in Genetics and Developmental Biology**
	Focus on Genetics and Molecular Pathology
	University of Vienna, Austria
Since 01/2009	**Master thesis**
	Max F. Perutz Laboratories, Department for Biochemistry

WORK EXPERIENCE (science related)

2008 and 2009	**Sandoz GmbH**, Kundl, Austria
(6 weeks each)	Work in an analytical laboratory
01/2011	**Workshop on synthetic life**, Basel, Switzerland
	Organized by the Swiss Academies of Arts and Sciences, the Austrian Academy of Sciences and the DECHEMA Society for Chemical Engineering and Biotechnology
02/2011	**Workshop on RNA biology**, Vienna, Austria
	Organized by the SFB17 (special research program 17) on Modulators of RNA Fate and Function

PUBLICATIONS

Mechanisms of StpA-mediated RNA remodeling.
Doetsch M, Gstrein T, Schroeder R, Furtig B.
RNA Biology (2010) **7**(6): 735-743.

The RNA annealing mechanism of the HIV-1 Tat peptide: conversion of the RNA into an annealing-competent conformation.
Doetsch M, Fürtig B, Gstrein T, Stampfl S, Schroeder R.
Nucleic Acids Res. (2011) [in process]